Asia Pacific Research Initiative for Sustainable Energy Systems 2016 (APRISES16)

Office of Naval Research
Grant Award Number N00014-17-1-2206

Ocean Thermal Energy Conversion (OTEC) Heat Exchanger Development

(February 2020 - July 2021)

Task 6.1

Prepared for
Hawai‘i Natural Energy Institute

Prepared by
Makai Ocean Engineering

August 2021

HNEI
Hawai‘i Natural Energy Institute
University of Hawai‘i at Mānoa

MAKAI OCEAN ENGINEERING

ANNUAL REPORT

Prepared For

HAWAII NATURAL ENERGY INSTITUTE

1680 East West Road, POST 109

Honolulu, HI, 96822

USA

Prepared By

MAKAI OCEAN ENGINEERING

PO Box 1206, Kailua, Hawaii 96734

August 2021

TABLE OF CONTENTS

LIST OF FIGURES

LIST OF TABLES

1. INTRODUCTION

Makai Ocean Engineering has been developing Thin Foil Heat Exchangers (TFHX) for use in seawater-refrigerant, air-water, and water-water applications. This report summarizes work performed between February 2020 – July 2021.

In this period, Makai's efforts focused on advancing the TFHX design, reducing TFHX fabrication time, and continuing to characterize TFHX thermal, hydraulic, and structural/mechanical performance.

TFHX Design

Makai designed a modular, 4-port, full-length (1-m), counterflow TFHX. 24 TFHX plates are stacked in a plastic, injection-molded module. Multiple modules can then be stacked together to form a heat exchanger unit. New fixturing was designed and procured to fabricate and pressure test individual plates as well as stack a module consisting of 24 plates.

Makai advanced the all-welded TFHX (AW-TFHX) technology by demonstrating the internal manifold weld. Makai completed the design and procurement of fixturing to weld and pressure test stacks of all-welded plates.

TFHX Fabrication

Makai commissioned the High Speed Welding Station (HSWS) and has been fine-tuning parameters to optimize weld quality. Fabrication time was reduced from ~30 minutes for a mid-length plate on the stage to 17.5 minutes for a full-length plate on the HSWS (2X heat transfer area in ~ 60% of the time).

TFHX Characterization and Performance

In this period, Makai introduced additional parameters that expanded TFHX pressure capacity and channel sizes and began geometric and mechanical characterization of these new combinations. Makai also added optical microscopy to the array of tools used in characterization.

Makai continues to conduct performance testing of different TFHX configurations. A new round of counterflow seawater-seawater performance testing was conducted at the 100 kW Test Station. Makai also completed modifications to the 100 kW testing station in preparation for full-length, modular, 4-port TFHX testing in counterflow seawater-seawater and seawater-ammonia configurations.

Testing capability was also expanded to include air in the external channels and non-seawater liquid-to-liquid tests. Both new testing required the design and installation of new test apparatuses. Makai conducted air-water testing of 11 configurations of TFHXs and liquid-liquid testing of 1 TFHX configuration.

2. TFHX DESIGN DEVELOPMENT

Makai continues to make design changes to improve TFHX performance, adapt the TFHX for different applications, reduce fabrication time and complexity, and reduce material cost. In terms of TFHX design work in the period covered by this report, Makai focused on developing the technology using different materials, adapting the TFHX manifold design for different applications, and overall heat exchanger design.

Material Selection. The TFHX was initially developed using titanium for marine-based applications; titanium provided the required corrosion resistance, reliability, and durability. In adapting the TFHX for other operating environments, Makai has started to evaluate stainless steel and nickel-based alloys as alternate material candidates suitable for the TFHX fabrication process.

External Channel Spacing. Makai developed the use of formed features, called dimples, to ensure the external channel spacing remains precisely spaced, as designed. Spacers/o-rings are still used for testing and prototype purposes, however, for larger, finalized, heat exchanger units, the permanent, integrated dimples are easier to manage and reduce overall complexity.

Gasketed TFHX Development. In this period, Makai addressed the need for a larger manifold duct to support more flow in a TFHX unit and explored designs that would enable tighter plate spacings without the use of interlocking plates.

All-Welded TFHX (AW-TFHX) Development. In the AW-TFHX, an internal manifold weld is used to seal the internal fluid channel. Makai demonstrated proof-of-concept of the internal manifold weld and then developed new fixturing and a new short-length TFHX plate design to further develop the AW-TFHX.

Short-Length TFHX Plate. The short-length TFHX plate was designed for the AW-TFHX platform. Fixtures for single plate fabrication on the HSWS and welding stacks of short-length plates together were also designed and purchased.

Modular, Full-Length, Four-Port TFHX Unit. Makai completed the design work for a modular heat exchanger unit targeted for seawater-seawater and ammonia-seawater applications. The modular design is intended to streamline the TFHX commercialization process by using one architecture to target applications with varying duty requirements.

2.1. TFHX MATERIAL DEVELOPMENT

Initial TFHX development has focused on using titanium foil as the primary construction material. The use of thin foils is enabled by selecting corrosion-resistant titanium, which mitigates concerns about seawater corrosion induced material loss.

For TFHX applications beyond marine environments, different materials, such as stainless steel and nickel-based alloys, may be better suited for the specific applications. For example, stainless steel may be a more cost-effective option if the corrosion-resistant properties of titanium are not required. Alternatively, higher cost nickel-based alloys may be warranted for high-temperature, high-pressure applications where the TFHX's novel use of thin foils, combined with internal

structural support provided by the weld pattern, still enable less overall use of material and provide a cost-effective solution to existing, available heat exchangers.

Determining material suitability for the TFHX process involves a preliminary evaluation of material reflectivity, the ability to source the material in foil form, and cost. Material reflectivity establishes a baseline feasibility of laser welding; highly reflective materials are difficult to weld and the laser welding process may not be the optimal fabrication method. Once a preliminary assessment indicates the material has potential for success in the TFHX method, in-depth research and testing is conducted to determine the necessary weld parameters to create strong, durable welds. Inherent material properties, such as the melting point, and design properties, such as foil thickness, both affect selection of weld parameters. Once a suitable set of weld parameters are selected, the characterization process must be repeated to account for how material properties affect the geometric, mechanical, and thermal performance.

Specifically, Makai has investigated stainless steel (SS316L) and, recently, a nickel-based alloy (Haynes 230) as potential new materials for the TFHX. Stainless steel development is more advanced; Makai has purchased 0.002” and 0.003” stainless steel foils, identified appropriate weld parameters, fabricated plates, and performed preliminary geometric, mechanical, and thermal performance testing. More extensive characterization is planned for the next work period. Haynes 230 has passed preliminary assessment and Makai has placed an order for Haynes 230 foil for foil thicknesses between 0.004” to 0.010”.

2.2. EXTERNAL CHANNEL SPACING

Maintaining uniform external channel spacing is another important consideration in maximizing performance. Uneven channel spacing can induce uneven flow distribution and uneven heat transfer between plates.

Makai has developed a scalable solution using formed features in the foil. Similar to how a 3E plate is received with manifold features, a grid of dimples (numbers and locations depend on the overall plate shape and size) can also be formed in the foil. Dimples are positioned to stack up and the dimple height is customizable for each plate spacing. This solution requires no additional components to assemble and no components that can become loose or lost during operation (and no longer provide the function of maintaining spacing).

Makai tested the dimple feature to maintain a 1-mm plate spacing with 24 and 60 plates during air-water testing (Figure 1). For the same air velocity, the 24-plate and 60-plate units produced the same pressure drop and thermal performance, strongly indicating the dimples were able to maintain uniform external channels across both units.

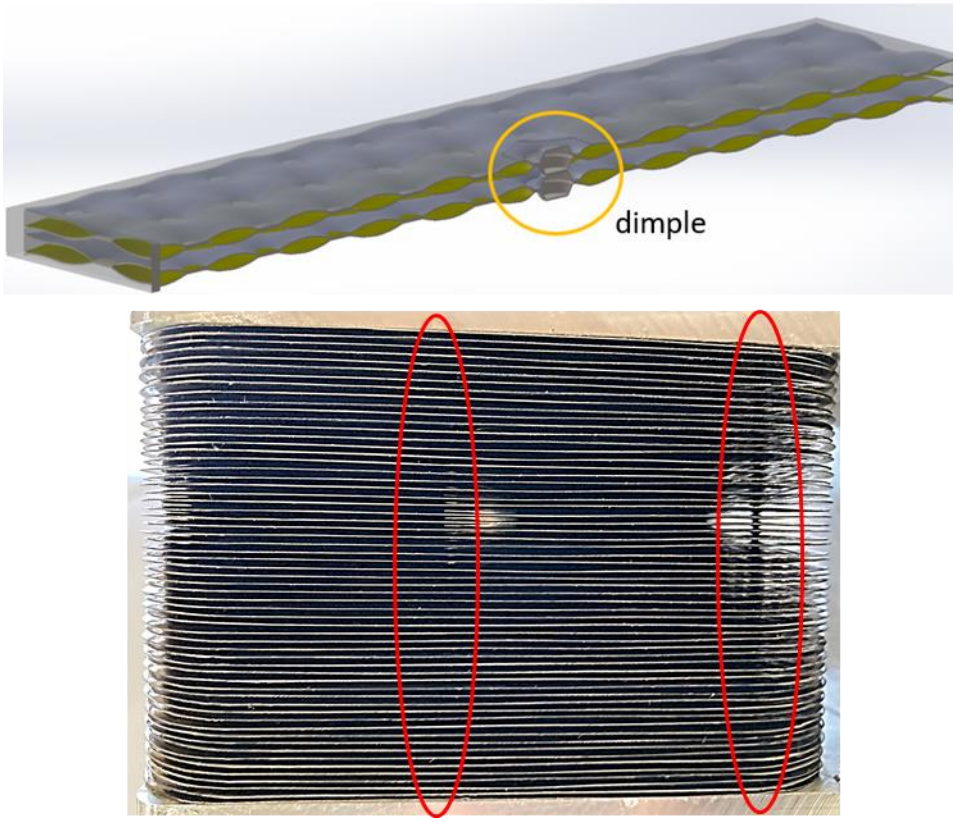

Figure 1. Dimple features used to maintain 1mm plate spacing for a 60-plate stack.

2.3. TFHX MANIFOLD DEVELOPMENT

Makai has been developing a gasketed and an all-welded version of the TFHX. In both versions, a TFHX plate consists of two sheets of foil welded together at varying locations and the internal passage is formed between the foil. The internal fluid is ducted into and out of each plate through manifold openings. The external fluid passage consists of the space between plates when individual plates are stacked together. In the gasketed version, the internal fluid is sealed from the external fluid using gaskets at the manifolds. In the all-welded version, the internal and external fluids are separated using an internal manifold weld.

2.3.1. Gasketed TFHX

The gasketed TFHX uses a manifold insert placed between the two pieces of foil at each of the manifold openings to direct the internal fluid into and out of each TFHX plate and to support gasket compression for sealing an assembled stack of TFHX plates. Each piece of foil has formed grooves which the gaskets sit in and also hold the insert in place. The manifold/manifold insert design affects the overall heat exchanger in multiple ways:

1) Minimizing the manifold footprint increases the active heat transfer area.
2) Reducing the manifold insert thickness decreases plate spacing and, therefore, increases the heat transfer area within a fixed volume.

3) Reducing the manifold insert thickness limits the available cross-sectional area for the internal fluid to flow from the manifold duct into the plate which increases the pressure drop across the insert and limits the per plate internal fluid flow rate.
4) The insert design dictates how closely welds can be made to the manifold opening and, whether a transition zone is required. More tightly spaced welds increase the pressure rating whereas more widely spaced welds result in lower head losses.
5) The size of the manifold opening, and associated pressure drop, limits the number of TFHX plates than can be stacked together in one heat exchanger unit.

Makai is currently using an insert suitable for applications using a 2-mm plate spacing; however, Makai has performed preliminary design work and is confident the same insert design can be adapted for plate spacings down to 1.4 mm.

The new "full-length" 860-mm TFHX plate requires a larger manifold opening to support more plates in one heat exchanger unit. A more detailed discussion on the full-length TFHX design is in Section 2.5.

Makai also designed and demonstrated the performance a new insert design for applications requiring 1-mm plate spacings without the use of interlocking plates. The new design was a technically viable but costly option; a more cost-conscious production method, which would require significant up-front tooling investment, would be more suitable for large applications that require plate spacings around 1mm.

2.3.2. Metal-Metal Seal

Makai developed a concept to utilize a metal-on-metal seal in place of gaskets. In this design, the bottom foil of one plate has a groove that nests in a groove on the top foil of the plate underneath (Figure 2). When the entire stack is compressed, the deflection provides enough force for the mating surfaces to form a metal seal without the use of a separate gasket. The compression and deflection are controlled by the design of dimple features formed in the foil around the manifold opening, which also provide a channel for the internal fluid to enter/exit each plate. Makai used FEA analysis to determine the appropriate dimple height, diameter, and spacing.

Makai procured the tooling, forms, and initial set of plates for seal testing and development. Although the formed foil pieces met the specifications as determined from FEA analysis, the plates did not pass a seal test. Additional analysis and re-design would be required to determine what modifications are necessary to produce a metal-metal seal.

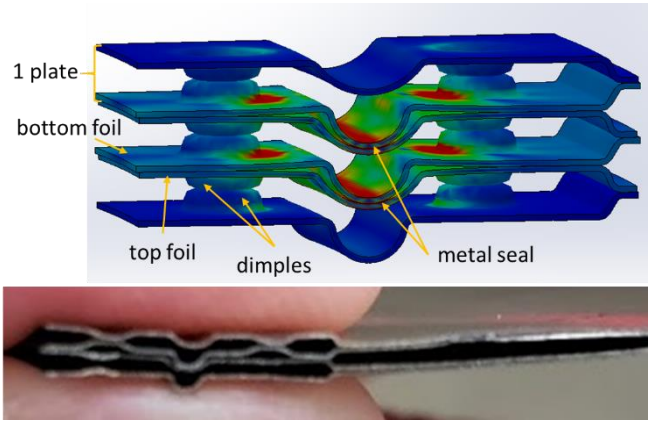

Figure 2. Metal-Metal seal concept and prototype

At this time, Makai has prioritized the all-welded development (Section 2.3.3) and has not pursued the metal seal concept further.

2.3.3. All-Welded TFHX

Makai has been developing the All-Welded TFHX (AW-TFHX), in which the internal fluid passage is sealed by welding along the thickness of two pieces of foil (0.002”-0.005”) rather than a gasket (Figure 3). An all-welded option minimizes the risk of leaks and misalignments during operation and installation but increases the difficulty of fabrication and maintenance/repair.

In an AW-TFHX, individual plates are assembled into a heat exchanger by welding sequential plates together at the manifold openings. Plate spacing, structural support, and rigidity are achieved by welding pillars at required locations on the plate. These pillars also form a continuous structural frame that provides rigidity. With each plate permanently joined the next, the assembled unit does not rely on external support (endplates or tie bars) or require compression for sealing. Because the AW-TFHX does not require gaskets for sealing, inserts are no longer required and the plate spacing can be reduced < 1mm if warranted by the application.

The novel approach to the AW-TFHX is in replacing the gaskets with an internal manifold weld. This technique requires precision optics and controls to identify and weld designated foil edges while leaving adjacent foil edges unaltered. For example, using 0.003” thick foil and a 0.028” (0.7-mm) plate spacing, the weld must be performed on a 0.006” seam with only a 0.022” gap separating adjacent foils that are not to be welded.

Makai identified and demonstrated the critical steps of the internal manifold weld, which are: 1) hold the edges together for welding, 2) identify edges to be welded together, and 3) weld only at the edge, leaving other parts of foil unaltered.

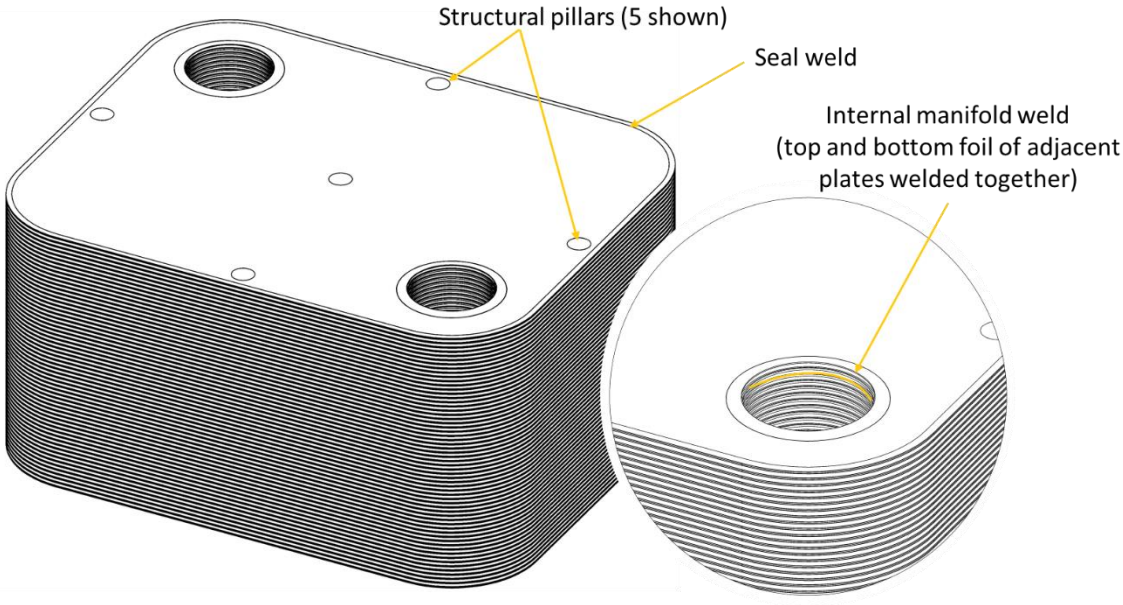

Figure 3. The key features of the AW-TFHX are the internal manifold seal welds and the structural frame welds. The perimeter seal weld and pattern welds remain the same.

Makai demonstrated the ability to identify the interface between two foils at the internal manifold and weld the foils together using a fold mirror technique (Figure 4) which used a rotating mirror placed within a 55-mm ID manifold opening to perform the internal manifold weld.

Makai conducted a series of tests to roughly define the parameters for a good internal manifold weld. The next steps are to refine the appropriate parameters, perform a series of internal manifold welds, and verify the weld seals off the internal channel and meets the required pressure rating.

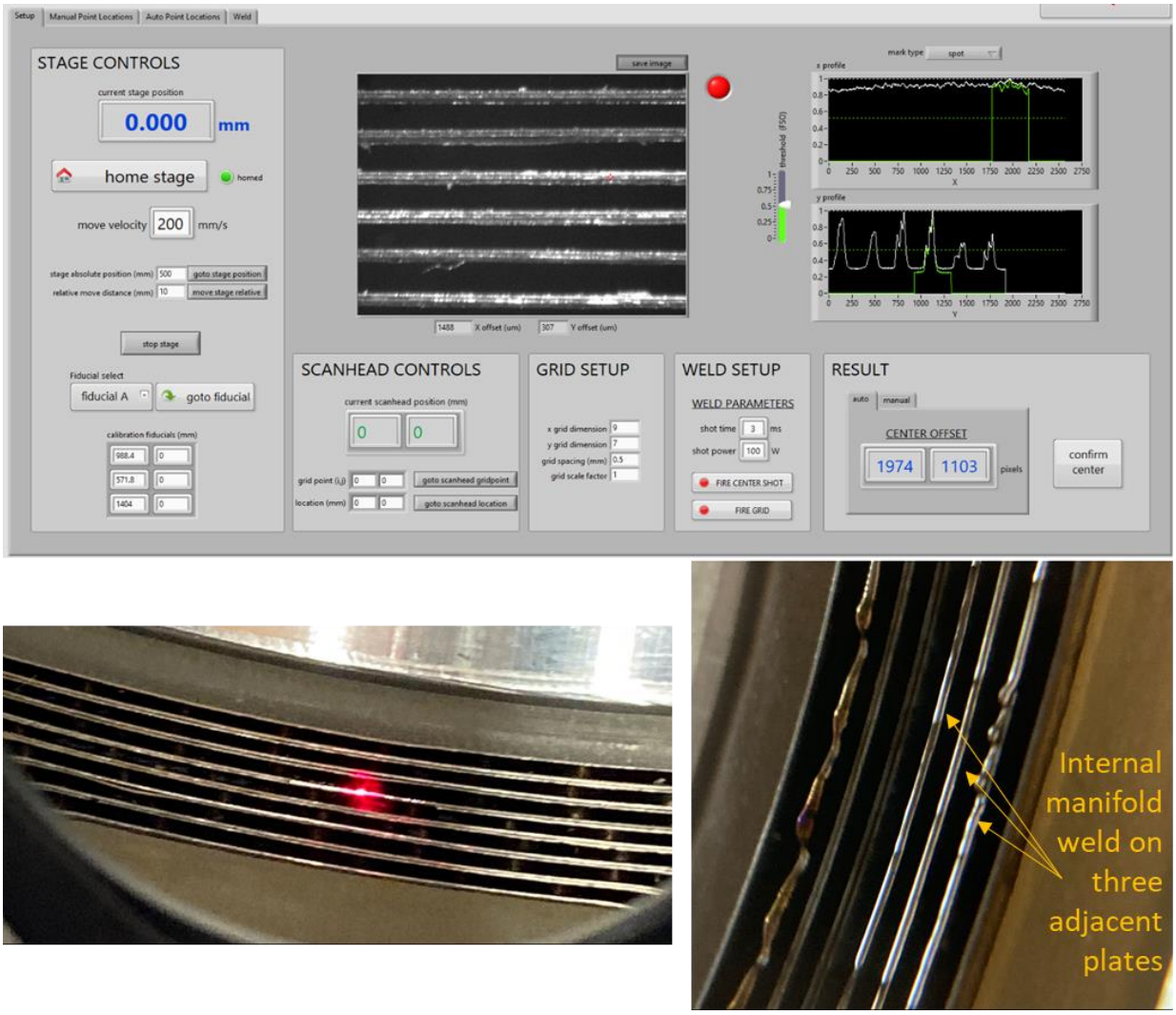

Figure 4. Steps to perform the internal manifold weld include (top) identifying the foil edges and (bottom) welding at the foil edges. The bottom right image shows welds on three adjacent plates.

For smaller or much larger manifold openings, it is impractical to place a rotating mirror inside the duct because the required focal distance may not match the manifold diameter. Instead, a method using a ring of angled mirrors positioned above the stack of plates and programming the scanhead to fire the laser at calculated locations within the ring of mirrors would be universally applicable to future TFHX designs.

Makai conducted the first test of the ring mirror method and was able to perform a complete, 360° internal manifold weld. The weld is currently performed in discrete sections corresponding to the field of view of each mirror (Figure 5).

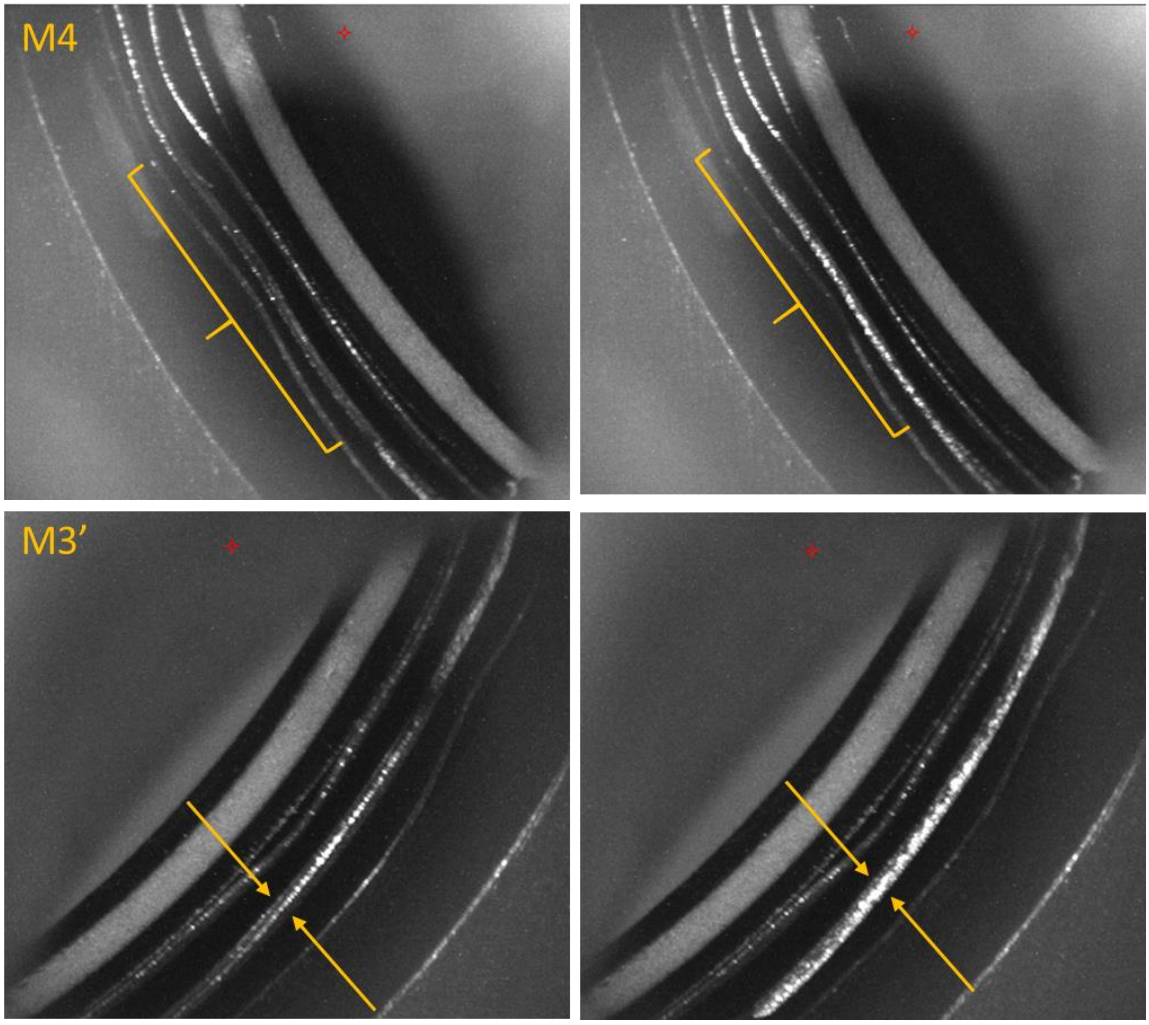

Figure 5. Working field associated with two mirrors. The images on the left show the unwelded foil edges and the images on the right show the welded edges.

The steps described above demonstrate the technical feasibility of the internal manifold weld. The next step is to weld several TFHX plates together, along with header and follower plates, and test the seal strength of the internal manifold weld. The initial seal test will be performed on a stack of five short-length TFHX plates, described in more detail in Section 2.4.

The current method to demonstrate stacking and sealing ability is time and labor intensive. Individual TFHX plates must be stacked one at a time, with multiple fixture change-outs as well as manual identification of the manifold weld locations. The economic viability of the AW-TFHX will require additional development, particularly in automation of the fabrication process:

- Automated sequential layering of individual TFHX plates and structural pillars to the welded stack
- Ability to perform the internal manifold weld and structural pillar weld in same fixture

- Automated calibration, identification, and programming of the weld locations

The automation steps are comparable to what Makai has already accomplished with the HSWS in automating the welding and forming steps of individual TFHX plates.

2.4. SHORT-LENGTH TFHX

The short-length TFHX plates were designed to prove out the AW-TFHX technology by demonstrating the ability to stack, weld, and pressure test a stack of AW-TFHX plates. The short-length plates also serve as a rapid prototyping platform for testing different combinations of weld parameters and establishing the relationship between weld patterns and plate geometry and strength.

The short-length blank plates can be cut to size from rolls of foil in-house. The cut piece of foil is then inserted into the shim punch fixture where the manifold openings are formed using a shim punch (Figure 6).

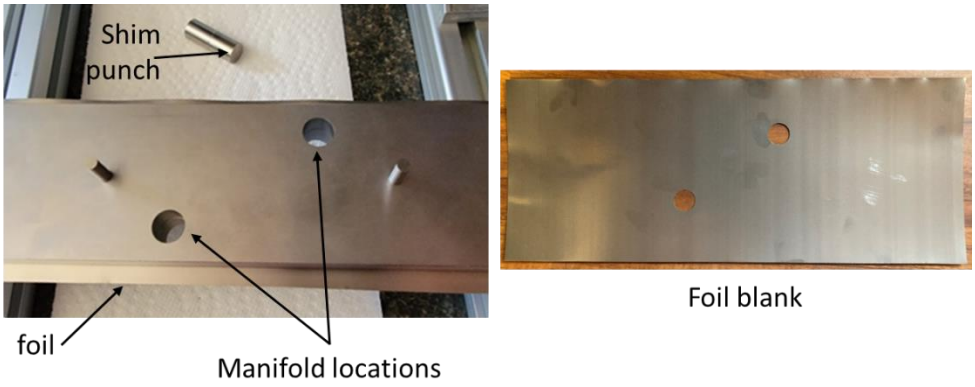

Figure 6. (left) 100mm x 300 mm foil inserted into the shim punch fixture and (right) foil ready for fabrication.

As with other TFHX plate shapes, custom fixturing was designed for to interface with the HSWS.

Although the AW-TFHX concept does not require manifold inserts for gasket support in the final assembled TFHX unit, manifold inserts are necessary in the fabrication process. Once a plate is welded and the internal passages are formed, the inserts are no longer required. Makai designed and tested several versions of removeable inserts and decided the spiral ring design was the easiest to handle and remove.

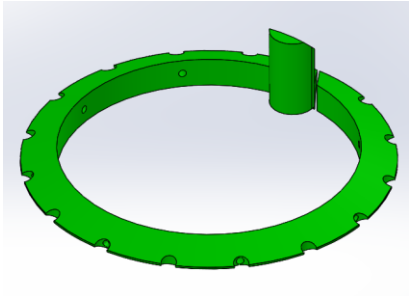

Figure 7. Spiral split ring design for the removeable insert.

2.4.1. Short-length Plates

Makai commissioned and tested the fixturing using 0.003”, 0.004”, and 0.005” foil thicknesses. For the same foil thickness, weld parameters for individual welds for the short-length plates are the same as previously used in mid-length plates. However, due to the speed of the HSWS and the limited area of the short-length plate, the wait time between welds had to be increased to minimize thermal distortion and allow enough time for heat to dissipate. For future work, Makai may evaluate active cooling systems or modifications to the welding sequence to reduce any waiting time between welds.

The short-length plates also provide a fast, low-cost platform for rapid testing of weld parameters as well as determining burst pressures and effective channel height. An initial check of effective channel heights aligned with previous data from plates fabricated on the stage and the HSWS.

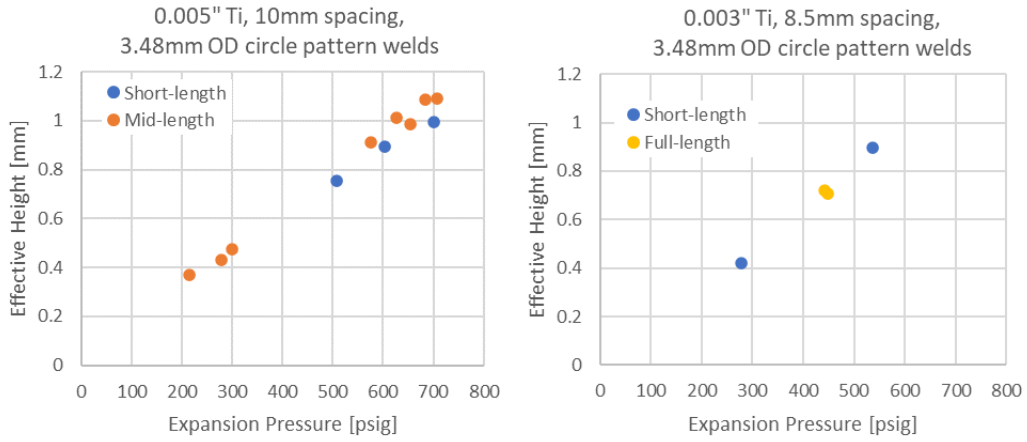

Figure 8. For the same pattern weld and foil thickness, effective heights on short-length plates line up with mid-length and full-length plates.

The smaller manifold openings also enabled pressurization over 1000 psi. With a tightly spaced pattern weld, Makai fabricated a short-length plate using 0.003” titanium that was pressurized to 1100 psig without bursting. Makai has plans to upgrade the existing expansion system to accommodate pressures > 3,000 psig and construct a separate system capable of pressurization > 15,000 psig.

Figure 9. 0.003" short-length plate pressurized to ~1100 psi.

2.4.2. Stacking Fixture

The stacking fixture is designed to be used in sequential stacking and welding of all-welded short-length plates, including header and follower plates to the first and last plates of a stack.

The stacking fixture design requirements are:

1) Maintain alignment (<25 micron) between the fixturing and the scanhead. The fixturing has components that are installed/removed/re-installed for each layer.
2) Repeatable (<10 micron) placement of the mirror mount assembly, which is removed and re-installed for each plate.
3) Provide means of ensuring contact between pillars and plate and between manifold edges for each weld.
4) Allow for shield gas coverage during pillar and internal manifold welding.
5) Complete calibration accomplished in minimal time (minutes).
6) Fixturing and methodology are fundamentally transferrable to high-speed automation.

The stacking fixture consists of a base assembly and the different additional plates and fixtures that are used for pillar welding versus manifold welding. The plate stack is held on a platform on the base assembly. The platform is moved vertically such that distance between the weld plane and the scanhead is maintained regardless of the height of the plate stack; i.e., as plates are welded together, the welded stack of plates is lowered when the next plate is placed on top.

For each plate, structural pillars are first positioned and welded to the plate using the appropriate fixtures. The internal manifold weld is then performed between the top plate and the plate below it. The stacking sequence is repeated for each plate required in an assembly to form an AW-TFHX unit.

Makai designed, procured, and is awaiting parts arrival of the short-length stacking fixture.

2.5. FULL-LENGTH, MODULAR, FOUR-PORT TFHX

The full-length, four-port modular TFHX is suited for seawater-seawater (or water) or seawater-ammonia applications using counterflow or parallel flow configurations. The modular construction can accommodate a variety of applications with different flow rates and duty requirements and provides a method for maintenance/replacement operations without replacing an entire unit.

2.5.1. Full-Length TFHX Plate and Manifold Design

In order to accommodate a range in flow rates and duties and efficiently utilize the thermal capacity of the heating/cooling fluids at a 2-mm plate spacing, the TFHX plate length and the manifold opening was increased.

The increased manifold opening is necessary to take advantage of the modular concept and enable multiple modules (up to 16 modules or 384 plates, depending on the application flow rates) to be stacked together in one TFHX unit while ensuring the manifold duct pressure drop is acceptable. The larger manifold insert is similar in design to the existing insert and is also nominally 1.8 mm thick, resulting in a 2.05-mm plate spacing when using 0.005” foil.

The external fluid ducting must also be designed to ensure the external fluid is evenly distributed between individual plates in a module and between modules that comprise a complete heat exchanger unit. In prototype-scale TFHXs, test housings included additional diffuser length for the external fluid to ensure even flow distribution. In a full-length plate, it is impractical to have additional diffuser length for the external fluid. Instead, utilizing the four-port design, external fluid flow distribution is managed similar to internal fluid flow distribution; dimples are used to maintain the flow channels for external fluid to flow between plates, similar to the function of the internal manifold insert. The dimple features around the external inlet/outlets are a new feature introduced for the full-length design.

Dimples have been successfully used in place of o-rings to maintain the external channel spacing (Section 2.2); however, the dimple forming process has not been fine-tuned, resulting in some wrinkles in the foil around the dimples. Slight wrinkling is not a concern for the external manifold duct but wrinkling in the pattern weld region requires an additional step to smooth out the wrinkles prior to welding and adds a non-trivial amount of time to the fabrication process. Therefore, for the initial full-length modules, previously used, reliable silicon o-ring spacers will be used to maintain uniformity in main heat transfer area of the plate.

Each full-length plate has 0.43 m^2 of heat transfer area. Although the overall dimensions and plate spacing are fixed, the internal channel size (and therefore the external channel size) is still customizable to fit the application’s flow rate, pressure drop, and pressure rating requirements.

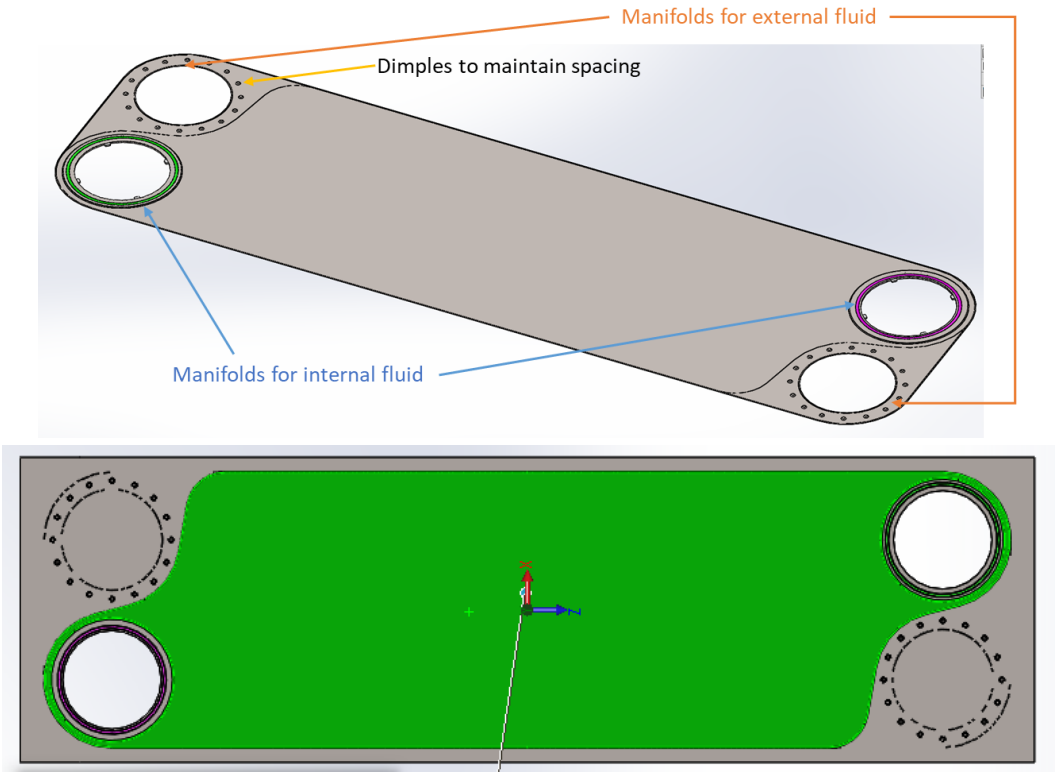

Figure 10. Full-length, four-port TFHX plate with internal fluid channel highlighted.

2.5.2. Tooling and Fixtures

The new plate design required new molds for the insert, new forms for the formed foil, and new fixtures for the HSWS, cutting, pressure testing, and stacking.

Manifold Inserts. The initial run of the new manifold inserts arrived with significant bowing. The non-uniformity was unacceptable as it may lead to sealing or flow distribution issues. After working with the vendor, additional features were added to the mold and the second set of inserts were acceptable. The averaged, as-received, insert thickness was 1.87 mm, resulting in a 2.13-mm plate spacing with 0.005" foil.

Foil Form. A new foil form was designed and procured to accommodate the longer plate, larger internal fluid manifold, and dimples for the external fluid. The first set of full-length plates was received in January 2021. After evaluating the plates, Makai determined the dimple density around the external manifold had to be doubled.

Figure 11. First full-length plates.

Makai received a second shipment of full-length plates in 0.003", 0.004", and 0.005", all with the increased dimple density in June 2021. Unfortunately, half the plates of the 0.004" and 0.005" had microcracks around the external dimples, which made it difficult to maintain contact between the two foils during the welding process. Makai has worked with the supplier and is confident the next shipment of foils will have all issues resolved.

Full-Length HSWS Fixture. A new full-length fixture was designed to accommodate the full-length plate and interface with the HSWS platform. The main functions of the full-length fixture are:

- Index and hold two pieces of formed foil, with manifold inserts between the foil at required internal fluid manifold locations.
- Deliver shield gas to the back side of the foil during welding
- Provide a means to hold the two pieces of foil together during welding
  Support and secure the welded plate in position while the internal channel is formed

A functional full-length fixture was delivered to Makai in February 2021.

Full-length plate demonstration. Full-length plate fabrication presented several challenges; however, Makai was able to produce several plates for economic analysis (Section 4).

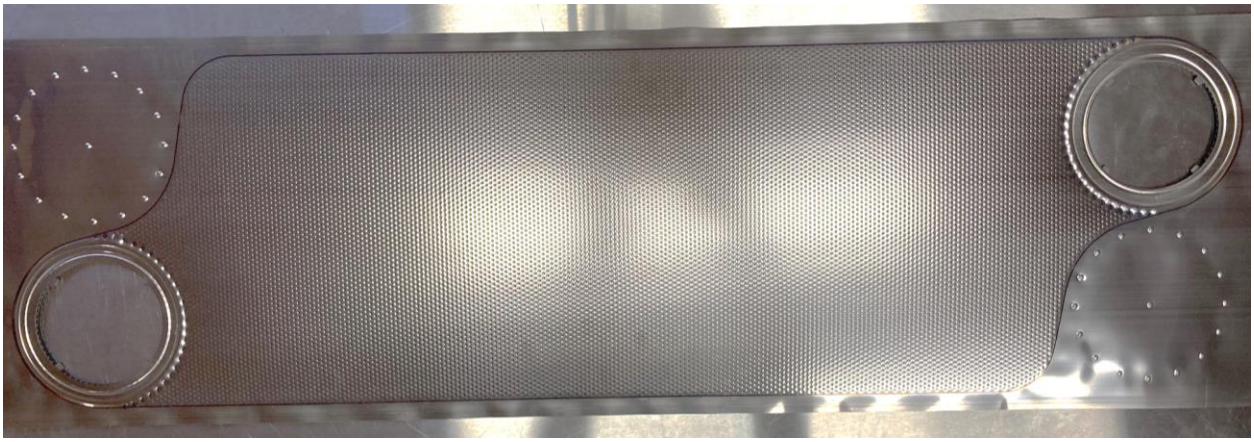

Figure 12. Full-length TFHX plate.

2.5.3. Module Design and Assembly

For applications requiring fully-enclosed heat exchangers, a modular approach leverages economic savings associated with using a standardized plate and heat exchanger design (e.g., tooling, fixtures, and design work) while maintaining the ability to tailor individual TFHX plate designs for the application. The final heat exchanger unit size is also customizable by adding/removing modules to meet the application's flow, pressure drop, and duty requirements.

A module houses 24 full-length TFHX plates and is constructed from two injection-molded Ryton halves that are snap fit together (Figure 13). The housing encapsulates the external fluid during operation. In this manner, the modular TFHX is able to avoid using large gaskets along the perimeter of each plate to seal the external channel that is commonly used in gasketed plate-and-frame heat exchangers while maintaining the ability to disassemble individual plates that is not

possible in welded and brazed heat exchangers. Only one large, perimeter gasket between the two halves of the module housing is required to seal the entire module.

Since the high-pressure fluid is contained in the internal channels where the weld pattern is designed to support the internal pressure, the module pressure rating is decoupled from the high-pressure fluid and determined by the external, low-pressure fluid. Makai has designed the module housing for a pressure rating of 50 psig.

With 24 full-length TFHX plates, each module has 10 m^2 of heat transfer area, provides nominally 125 kW of duty, and weighs 10 kg. The 24-plate size balances customizability, ease of handling, and cost-effectiveness.

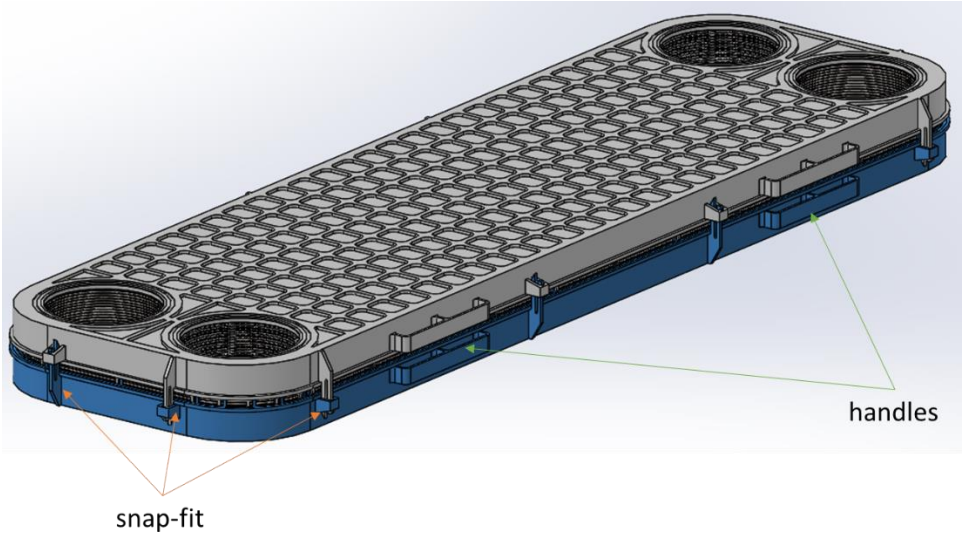

Figure 13. Module housing design.

Module Inspection

Makai received a preliminary run of 8 modules. Two issues were identified upon inspection: 1) "teeth" features used to position the gasket between the module halves were broken off in transit, and 2) the manifold openings (in the long/flow direction) were 1.62mm too far apart.

The first issue was readily resolved with modifications to the shipping crate and module packing.

The second issue does not have a straightforward resolution. The mold can be modified, but it is an expensive correction. It is also impractical to modify the plates to match the manifold spacing in the module because that would require modification to the foil forms and HSWS fixtures. Without a favorable solution, Makai will first determine whether the module will seal to the plates without modification, and then, if necessary, evaluate options for post-fabrication modifications to the module halves.

At least 4 full-length plates are required to perform the module seal test in the stacking station. Makai is awaiting the arrival of additional foil to fabricate plates to conduct the module seal test.

Single-Plate Pressure Tester

The single-plate pressure tester was designed to aid in pressure checking of completed full-length TFHX plates. After a plate is cut, it can be installed in the single-plate pressure tester and pressurized to 150 psig for quality check (Figure 14). The fixture was designed such that as much of the plate as possible is visible to facilitate leak detection.

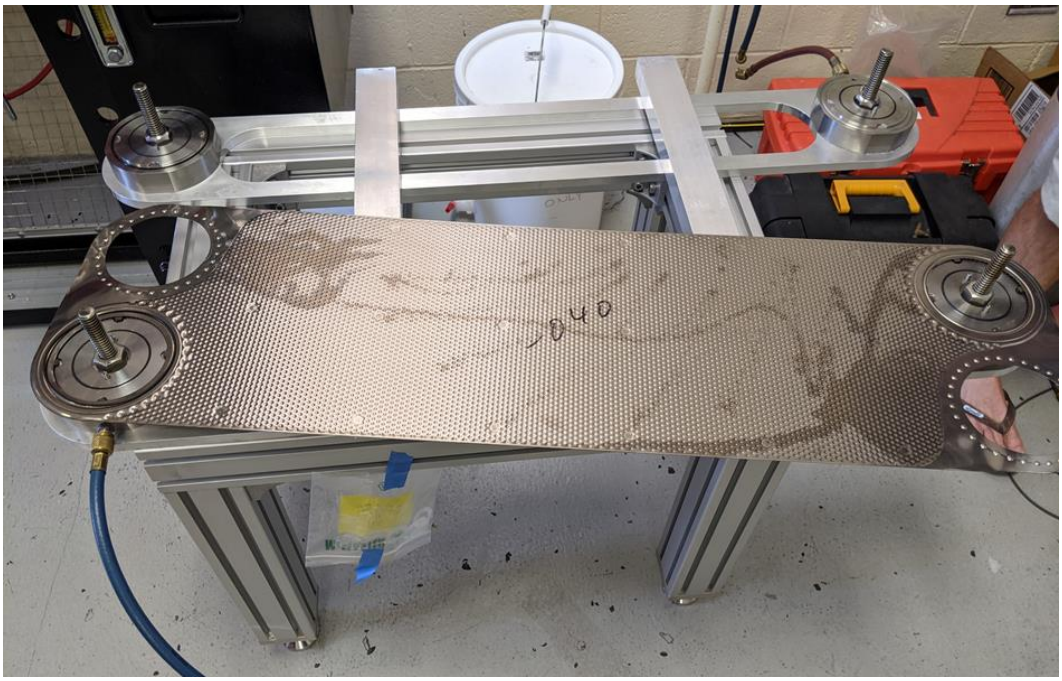

Figure 14. Full-length TFHX plate installed in single plate pressure tester.

Stacking Station

A stacking station was designed for module assembly. A module is assembled by sequentially stacking TFHX plates with gaskets in between plates on top of the bottom half of the module. To ensure sealing, it is crucial that gaskets are placed and remain in position. The stacking station contains guides to ensure plates and gaskets are properly indexed and also enables pressure testing (up to 125 psi) every 2 plates up to the full stack of 24 plates, which allows for early identification of misaligned gaskets or inadvertent damage to plates during the assembly process.

Compression during pressure testing is accomplished using a push plate attached to air cylinders (Figure 15). Two air cylinders are used to provide compressive force during pressure testing and one cylinder is used to retract the push plate after pressure testing is complete. A custom Labview-based program is used to pressurize/hold/vent compressed air to the module and TFHX plates during testing as well as monitor pressure to identify leaks. By incorporating these semi-automated features, Makai's goal is to assemble a module in 2 hours, or 10 minutes per plate pair, including holding time at pressure.

The final assembly, including the external fluid space can also be pressure tested in the stacking station. Once a module is assembled and pressure tested, the module is removed from the stacking station. At this point, the assembly is held together by the snap fit halves of the module housing which do not provide full compression; the manifold gaskets and external channel spacers are

compressed ~10%, which is sufficient to hold the plates and gaskets in place. Complete compression is provided by endplates and tie bars once a complete unit is assembled.

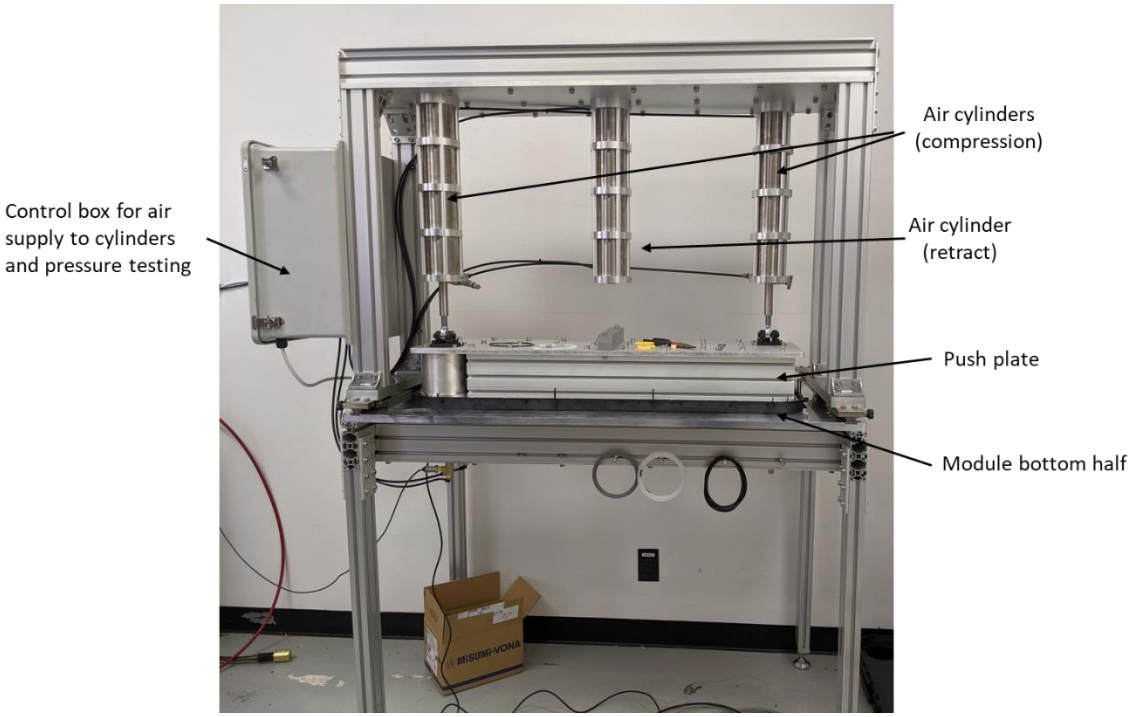

Figure 15. Stacking station with push plate lowered, ready to pressure test a pair of plates.

2.5.4. Complete HX

Multiple modules are stacked together to form a heat exchanger unit. The number of modules that can be stacked in a unit depends on the flow rate and pressure drop allowances; up to 16 modules can be stacked together to form a nominally 2 MW heat exchanger unit with 160 m^2 of heat transfer area. Module-to-module sealing is accomplished using gaskets at the manifold interfaces. Endplates and tie bars are used to provide complete compression of plate-to-plate gaskets (within a module), module perimeter gaskets (one per module), and module-to-module gaskets (four per module). The use of endplates and tie bars is similar in appearance to conventional gasketed plate-and-frame heat exchangers, however, in the TFHX, the endplates and tie bars are rated to support gasket compression and external fluid pressure and are not required to handle the high pressure of the internal fluid.

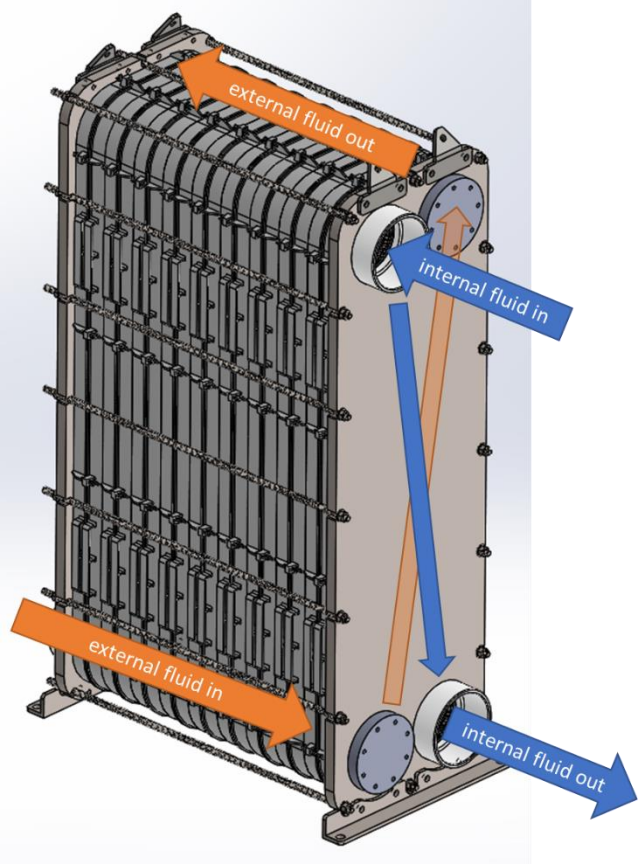

Figure 16. TFHX unit with 9 modules stacked together. The internal and external fluid connections are on opposite endplates.

2.5.5. Status of Full-Length TFHX Plate Production

In this period, Makai was unable to produce a complete module for performance testing. After resolving issues with micro-cracks in the delivered foil and troubleshooting weld parameters on the HSWS, not enough foil was left for a complete module. An additional order of 0.005" foil was placed and Makai will resume full-length fabrication once foil arrives.

3. TFHX FABRICATION

In this period, Makai's efforts were directed at transferring the successful, reliable production of TFHX plates on the stage to a semi-automated process on the High-Speed Welding Station (HSWS). The HSWS has the potential to reduce production time by 10X and is an important stepping to making the TFHX cost-competitive. Makai continues to methodically resolve issues that arise and further our expertise in the nuances of each step of TFHX fabrication.

4. ECONOMIC ANALYSIS

There are two broad categories in heat exchanger design, pass-through vs. 4-port. In a pass-through design, the external fluid is not contained within the heat exchanger; the heat exchanger is immersed in the external fluid. Makai previously installed a pass-thru TFHX unit at Cyanotech and has been working on pass-through TFHXs that use air as the coolant. In contrast, in a 4-port design, the external fluid must be encapsulated within a housing and ducted to and from the heat exchanger. Makai's full-length modules address applications which require the 4-port design.

Individual TFHX plate fabrication is the same for both types of heat exchangers. Both 4-port and pass-through heat exchangers also require header and follower plates to provide gasket compression to seal the internal channels, but the 4-port design requires additional module housing components to contain the external fluid (see module discussion in Section 2.5.3).

As Makai continues to advance the TFHX technology and approaches commercialization, housing and assembly costs, not just TFHX plate production costs, have been added to the economic analysis. Previous versions did not account for these added costs or include capital required to invest in equipment (fixturing, molds, etc.).

Production times used in this economic analysis are based on the full-length TFHX plates produced on the HSWS during testing and commissioning. Currently, it takes approximately 17.5 minutes to fabricate a full-length TFHX plate (0.43 m^2 of heat transfer area); active welding time is around 12.5 minutes, with the pattern weld requiring 10.5 minutes.

Although higher pressure ratings can be achieved with large circle welds, spot welds can be performed faster and are preferred if the pressure rating requirement can be met. Makai expects to further reduce the pattern weld time to under 1 minute. This means a full-length plate can be welded in 2.6 minutes, reducing the overall plate fabrication time by almost 10 minutes (from 17.5 to 7.6 minutes). The faster weld time not only increases productivity, but substantially reduces the shield gas cost by (nearly) a factor of 5, from \$31.80/m^2 to \$6.67/m^2 (Figure 17).

Even at current fabrication times and added cost housing/assembly/capital costs, Makai continues to improve the economics of the TFHX (Figure 18). In terms of fabrication time, a TFHX-3B plate had 0.58 m^2 of heat transfer area and required 374 minutes to fabricate. A TFHX-3C plate has 0.21 m^2 of heat transfer area and requires 120.5 minutes to fabricate. A mid-length TFHX-3E plate had 0.2 m^2 of heat transfer area and required 25 min to fabricate. A full-length TFHX plate has 0.43 m^2 of heat transfer area and currently takes 17.5 minutes to fabricate but is expected to require only 7.6 minutes to fabricate in the near future. With the HSWS, more than double the area can be fabricated in less than 1/3 of the time. Material selection also affects economics. At current fabrication times, a plate made from 0.002" SS316L is \$512/m^2 compared to \$679/m^2 using 0.005" Ti, a reduction of 25%.

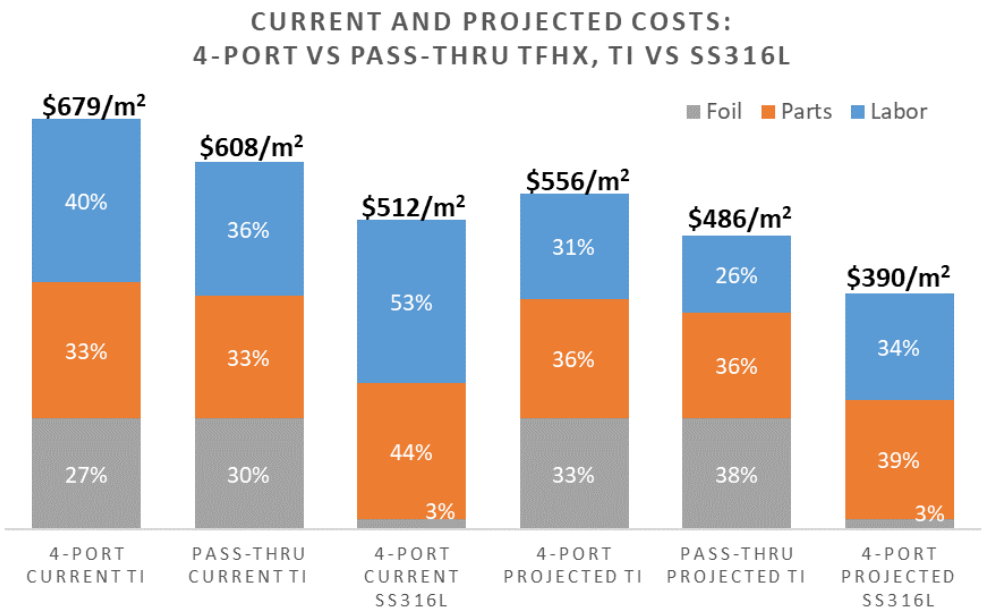

Figure 17. Current vs projected costs for 4-port and pass-through TFHX designs.

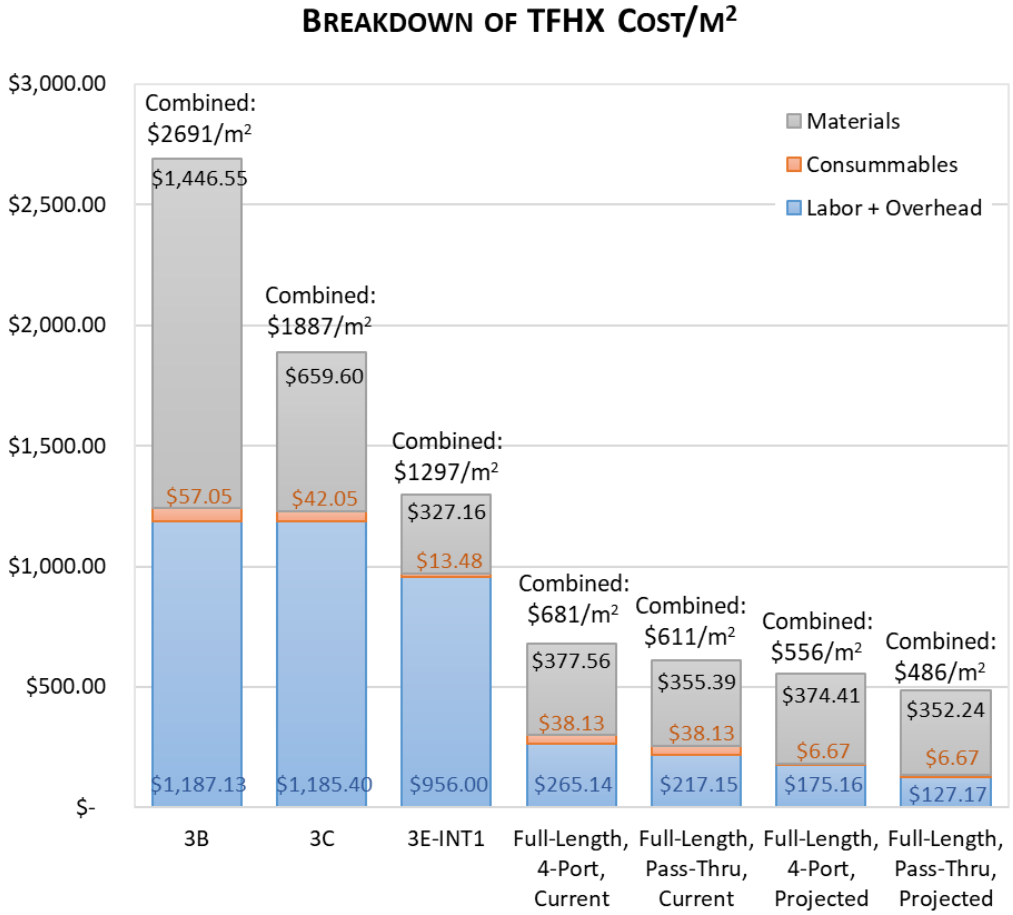

Figure 18. Makai continues to improve TFHX economic outlook. Current, non-optimized fabrication rates represent nearly 50% reduction in previous 3E-INT cost/m².

5. TFHX CHARACTERIZATION

Makai continues to compile a comprehensive database of empirical measurements to characterize the TFHX's geometric and mechanical properties; these data are intended to be incorporated in a design tool used to drive TFHX design decisions for future applications and provide foundational data for expected operational limits and service life.

Laser welding of thin foils is a critical component of the TFHX technology. Makai continues to further our research and understanding of the parameters that affect the strength and durability of the weld, and ultimately, the TFHX. In this period, Makai expanded the capabilities of the laser welding system and added polishing and optical microscopy to our analysis tools to characterize the effects of changes in weld parameters are reflected in the weld microstructure. Makai also expanded the geometric and mechanical testing database and performed initial durability testing under environmental exposure.

5.1. LASER WELDING PARAMETERS

Weld parameters affect the size, strength, and reliability of the weld. A single TFHX plate can have over 10,000 welds; it is crucial that weld parameters are chosen such the weld success rate is > 99.999%. In addition, for a cost-effective TFHX, weld parameters must also be selected with fabrication speed in mind.

Once appropriate weld parameters are identified, static and cyclic pressure testing and comparison of fabrication time can be used to determine the best set of parameters. Makai has also invested in optical microscopy (and associated equipment to mount and polish samples) as another method to assess weld quality. Makai previously sent out specific samples for processing and imaging which provided valuable insight into weld grain structure, weld penetration depth, heat affected zone, and geometry features (Figure 19 and Figure 20).

An example of a good weld is shown in Figure 19. The weld appears to fully and evenly extend through the bottom foil thickness, i.e., at the weld location, both pieces of foil appear as one homogenous component with similarly distributed grains. There are no pockets or gaps in the weld and the weld surface is smooth, without divots or undercut areas. The grain structure of the weld and heat affected zone are visibly different (larger) than the initial titanium foil.

Microscopy can also provide insight into the fabrication process and fatigue life. In Figure 20, a fabricated sample is examined under microscopy to confirm the process used to form the internal channels does not introduce cracks. A post-fatigue testing sample indicates fatigue failure is a result of crack initiation and propagation. One method to extend fatigue life is to reduce stress concentration site. In the post-fabrication sample of Figure 20, the radius of the weld joint appears non-uniform; the left channel is more rounded at the weld joint whereas the right channel is more pointed at the weld joint. The weld joint with the smaller radius will have a higher stress concentration.

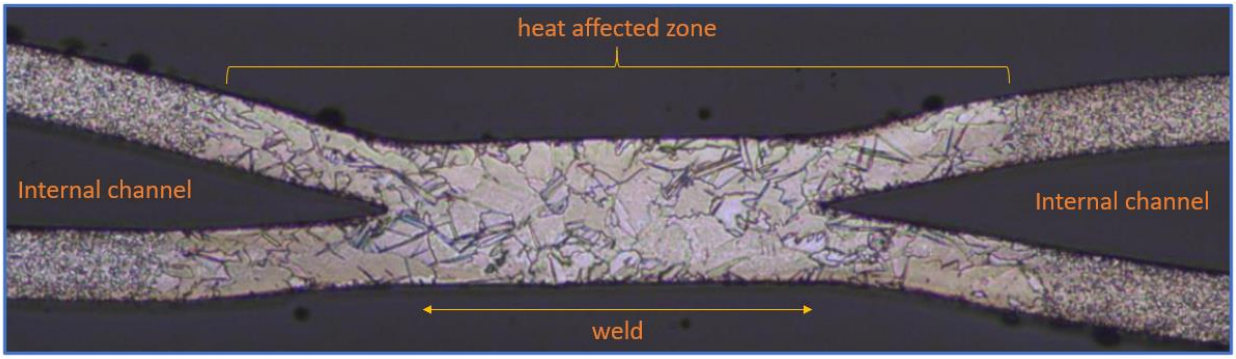

Figure 19. Optical microscopy of cross section of a weld. The TFHX diagram shows the area of the image for reference.

Makai suspects, and will verify, that the differences in burst pressure and fatigue life can be explained by differences microstructure within the weld and heat affected zone and presence/absence of post-forming stress concentration areas (i.e., sharp or blunt radii at the weld joint) produced by the different combinations of weld parameters.

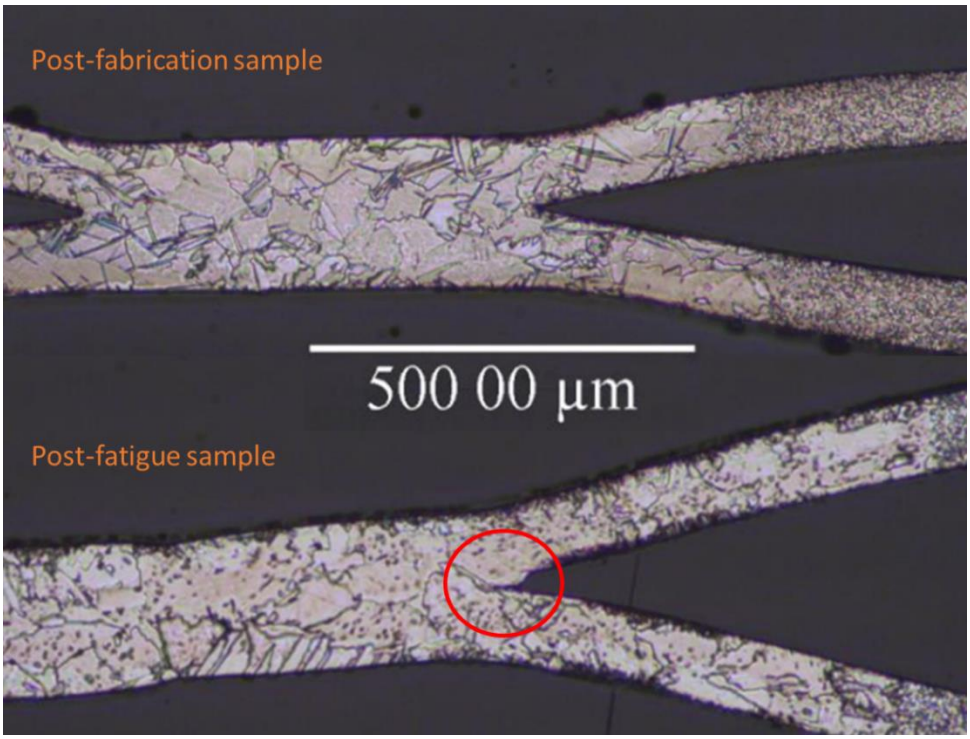

Figure 20. Images of post-fabrication and post-cyclic testing weld joints. A small crack appears to be present in the post-fatigue sample.

Makai plans to systematically identify the optimal combination of weld parameters for each material and foil thickness. The short-length platform is well-suited for this development effort, since plates can be made entirely in-house and each plates uses substantially less foil than other TFHX platforms.

5.2. GEOMETRIC CHARACTERIZATION

With geometric characterization, the goal is to establish the design parameters – material, foil thickness, weld diameter, and weld spacing – required to create a specific channel size and shape. The optimal weld parameters are unique to each material and foil thickness and will be identified first, prior to detailed geometric characterization. The TFHX internal channel shape is ellipsoid in one direction and saddle shaped in another direction. Makai has defined the following terminology used to characterize the internal channel (Figure 21):

- Weld diameter – the diameter of the weld
- Weld spacing – the distance from weld center to weld center
- A-A height – the height of the saddle
- B-B height – the maximum height of the internal passage

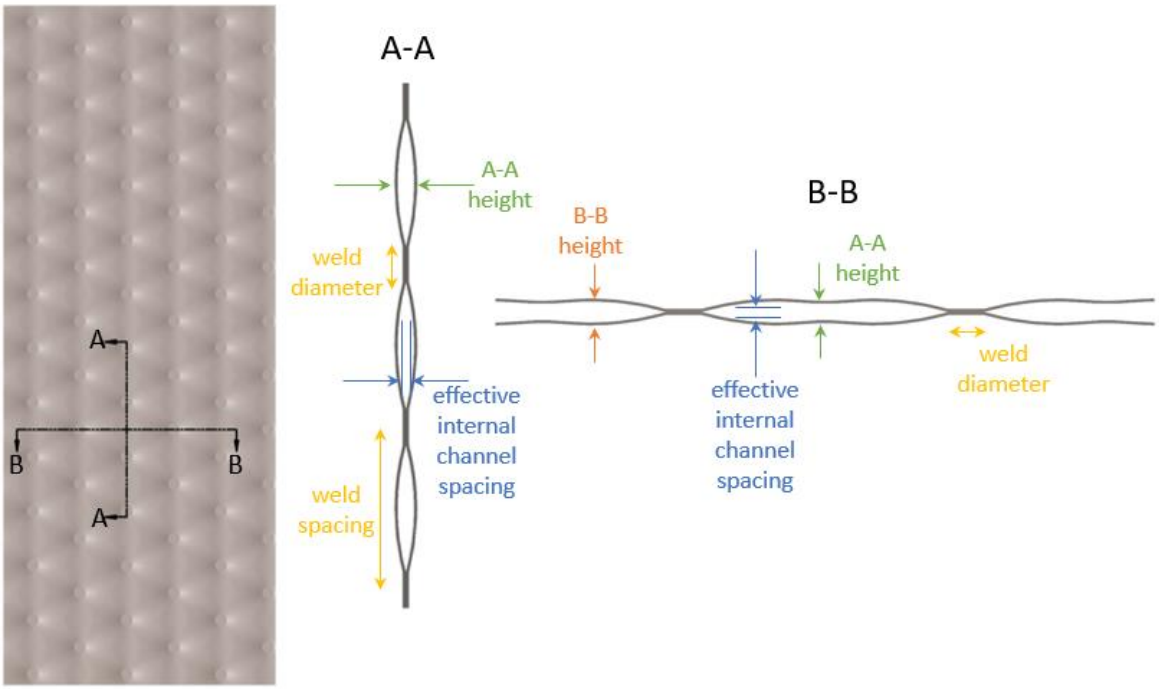

Figure 21. Schematic of geometric definitions.

- Effective internal channel spacing – the effective channel spacing is calculated by finding the internal volume of a hexagonal area outlined by the centers of the six nearest welds surrounding a single weld (in the main heat transfer region) and dividing it by the surface area. Volume is calculated from height measurements taken by scanning the surface with a profilometer. Surface area is the two-dimensional hexagonal area minus the weld area, it does not account for any increase in surface area due to curvature.

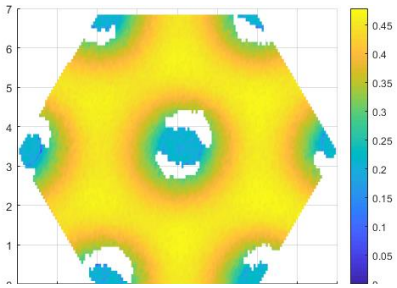

Figure 22. Hexagonal area used to calculate effective internal channel spacing.

To date, geometric characterization has focused on how the effective internal channel spacing is affected by foil thickness, weld spacing, and expansion pressure. Preliminary studies indicate the foil thickness, weld spacing, and expansion pressure are still the primary variables that affect the effective internal channel size; larger weld diameters do not impact the internal channel spacing *as long as the weld diameter is less than 50% of the weld spacing*.

The effective internal channel spacing variation with expansion pressure for weld spacings between 3 mm to 10 mm and titanium foil thicknesses of 0.003”, 0.004”, and 0.005” is shown in Figure 23. Smaller weld spacings, lower expansion pressures, and thicker foil produced smaller effective spacings. The effective spacing is measured at several different locations for each plate and averaged. For some combinations of plate type and expansion pressures there is significant variability in the effective channel spacing within a single plate. This variability is attributed to the way the effective spacing is measured; if the plate is not flat (parallel) to the plane of measurement or if the surface angle of the channel is too steep (e.g., at the edge of a weld), the profilometer measurements will be biased.

Although lower effective heights can be achieved with lower expansion pressures, insufficient expansion pressures (e.g., <85% of supported burst) result in deformation of the channel during operation. This is undesirable because it affects performance and shortens fatigue life. Makai’s design approach is to change the weld spacing and weld diameter to change the effective height. In this manner, for the same foil thickness and weld spacing, a larger weld increases the supported burst pressure and indirectly increases the achievable effective internal channel size by increasing the expansion pressure.

Makai has been able to use previously collected data to reasonably estimate the required weld spacing to produce a specified effective channel spacing; however, Makai anticipates another round of characterization for the additional weld diameters.

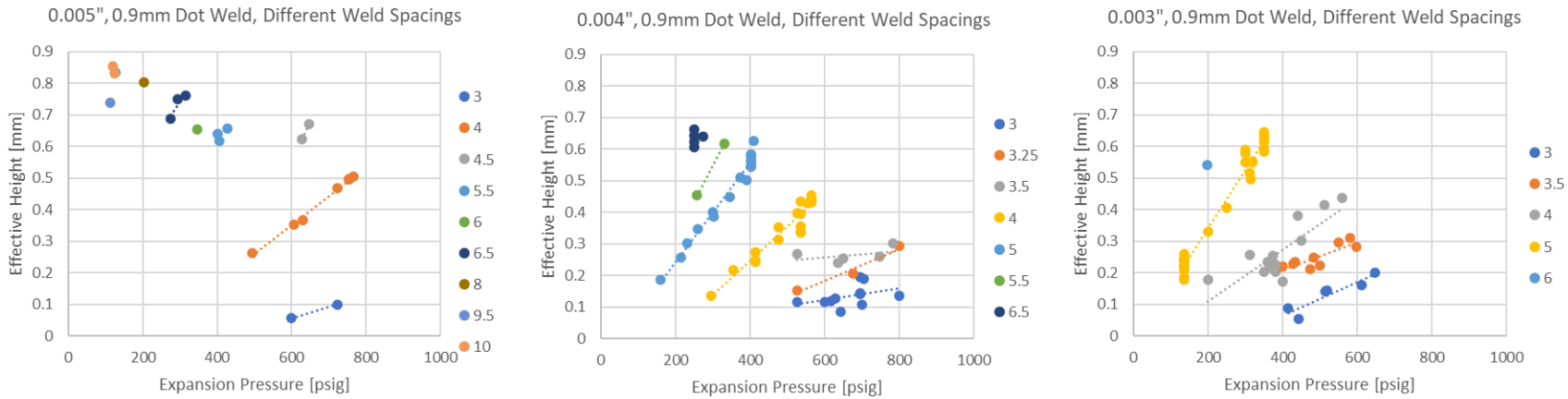

Figure 23. Average effective internal channel spacing for titanium foil using dot welds depends on foil thickness, weld spacing, and expansion pressure. Smaller spacings, lower expansion pressures, and thicker foils lead to smaller channel spacings.

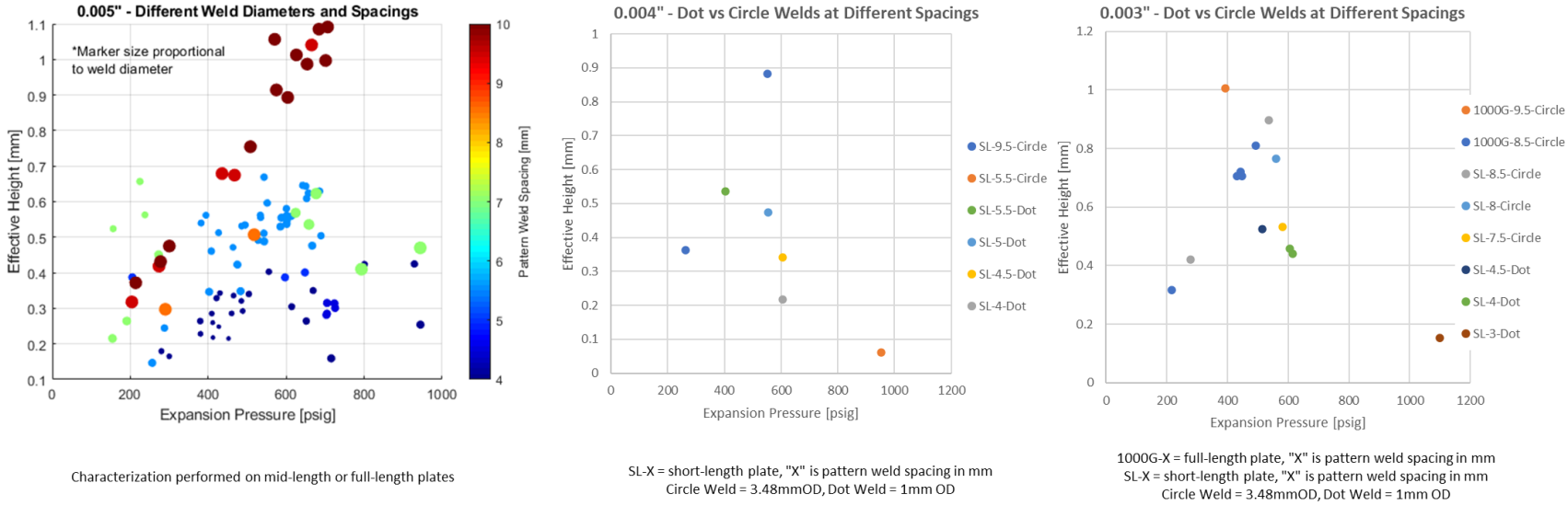

Figure 24. Effect of weld diameter, weld spacing, and expansion pressure on effective channel height.

5.3. MECHANICAL CHARACTERIZATION

Makai previously reported variations in supported burst pressures associated with the overall TFHX shape. Asymmetrical plates with sharp angles likely introduced stress concentration zones that resulted in lower supported burst pressures. Limited data suggests the supported burst pressures of the short-length plates are comparable to that of mid-length or full-length plates with the same design (Figure 26). Some issues with weld reliability on the full-length plates make the preliminary data inconclusive. Makai intends to perform rapid prototyping to identify the weld parameters using short-length plates and will recheck channel heights and burst pressures for each actual plate shape/size.

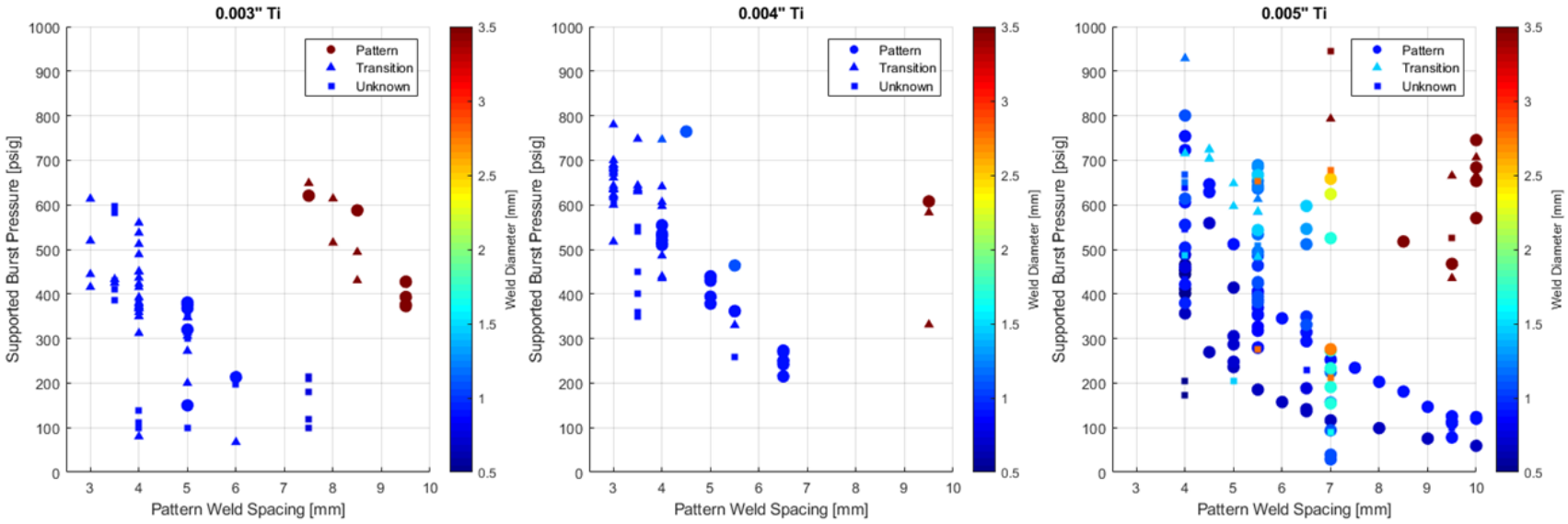

Figure 25. Supported burst pressure dependence on weld spacing, weld diameter, and foil thickness.

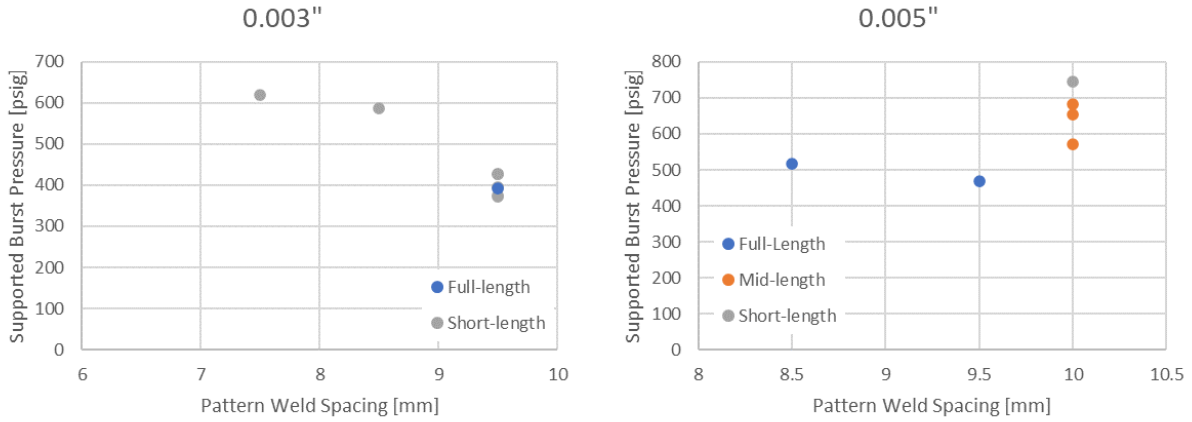

Figure 26. Supported burst pressure for the same pattern weld at different plate shapes/sizes.

In the unsupported test, a fabricated plate (with the excess foil removed) is placed into a single-plate pressure tester in which only the manifolds are clamped (to provide the seal for pressurization with compressed air). The plate is then pressurized until failure. The unsupported burst pressure test is used to establish the pressure rating of a TFHX plate. Pressurization in the unsupported burst test is representative of loading in an operational TFHX heat exchanger where each individual TFHX plate meets the pressure rating and external support is provided only to compress the o-rings used to seal the internal from the external passages.

Unsupported burst pressure testing has only been conducted on a few samples and the results are so far inconclusive (Figure 27). As expected, thinner foil, smaller weld diameters, and larger weld spacings lead to lower overall burst pressure. Additional testing is recommended before drawing conclusions on the relationship between expansion pressure (i.e., whether the 85-95% range leads to variability) and the overall plate shape on unsupported burst pressure.

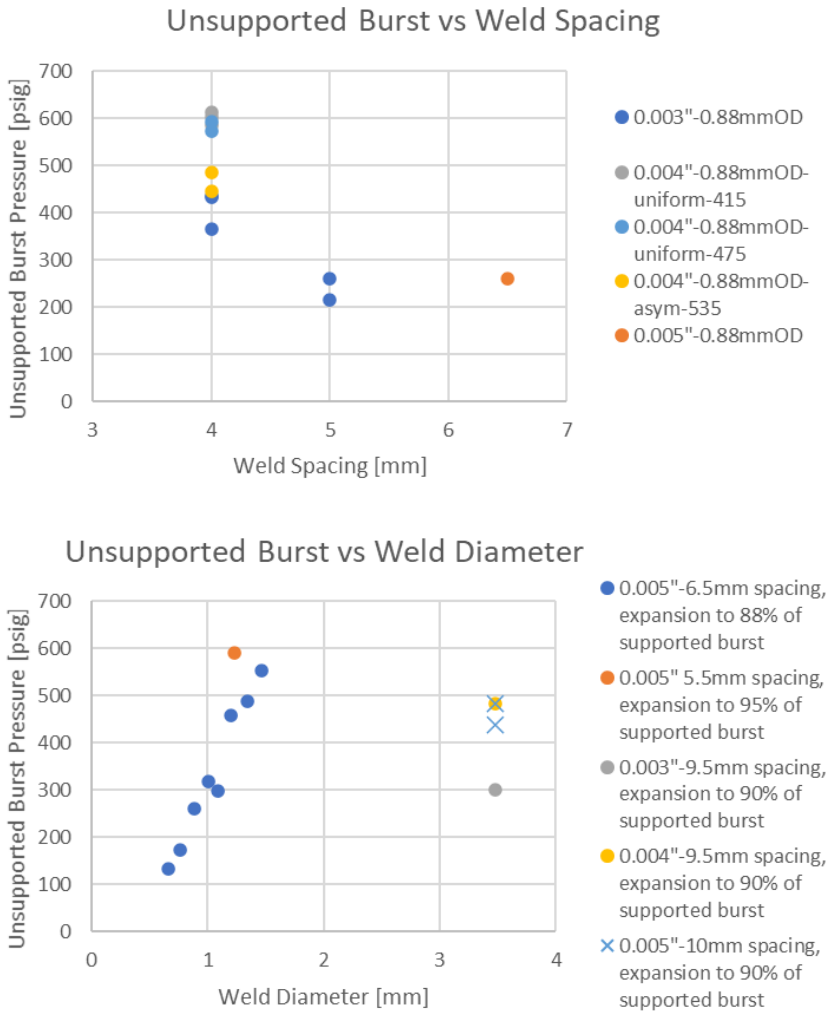

Figure 27. Unsupported burst pressures for varying foil thicknesses, weld diameters, and weld spacings.

5.3.2. Cyclic Pressure Testing

Initially, fatigue testing used high pressure compressed air from a cylinder to pressurize a water-filled TFHX plate. A regulator controlled the pressure amplitude and a solenoid valve controlled the cycling time. This initial test setup was inefficient because the compressed air cylinders would have to be replaced daily. A revised design used linear motors to provide the pressure cycling. The amplitude of cycling can be set by changing the stroke length. Twelve plates can be simultaneously tested in the revised fatigue testing apparatus.

In this period, Makai further modified the fatigue testing apparatus such that one slot is capable of high pressure cycling, 0-200 psig, (Figure 28) and testing representative TFHX plate shapes/sizes.

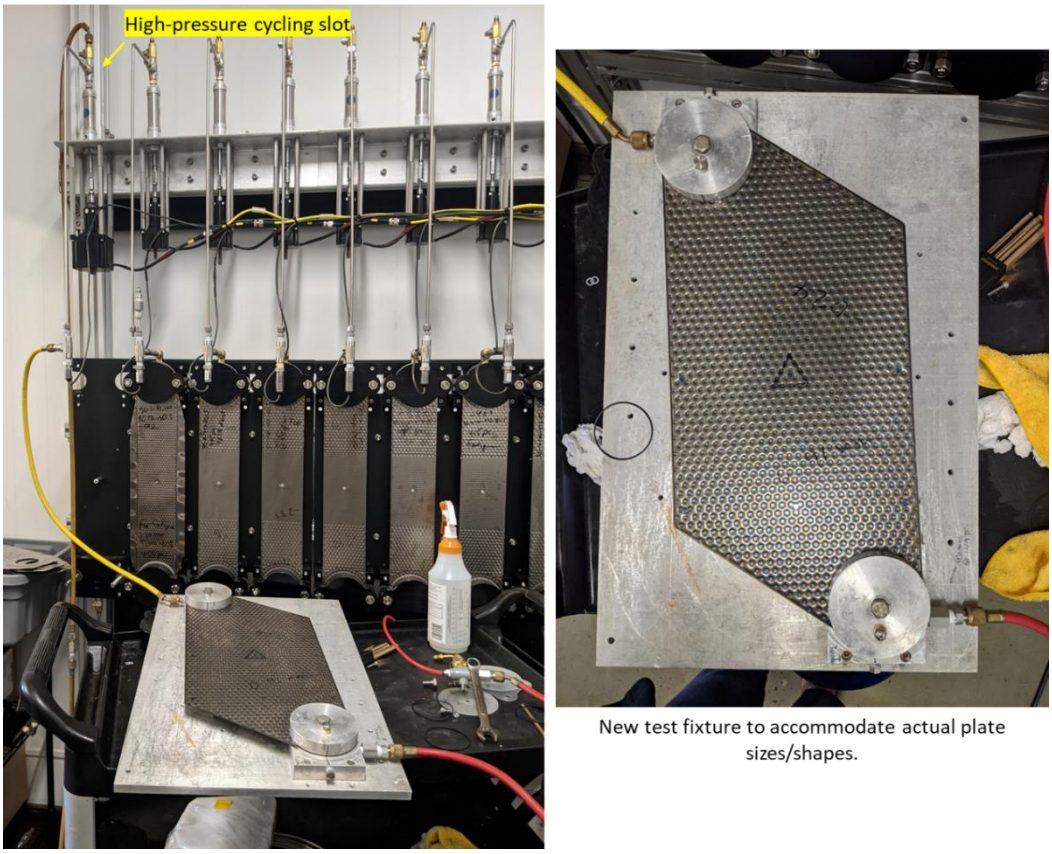

Figure 28. Revised fatigue testing apparatus. Twelve plates can be (independently) tested simultaneously.

In previously reported fatigue testing results, pressure was cycled between expected application pressures (e.g., for OTEC, 0-120 psig to replicate start-up/shut-down cycles and 60-120 psig to replicate operating pressures). A standardized plate (100 mm wide by 596 mm long) with 3E-style manifolds was designed for fatigue testing. The majority of testing was performed with a 0.88-mm OD weld at 4 mm pattern spacing with 0.003” and 0.004” titanium foil. Variations in expansion pressure and cycle pressure were studied. The effect of increasing pattern spacing to 5 mm was also investigated. Preliminary results suggested fatigue life is extended by reducing the alternating pressure and for the same alternating pressure, increasing the expansion pressure, reducing the pattern spacing, and increasing the foil thickness extends fatigue life (Figure 29).

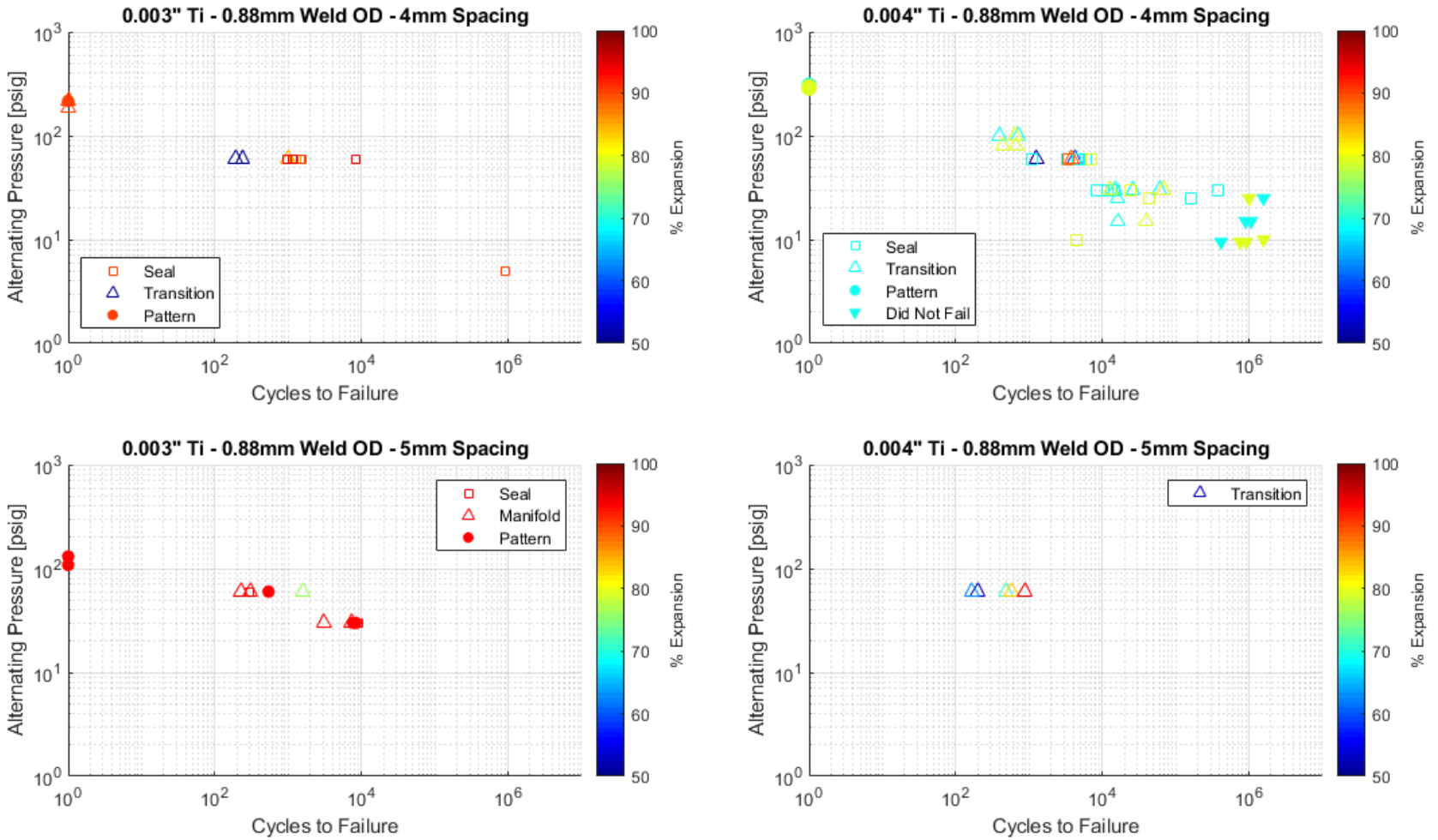

Figure 29. Preliminary testing fatigue testing using 100-mm wide standardized plates. Alternating pressure, expansion pressure, pattern weld spacing, and foil thickness affect fatigue performance.

Based on previous testing, Makai suspects fatigue life may be predicted as a percentage of the unsupported burst pressure. This hypothesis will be explored by testing at various percentages of the unsupported burst pressure in an attempt to identify common trends, e.g., for all designs, if the alternating pressure is 10% of the unsupported burst pressure, the sample will last 10^6 cycles.

In previous tests, most fatigue failures occurred at the seal or transition welds and the supported and unsupported bursts also occurred at transition welds. While all aspects of a TFHX plate must meet the required pressure rating and fatigue life requirements, failures at the transition or seal weld are not necessarily an accurate reflection of TFHX durability. The pattern weld drives TFHX thermal and hydraulic performance and, if practicable, should also be the limiting factor in durability performance, i.e., the transition and seal welds should be modified to be stronger than the pattern weld. This may not be practical if the seal weld cannot be reliably welded in the required location or if the transition zone ends up being more restrictive than the pattern zone.

In the latest round of fatigue testing, Makai tested the 3E-style, mid-length TFHX plates after they were used in seawater-seawater performance testing. For the two plate designs (Table 1) tested, pressure was cycled between 0 psig and a maximum pressure that was 15-40% of the unsupported burst pressure (Figure 30).

Table 1. Summary of plate designs used in fatigue testing.

Design	A	B
Weld Diameter [mm]	1.23	3.48
Weld Spacing [mm]	5.5	9.5
Supported Burst Pressure [psig]	660	668
Expansion Pressure [psig]	650	570
Unsupported Burst Pressure [psig]	590	483

For both designs, supported and unsupported bursts occurred at pattern welds. Fatigue failure locations occurred at the seal, transition, and pattern welds; however, in some tests, failure locations could not be definitively identified. Makai suspects some failures are not due to cracks in the foil but rather wear in the o-ring groove interface of the caps on the test fixture. Furthermore, it was difficult to identify any failures under the test fixture cap, which includes portions of the seal weld and transition welds. These unclear failure locations (and whether or not the plate actually failed) have been labelled as “other” in the results. The fatigue test fixture has been modified with more durable stainless steel caps for pressure testing and clear caps that can be used at lower pressures to aid in identifying the failure location.

One additional consideration must be mentioned while evaluating this set of fatigue data. The weld parameters were chosen to produce plates with an effective channel height and minimum expansion pressure in mind. The plate success rate for both designs was ~75%. It is possible fatigue performance will improve when similar designs are tested with optimum weld parameters.

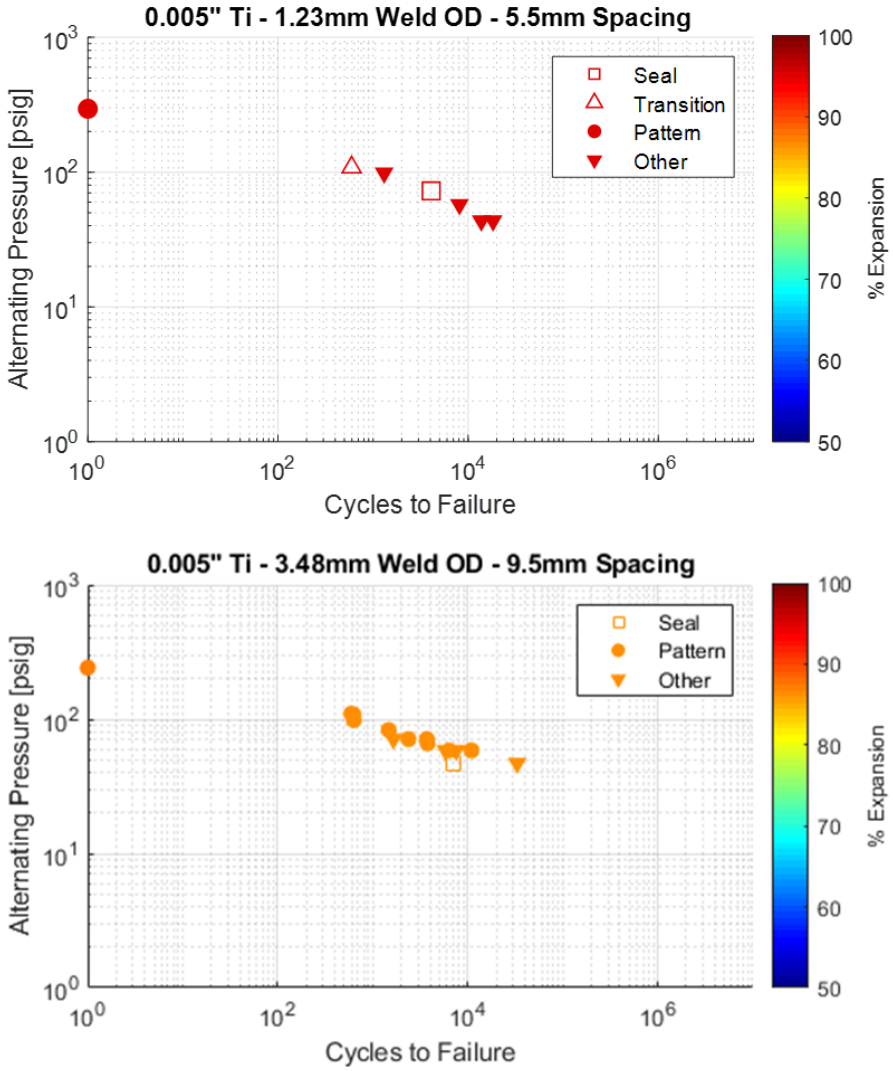

Figure 30. Fatigue testing of two plate designs.

Makai previously concluded an exhaustive set of fatigue data on uniform plates is impractical, unlikely to be representative of a custom plate design, and may inadvertently bias design decisions. While the most reliable and representative data test the final plate design under applicable loading conditions, Makai will continue to fabricate and test sets of plates to determine if fatigue life can be estimated as a percentage of unsupported burst pressure.

5.4. ENVIRONMENTAL EXPOSURE TESTING

In addition to durability under pressure cycling conditions, the TFHX must also perform under various environmental conditions. Makai conducted two environmental exposure tests: a high pressure water spray, which simulates cleaning operations, and a sand exposure test, which simulates the operating environment of air-water heat exchangers.

5.4.1. High-Pressure Water Spray

Makai conducted high-pressure water spray tests on two different TFHX units. The first test was conducted on TFHX-3C-3, after completion of a biofouling test. The spray test also provided some feedback on cleaning methods. The second test was conducted on a stack of 24 smaller plates. For both tests, the unit was pressure checked before testing to verify the internal channels were sealed and the plates were intact.

In the first test, a high pressure water spray was directed at the inlet face. The nozzle was held about 4" from the inlet of the plates. No damage was observed post-cleaning.

Figure 31. TFHX plates after water nozzle test.

In the second test, the inlet and outlet faces were sprayed using a 15° nozzle attached to a pressure washer for 30-60 seconds per face (Figure 32). Visual inspection of the inlet face showed no discernable change after the water nozzle spray (Figure 33). The unit was then re-pressurized to 150 psig for 1 hour to verify the integrity of the internal passages and air dP vs flow was re-measured. There were no leaks and also no significant difference in dP vs flow (Figure 34). The high pressure water spray neither damaged the integrity of the plates nor had a significant effect on the air passages.

Figure 32. Water spray test setup.

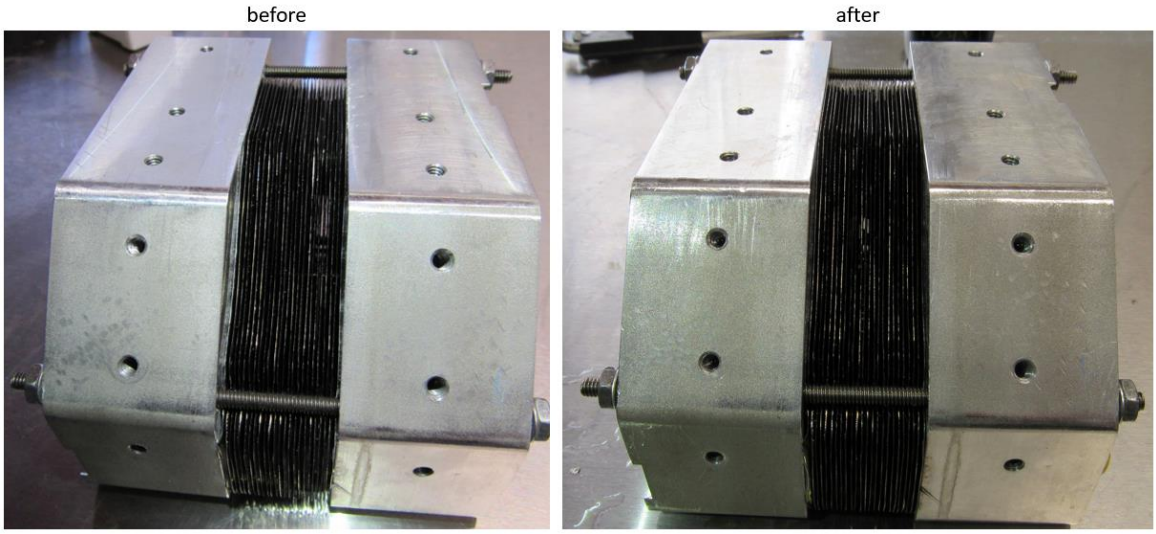

Figure 33. No discernable differences identified by visual inspection of inlet face before and after high-pressure water spray.

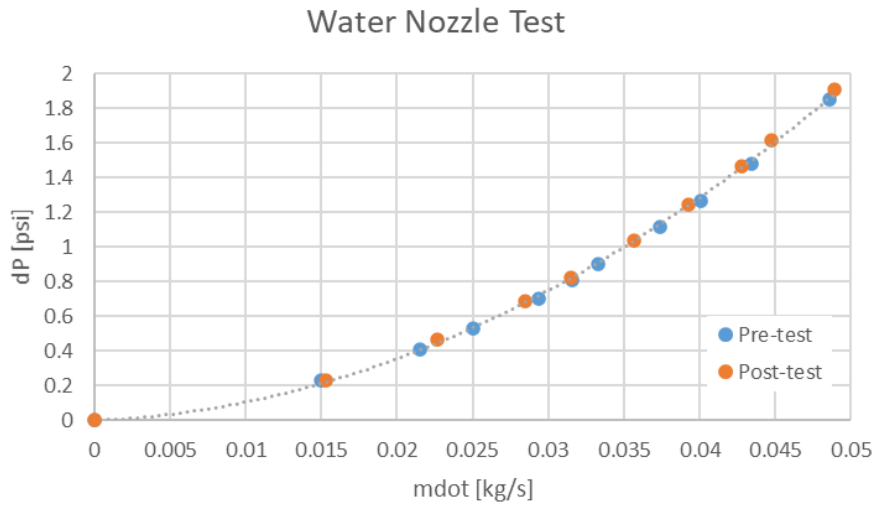

Figure 34. Pre and post water nozzle test air dP vs flow. No significant changes in dP indicate the TFHX plates and air passages were unaffected by the high pressure water spray.

5.4.2. Sand Exposure

A separate 24-plate TFHX unit was subjected to a sand exposure test, where an air/sand mixture was blown into the unit for 2 hours. As expected, sand particles that were larger than the external channel size were caught in the unit and increased the pressure drop by up to 40% (Figure 35). However, internal pressure checks performed before and after the test verified the plates were not damaged due to sand abrasion or erosion.

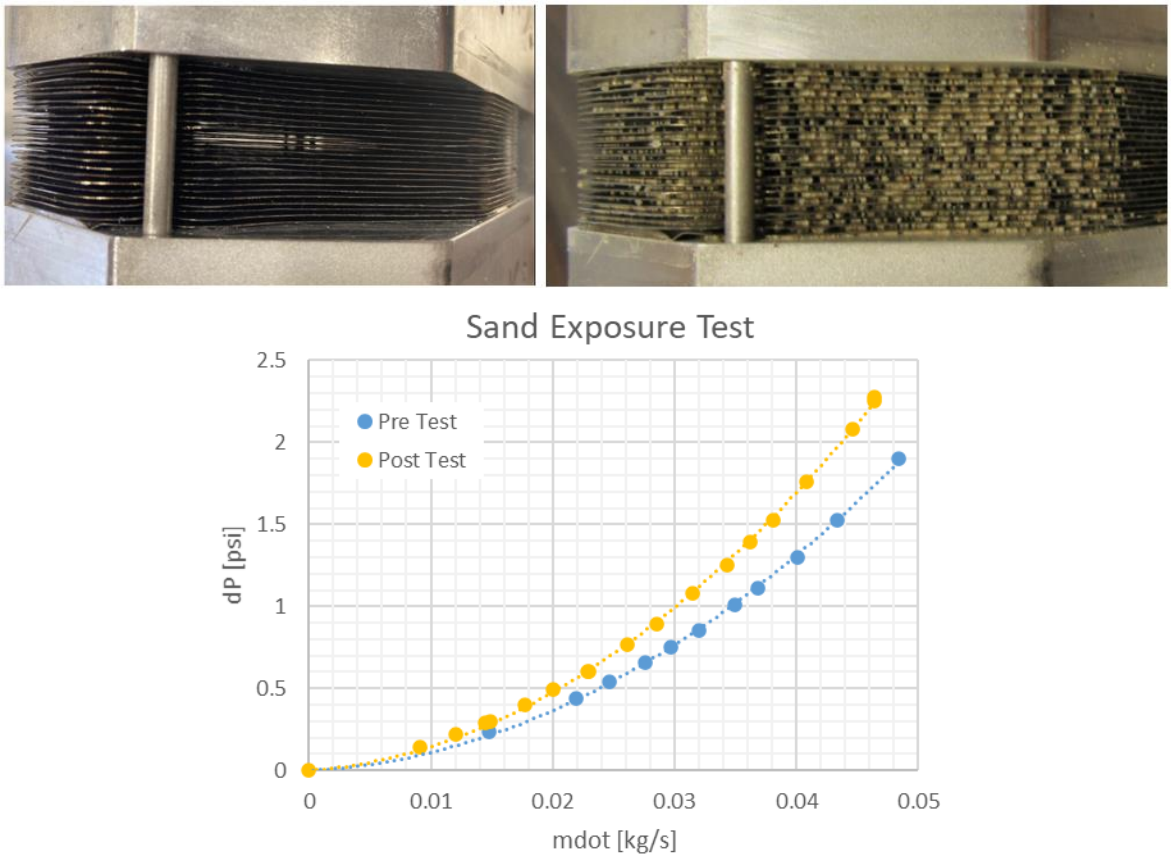

Figure 35. (top) Inlet edge of test unit before (left) and after (right) sand exposure test. (bottom) For the same mass flow rate, pressure drop increased 30-40% after sand exposure test.

6. TFHX PERFORMANCE TESTING

In this period, Makai designed, built, and tested 7 counterflow seawater-seawater and 11 crossflow air-water TFHX configurations. Makai also performed a case study for a desalination project. In preparation for future full-length, counterflow, seawater-seawater and ammonia-seawater testing, Makai also completed modifications to the 100 kW Test Station.

6.1. 100-KW TEST STATION MODIFICATIONS

Makai completed modifications to the 100 kW Test Station in preparation for ammonia-seawater and seawater-seawater full-length module performance testing. Ammonia-seawater testing will occupy the old 3B test station and seawater-seawater testing will occupy the old seawater-seawater test station.

A single module (24 full-length TFHX plates) will be tested first as an ammonia-seawater condenser and evaporator and then as a seawater-seawater heat exchanger. Makai has plans to test 3 or 4 modules with different TFHX plate designs. To facilitate easy installation and removal, an interface plate is mounted in place at each test station. The interface plate remains installed as part of the 100 kW Test Station and contains connections to seawater and ammonia piping. Modules will be installed to the interface plate and clamped using a follower plate and threaded rods and nuts. This configuration mimics the header and follower plate in a functional TFHX unit.

For the new ammonia-seawater test station, seawater piping was modified to accommodate the height of the module and to enable counterflow testing in both evaporator and condenser configurations. A new section of ammonia piping was also installed.

Figure 36. Ammonia-seawater test station modified for full-length module testing.

For the new seawater-seawater test station, seawater piping was modified to accommodate the height of the module (Figure 37). Seawater testing will only be conducted in the counterflow orientation and use cold seawater as the internal fluid and warm seawater as the external fluid.

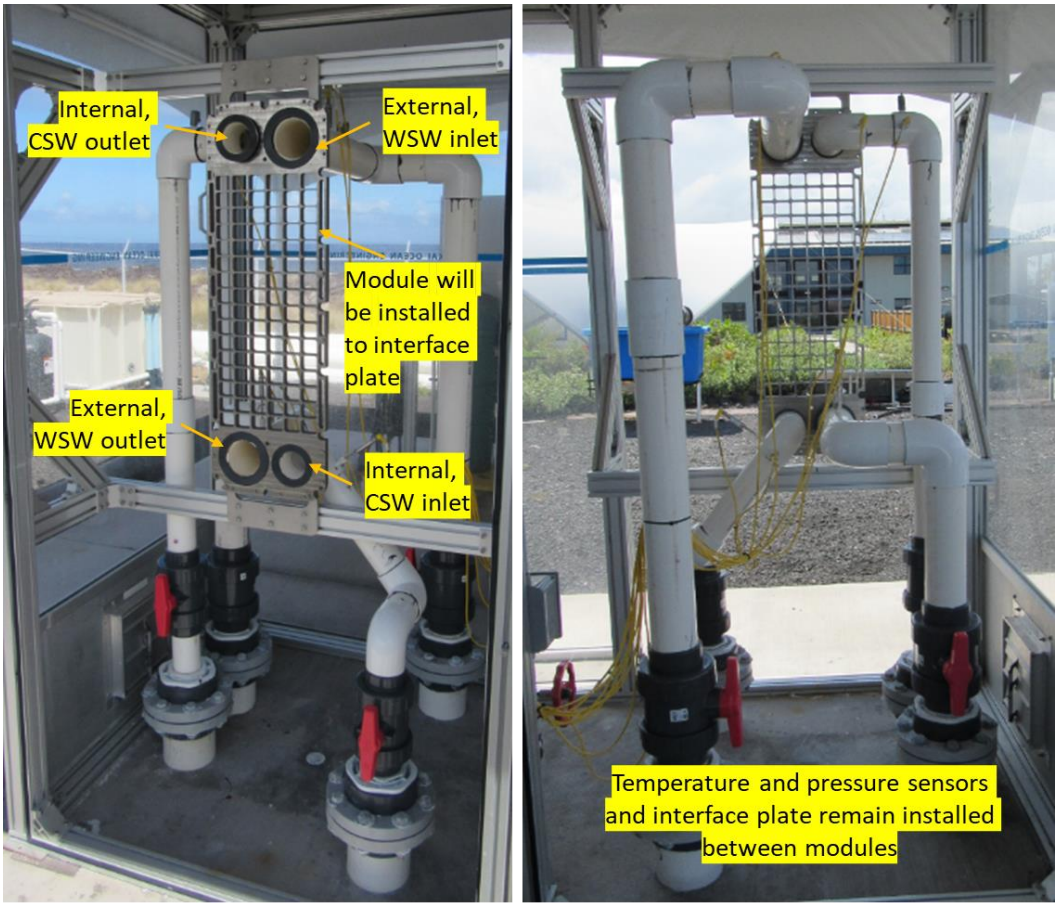

Figure 37. Seawater-seawater test station modified for full-length module testing.

The existing control program and instrumentation will be used for data collection. Temperature and pressure sensors were calibrated in June 2021 prior to re-installation. A new revision to the control program was completed to accommodate counterflow and parallel flow configurations during ammonia-seawater testing.

6.2. SEAWATER-SEAWATER TESTING

In this period, Makai built and tested 7 TFHX designs in a counterflow seawater-seawater configuration (Table 2). The heat exchanger units were mid-length, 3E-style,460-mm manifold center-to-center distance. A mid-length TFHX test housing was designed with the ability to interlock (12 plates for 2-mm plate spacing and 24 plates for 1-mm plate spacing, Figure 38).

The purpose of this testing is to determine convective coefficients to use in future TFHX designs and to provide a baseline for comparison with full-length, modular TFHX testing.

Table 2. Summary of seawater-seawater test units.

Configuration	Plate Spacing [mm]	Foil Thickness ["]	Internal Effective Channel [mm]	External Effective Channel [mm]	Internal Fluid Length [m]
1	1	0.004	0.25	0.55	0.46
2	1	0.005	0.37	0.44	0.46
3	2	0.004	0.25	1.55	0.46
4	2	0.005	0.37	1.44	0.46
5	2	0.003	0.55	1.36	0.46
6	2	0.005	0.62	1.18	0.46
7	2	0.005	0.91	0.90	0.46

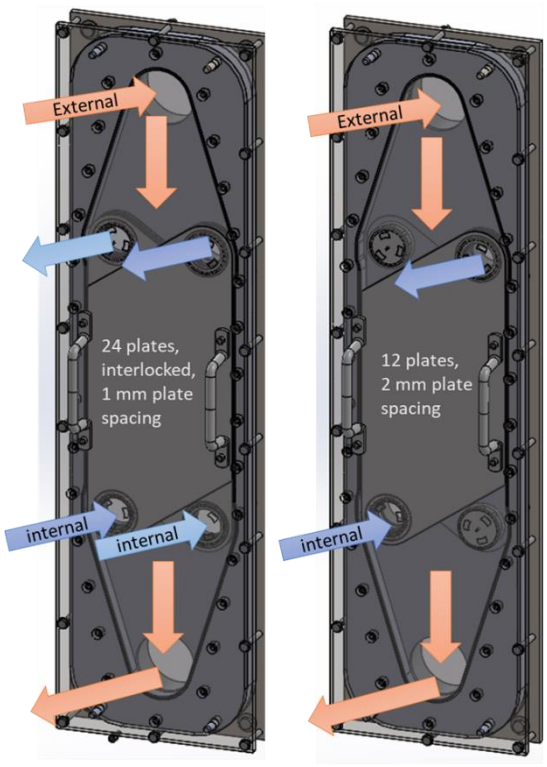

Figure 38. Mid-length, 3E-style, counterflow seawater-seawater test housing with the option to test at 1 or 2-mm plate spacing by interlocking or not interlocking plates.

Each heat exchanger was tested at 8-15 internal (cold) seawater velocities between 0.05-0.85 m/s and 9-16 external (warm) seawater velocities between 0.03-1.16 m/s. Seawater flow was controlled by setting the control valves to preset positions. Some flow variation was observed due to changes in seawater supply pressure. Inlet and outlet temperature and pressure and flow rate was measured for both internal and external fluids.

6.2.1. Pressure Drop

To prepare for future comparisons between full-length heat exchangers, pressure drop for this data set is normalized to a 1m path length and plotted versus Reynolds number.

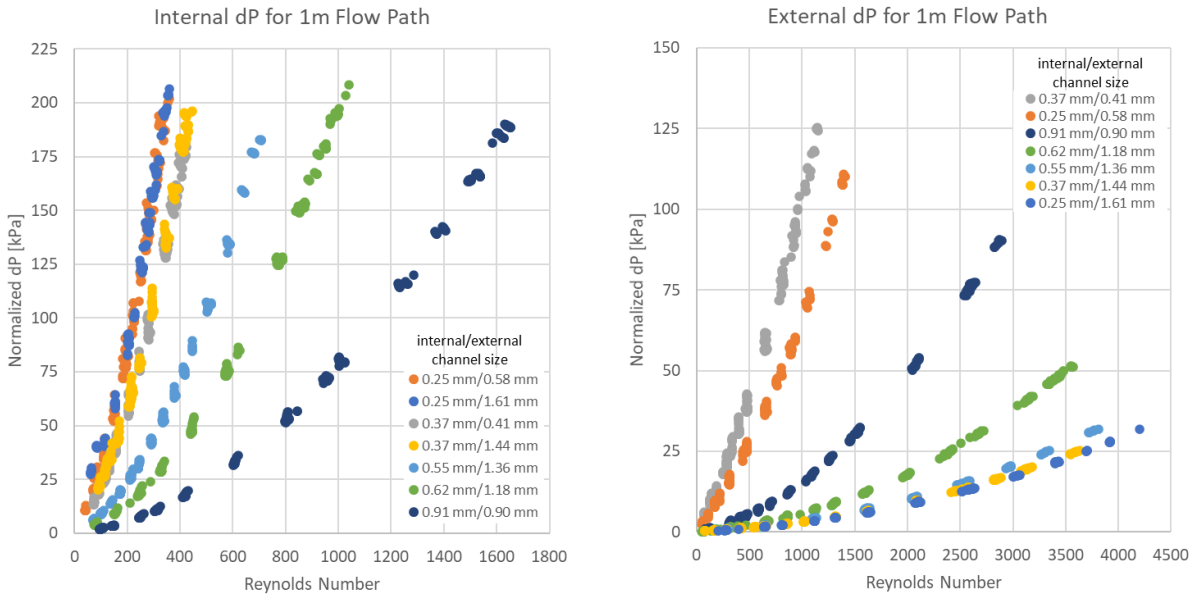

Figure 39. TFHX SW-SW internal and external pressure drop.

Internal flow rates up to 3 gpm per plate were tested in the largest internal channel size. Makai suspects a significant portion of the pressure drop at those high per plate flow rates is attributed to the manifold insert, which was designed for ~ 1 gpm per plate flow. Testing a full-length plate with similar internal channel size but a larger manifold insert will provide clarification.

6.2.2. Convective Coefficients

In seawater-seawater testing, the internal and external seawater convective coefficients are comparable. Since the overall heat transfer coefficient is sensitive to both internal and external seawater flow rates, when comparing different heat exchangers, it is more useful to compare the internal/external convective coefficients versus pressure drop and Reynolds number (Figure 40 and Figure 41).

For the same Reynolds number, smaller channels were previously observed to have higher convective coefficients. This trend was generally observed for both internal and external channels. Similarly, for the same pressure drop, larger channels are expected to have higher convective coefficients; this was also observed for both internal and external channels.

One exception is noted for the 0.55mm internal channel/1.36mm external channel configuration (#5 on Table 3). The internal convective coefficient is lower than expected and the external convective coefficient is higher than expected, particularly when plotted versus external pressure drop. Since the pressure drop vs Reynolds number data lines up well with other data, the discrepancy is unlikely to be attributed to poor data collection or data quality. The cause remains unknown but Makai expects additional data from full-length testing will provide clarity.

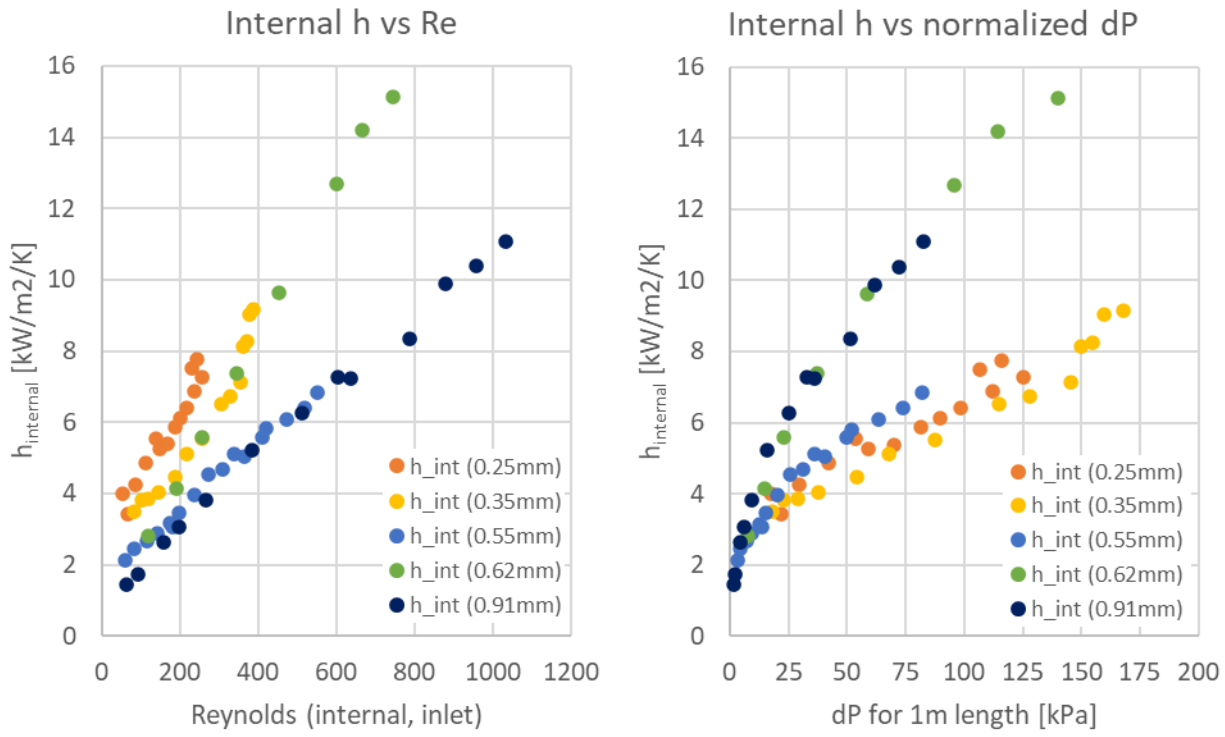

Figure 40. TFHX SW-SW internal convective coefficients.

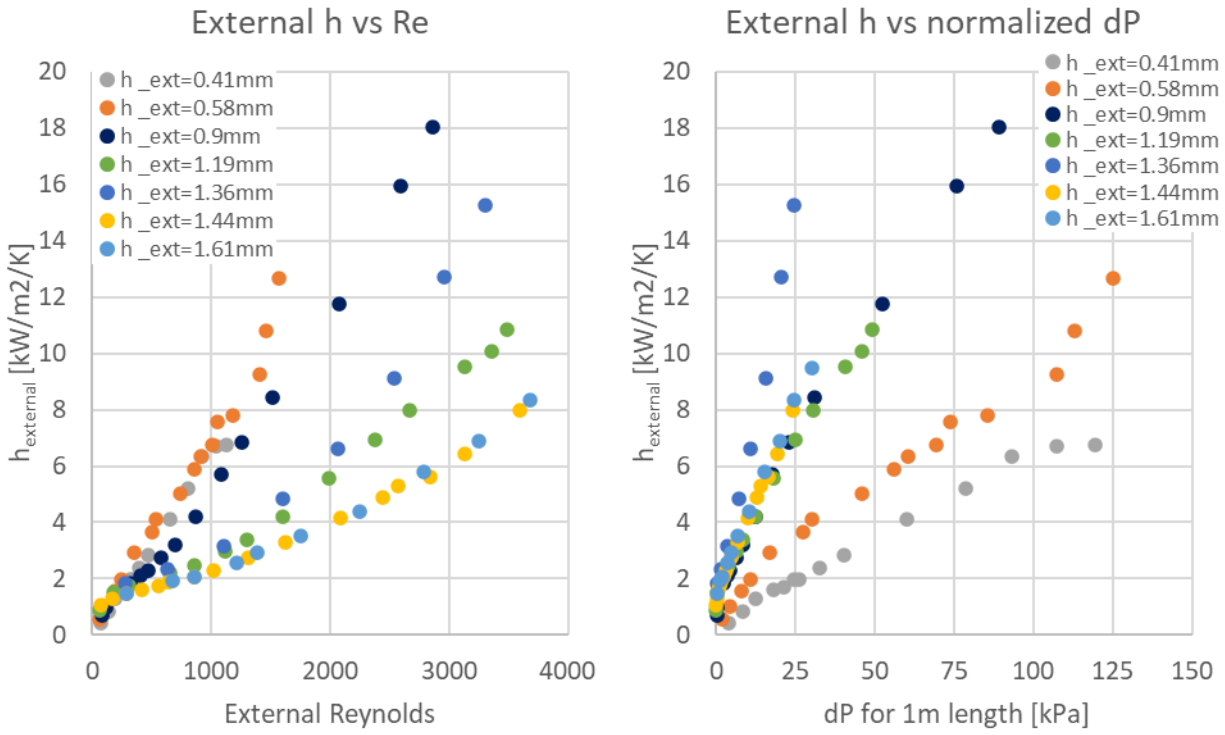

Figure 41. TFHX SW-SW external convective coefficients.

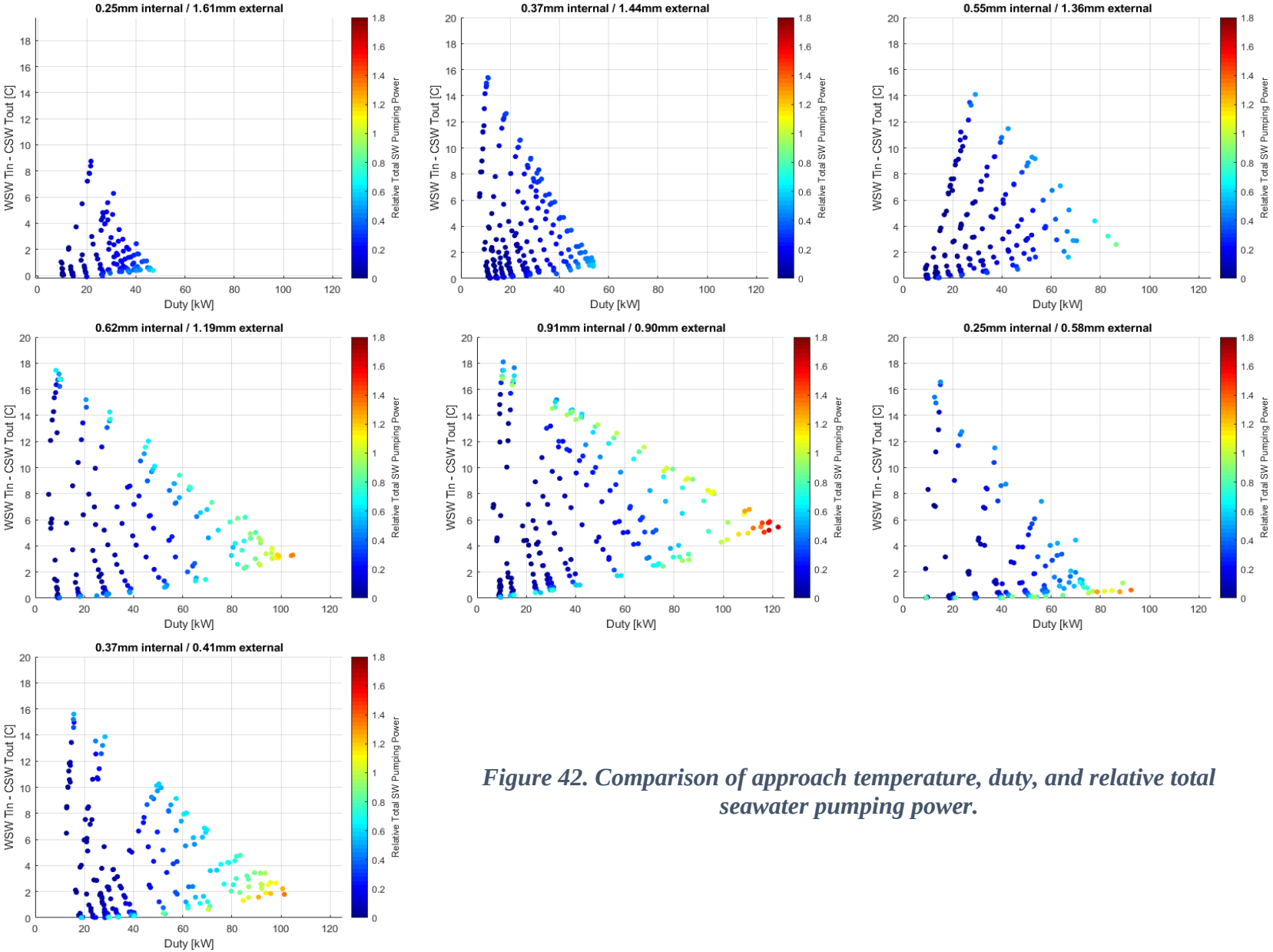

Figure 42. Comparison of approach temperature, duty, and relative total seawater pumping power.

6.2.3. Approach Temperature

Another consideration in the design of seawater-seawater heat exchangers is the approach temperature (warm seawater inlet temperature – cold seawater outlet temperature). The most efficient design would meet both pressure drop and duty requirements while having cold seawater exit as close to the warm seawater temperature as possible, extracting as much cooling capacity from the cold seawater as possible. For a fixed heat exchanger, this can be accomplished by varying the water flow rates (Figure 42). Alternatively, in the design process, the internal/external channel size and the flow path can be adjusted to meet the application requirements.

6.2.4. Discussion

Seawater-seawater testing revealed for similar internal and external fluids, both internal and external fluid flow rates significantly affect duty and overall heat transfer performance. For all tests, the internal convective coefficients varied almost linearly with Reynolds number and the external convective coefficients increased logarithmically at $Re < 500$ and increased almost linearly at $Re > 500$. This is likely the transition between laminar and turbulent flows.

By changing the internal/external channel sizes, the TFHX can be designed to fit an application's requirements. The tested TFHXs all fit in the same volume but required different combinations of flow rates and had different approach temperatures to produce the same duty.

These data will be compared to full-length seawater-seawater test results. Makai intends to use these data to design a seawater-water heat exchanger using warm surface seawater to cool auxiliary equipment at a HECO power plant on Oahu.

The issue of biofouling in seawater remains unresolved. Makai also plans to begin a long-term biofouling experiment using 1 or 2 full-length modules. The goals of the biofouling experiment will be to determine whether operational decisions such as flow velocity affect the required cleaning interval, establish cleaning intervals, and test different filtering and/or cleaning methods. Makai's initial focus will be on mechanical cleaning options to minimize additional subsystems required in chemical cleaning methods.

6.3. AIR-WATER TESTING

In this period, Makai tested 11 air-water TFHX configurations. This data set tested a practical range in air channel sizes (between 0.7 to 1.2 mm) and investigated the effect of stacking orientation (stacked vs. staggered) as well as the effect of different water (internal) channel sizes on similar air channel sizes (Table 3).

In order to minimize the effects of instrument accuracy and environmental heating on data quality, Makai increased the test section area by a factor of 4 over previous air-water testing, from 0.05m x 0.05m to 0.1m x 0.1m (Figure 43), and more than doubled the number of plates in a test from 4-8 to 16-22. As a result, the heat transfer area increased over 10X. As in previous testing, the external channel spacing in the test section was set using comb spacers at the inlet and outlet edges (Figure 44).

To accommodate the larger areas and higher duties, the air convection testing station was upgraded with a larger blower, a water pump with variable speed control, additional heating elements, and a new test housing (Figure 45).

Table 3. Air-water TFHX configurations.

	Internal	External	Stacked/ Staggered	Plates	Area
TFAC-3E-10	0.342	0.771	Staggered	18	0.3564
TFAC-3E-11	0.342	0.771	Stacked	18	0.3564
TFAC-3E-12	0.342	0.932	Stacked	16	0.3168
TFAC-3E-13	0.342	1.136	Staggered	14	0.2772
TFAC-3E-14	0.144	0.965	Stacked	18	0.3564
TFAC-3E-15	0.144	0.836	Stacked	20	0.3960
TFAC-3E-16	0.144	0.730	Stacked	22	0.4356
TFAC-3E-17	0.144	0.730	Staggered	22	0.4356
TFAC-3E-18	0.229	0.803	Stacked	20	0.3960
TFAC-3E-19	0.229	0.931	Stacked	18	0.3564
TFAC-3E-20	0.229	1.091	Stacked	16	0.3168

In air convection testing, test plates are installed in an air convection test housing with connections for water to be pumped through the internal channels of the test plates and air ducted to flow between the plates (external channels). The water is heated with heating elements to 50°C and water flow was controlled by adjusting pump speed. Air flow was provided by a blower and air mass flow rate was measured using a Coriolis flow meter. Air flow through the test section was changed by operating a bypass valve. Air temperature was not controlled. Temperature and pressure sensors measured the air and water inlet and outlet conditions.

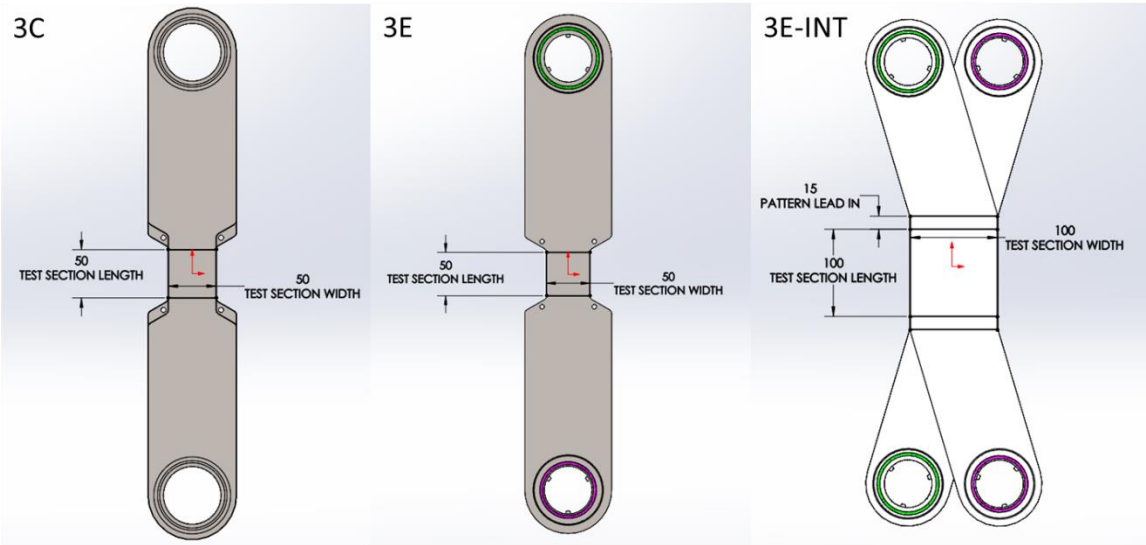

Figure 43. Per plate test area increased by 4x in latest air-water TFHX plate design.

Figure 44. 18-plate stack of TFHX plates. Green comb spacers on the inlet and outlet edges are used to maintain uniform air channels through the test section.

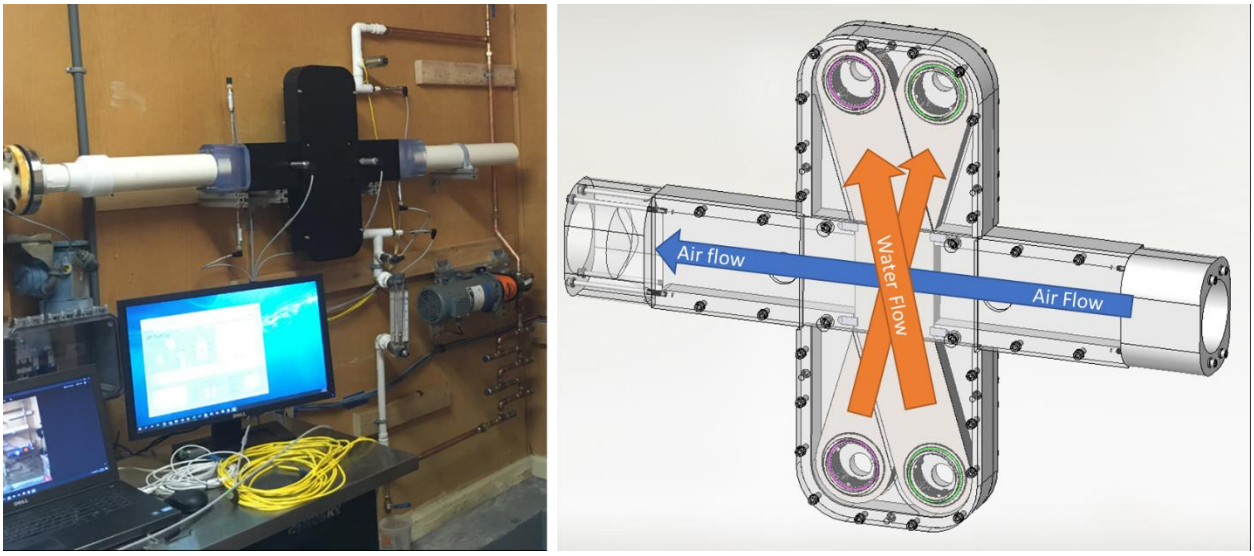

Figure 45. Air-water testing station and custom housing.

A test point is defined by specifying the air- and water-side flow rate. The water-side flow rate is set first and different air-side flow rates are tested for the fixed water-side flow rate. The process is repeated for each new water-side flow rate using the same air-side flow rates. Air-side flow rates were selected to produce up to 0.4 psi pressure drop, but were limited by the capacity of the blower.

Summarized data points were then obtained by reviewing the test point and selecting a span of data that was representative of steady-state conditions. This was typically the last 5 minutes of a 45-minute long test point. Measurements were then averaged over the selected stable span. Detailed description of calculations and data processing are included in Appendix B.

6.3.1. Test Results

Air-side pressure drops and convective coefficients are plotted versus air inlet Reynolds number to account for the difference in channel sizes and variations in air inlet temperatures while testing the different heat exchangers.

Over the same range in Reynolds number, the external channel size determines the air-side pressure drop (Figure 46). The effect of varying internal channel sizes does not appear significantly affect the pressure drop; i.e., for configurations that produced air channel spacings between 0.93-0.96mm, the pressure drop was the same for all three internal channel sizes.

For the same Reynolds number and similar external channel sizes, the configuration with the larger internal channel had a higher air convective coefficient by up to 10%. Additionally, for the same pressure drop and similar external channel sizes, configurations with larger internal channels had higher air convective coefficients.

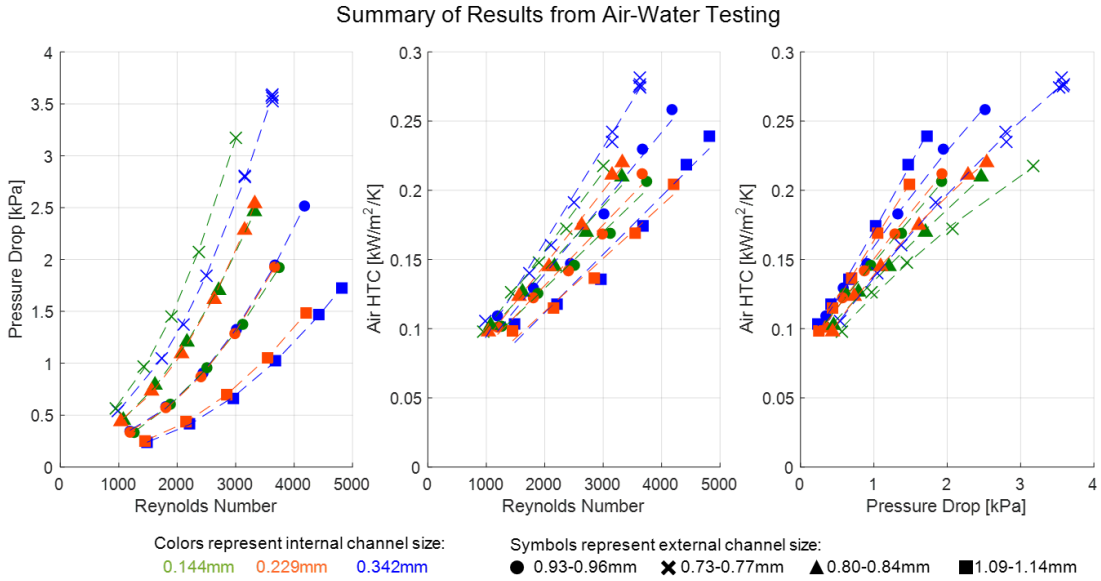

Figure 46. Combined air-water test data.

The stacking orientation had a significant effect on the 0.771 mm/0.342 mm (external/internal channel size) configuration and no effect on the 0.73 mm/0.144 mm configuration (Figure 47). This is attributed to the ratio of the internal channel size to the external channel size which was 0.44 in the 0.771 mm/0.342 mm configuration compared to 0.20 in the 0.73 mm/0.144 mm configuration.

For the same pressure drop, larger air-side channels produced higher duty because more air can be passed through the heat exchanger, which is why smaller air channels have higher duty and heat transfer efficiencies for the same Reynolds number (Figure 48).

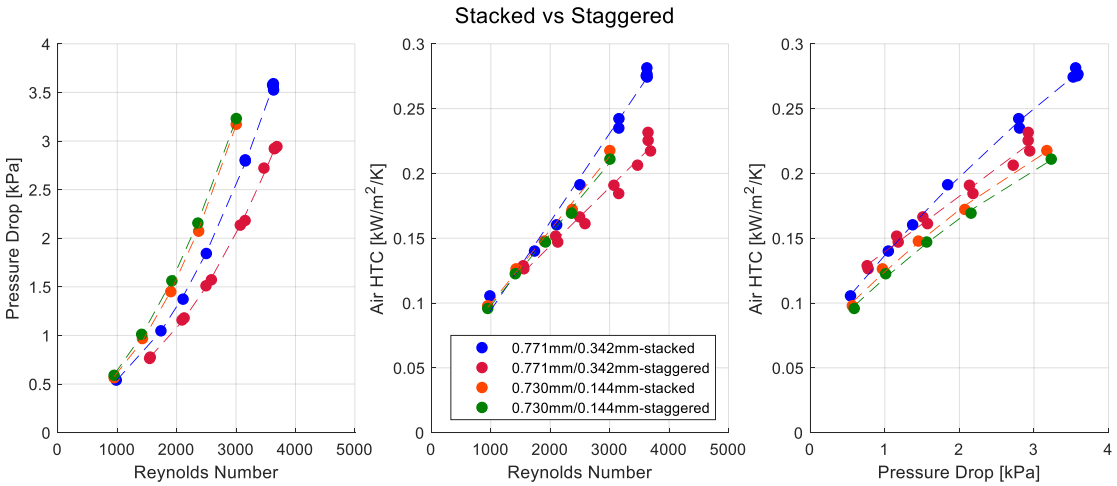

Figure 47. Effect of stacked vs staggered orientation.

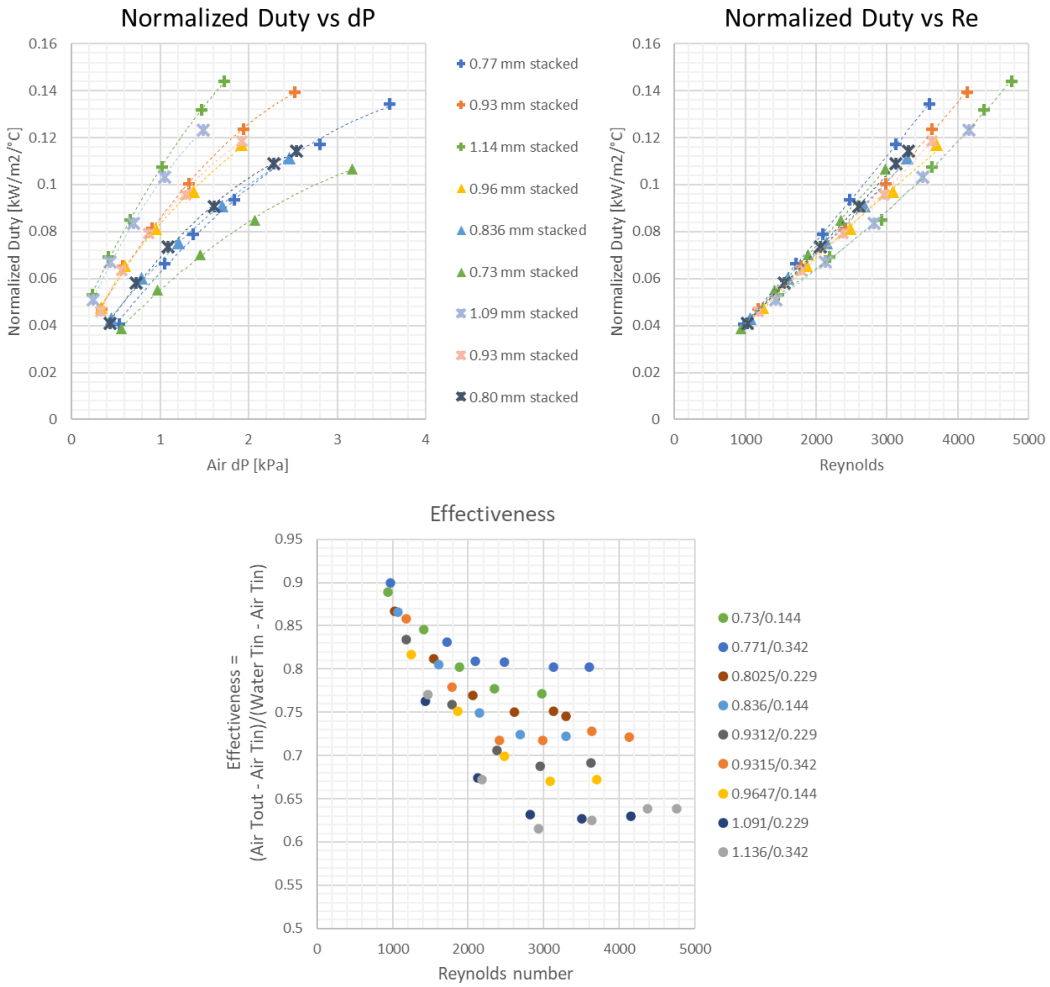

Figure 48. At the same pressure drop, duty was higher for larger air channels but at the same Reynolds number, duty was higher for smaller air channels. Heat transfer is more effective for smaller air channels.

6.3.1. Discussion

After two previous rounds of air convection testing, there were some data inconsistencies that were attributed to inaccurate plate spacings and the relative effective of measurement accuracy and environmental input at low duties (due to using low heat transfer areas). In this round of air convection testing, the interlocking design minimized plate compression in the test section and therefore, the previously observed concave/convex plate shapes were not an issue and air channel spacings were consistent. To address low heat transfer area, the per plate heat exchanger area was increased 4X by doubling both the air and water passage lengths and more than double the number of plates were used for each test.

Comparing pressure drops provides a preliminary check of previous data (Figure 49). The current data set is shown using closed circle markers and dotted lines show the boundaries of the current data range. For previous data sets, pressure drop has been adjusted to match the current 100mm air path length. Previous 3E data is shown with open diamond markers and previous 3C data is shown with x's and triangle markers. Each series is named by the air channel size / water channel size.

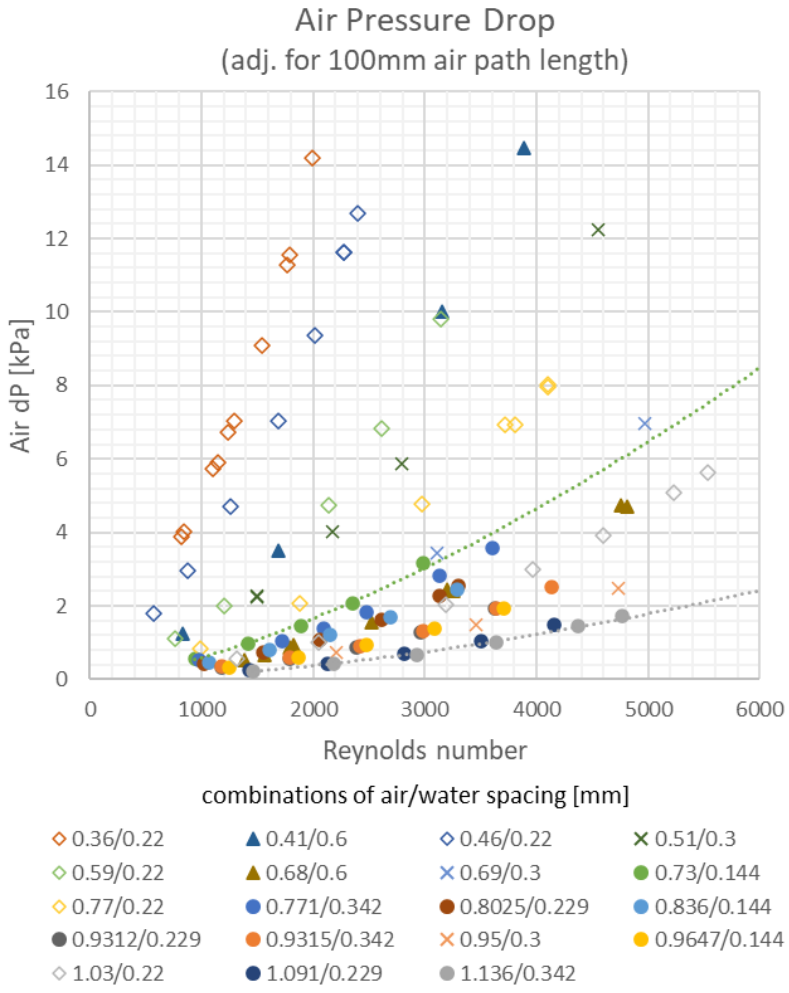

Figure 49. Air-side pressure drop comparison for all tested configurations.

The previous 3E pressure drops do not align with the rest of the data. For comparable air channel sizes, the pressure drop is over 2X higher at the same Reynolds number. This is likely due to uneven channel spacing. Similar inconsistencies are observed when compare air-side convective coefficients across all tested configurations (Figure 50). Therefore, Makai will exclude the 3E data from further use.

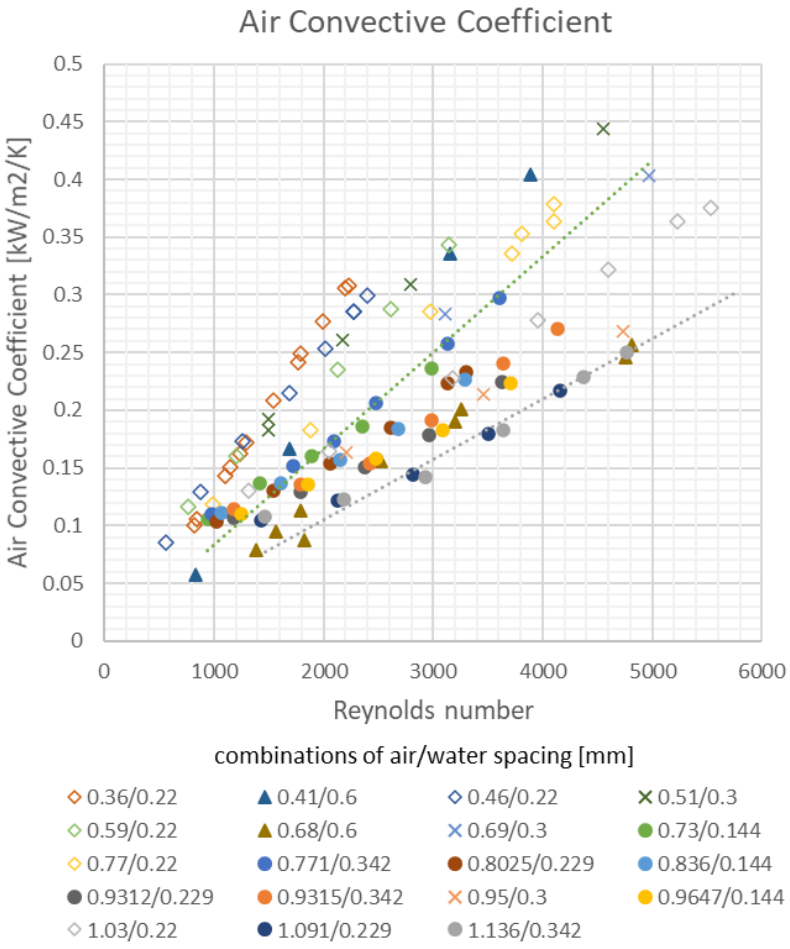

Figure 50. Air convective coefficient for all tested configurations.

One way to evaluate the effect of changing the air path length is to compare the effectiveness of the different plate sizes and configurations. Effectiveness is defined as the ratio of the actual increase in air temperature over the maximum possible increase air temperature. In comparable air channel sizes, for the same pressure drop, effectiveness is lower for shorter air passage lengths (Figure 51). However, for the same pressure drop, smaller channels can be used to the same effectiveness. For example, at 2 kPa dP, at 0.51mm air channel has about the same effectiveness as a 0.93mm air channel.

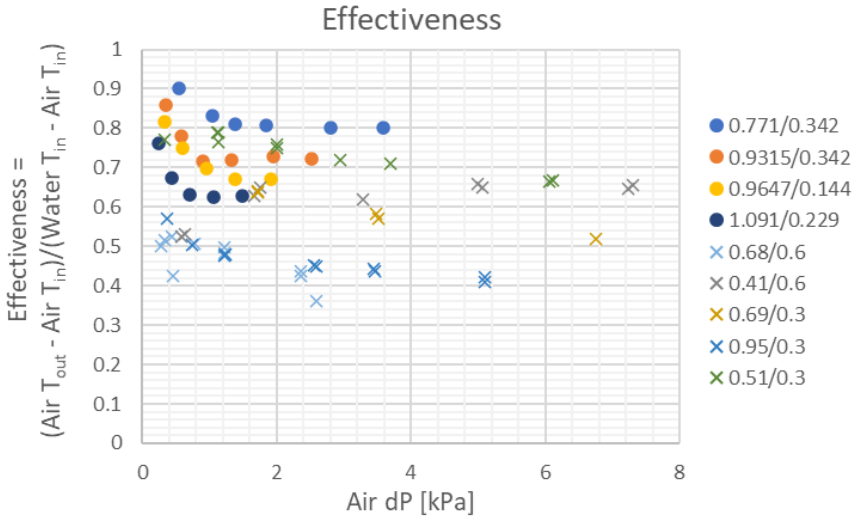

Figure 51. Temperature effectiveness vs air pressure drop for configurations with 100-mm long air path (circles) and 50-mm long air path (x).

For a given air channel size, air convective coefficient continues to increase almost linearly with increase air mass flow rate; i.e., at the tested velocities (up to 80 m/s in previous 3C data), the TFHX does not exhibit a saturation point. Typical finned-type heat exchangers display a saturation point where increasing air flow rate produces a diminishing increase in duty (Figure 52). Because the TFHX is direct heat transfer area, i.e., the air and hot fluid are only separated by the foil thickness, the TFHX is not limited by fin effectiveness and therefore, does not exhibit a saturation point (at practical air flow rates/velocities).

For most applications, the optimal TFHX design optimizes the allowable pressure drop, available air flow rate, and required duty. Tradeoffs between improved efficiency and increased heat transfer area density in smaller air channels versus lower pressure drops in larger air channels are evaluated depending on the application constraints. The absence of saturation point is also an important consideration; existing subsystems, designed for finned heat exchangers, may not be able to take full advantage of the TFHX capabilities. A holistic, systems-level engineering evaluation is recommended to maximize benefits of the TFHX rather than a direct, drop-in replacement.

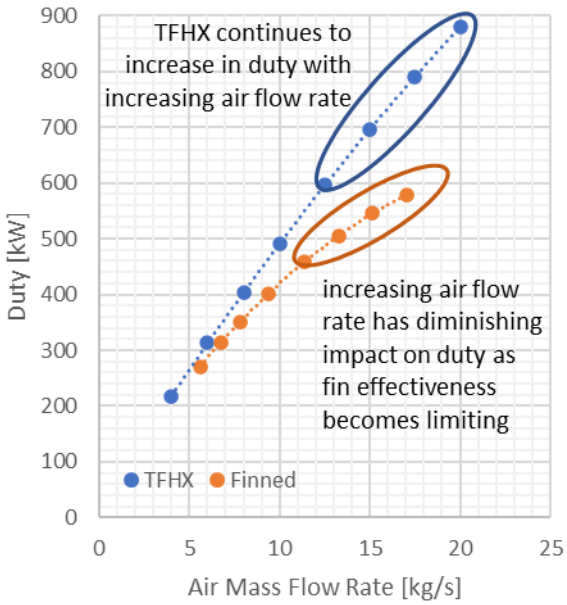

Figure 52. Unlike finned heat exchangers, TFHX does not exhibit a saturation point.

6.4. CASE STUDY: DESALINATION PROJECT

Makai pursued a commercial opportunity for the TFHX in a desalination project with Trevi Systems, Inc. The Trevi desalination process uses a specialized fluid, called the draw solution, with unique thermally dependent water absorption properties that are leveraged for desalination. Heat input is provided through solar heating and three heat exchangers are used in the system to recuperate as much heat as possible.

Important aspects of the heat exchanger design included targeting a tight approach temperature and minimizing the pressure drop. Both aspects are complicated by the properties of the specialized fluid. With respect to approach temperature, the fluid undergoes a pseudo phase change which requires a heat of mixing; i.e., heat input goes into converting the fluid from one phase to another (not a change of state) instead of increasing the temperature. This is characteristic impedes a tight approach temperature because it limits the temperature differential driving heat transfer. With respect to maintaining a low pressure drop, the draw fluid undergoes significant changes in viscosity with temperature and phase; i.e., the inlet viscosity of the fluid is significantly different than the outlet viscosity. To minimize pressure drop, the heat exchanger design must account for the most viscous state. Finally, the system flow rates are proportionally fixed and depend on the water absorption ratio; this means the flow rates cannot be changed to improve heat transfer efficiency.

The TFHX's customizable features, from matching the internal and external channel sizes for the application (compared to uniform channels on a plate-frame heat exchanger) to changing internal channel sizes along the flow path to accommodate the changing fluid viscosity make it a unique fit for the challenging application.

To gain experience with the draw solution and determine the pressure drop and convective coefficients required for a TFHX design, Trevi supplied Makai with draw fluid and Makai constructed a single individual TFHX plate for pressure drop testing and a 24-plate TFHX for performance testing. Performance testing was conducted under 2 different operating conditions provided by Trevi, denoted 2B and 1C.

6.4.1. Pressure Drop Testing

A single 0.1m x 0.5m plate was constructed for dP testing. The plate had a custom designed weld pattern to achieve the desired 0.57 mm internal effective spacing (Figure 53). The internal fluid path length of the pattern region is 0.39 m. Testing was conducted over a range in temperatures because the temperature-related changes on hydraulic properties were expected to be significant. Two concentrations of the draw solution, 80% and 47%, used in the desalination process were incrementally heated from 25°C to 90°C. Density and temperature were recorded by the Coriolis as the fluid was heating up (Figure 54). At each temperature, a dP vs mass flow rate test was performed.

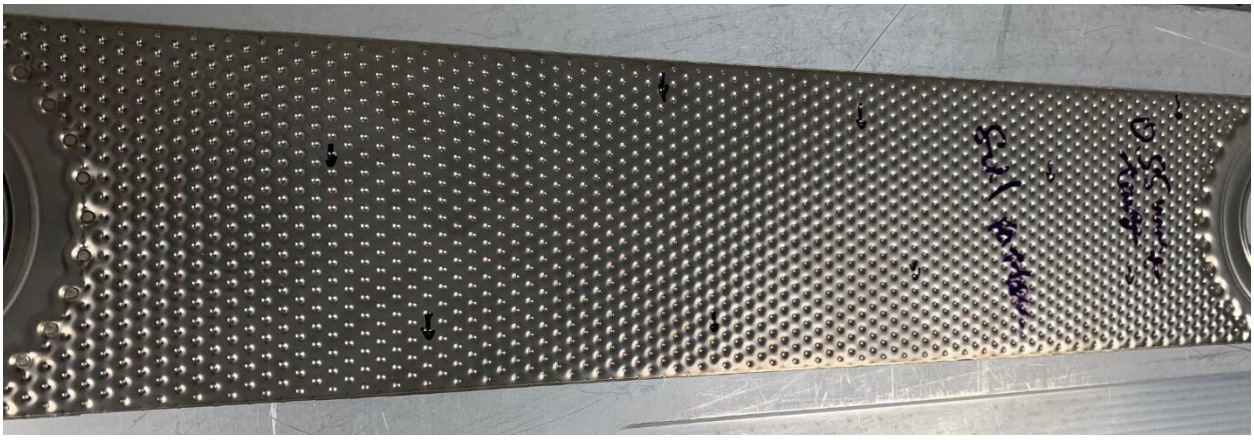

Figure 53. Trevi pressure drop test plate.

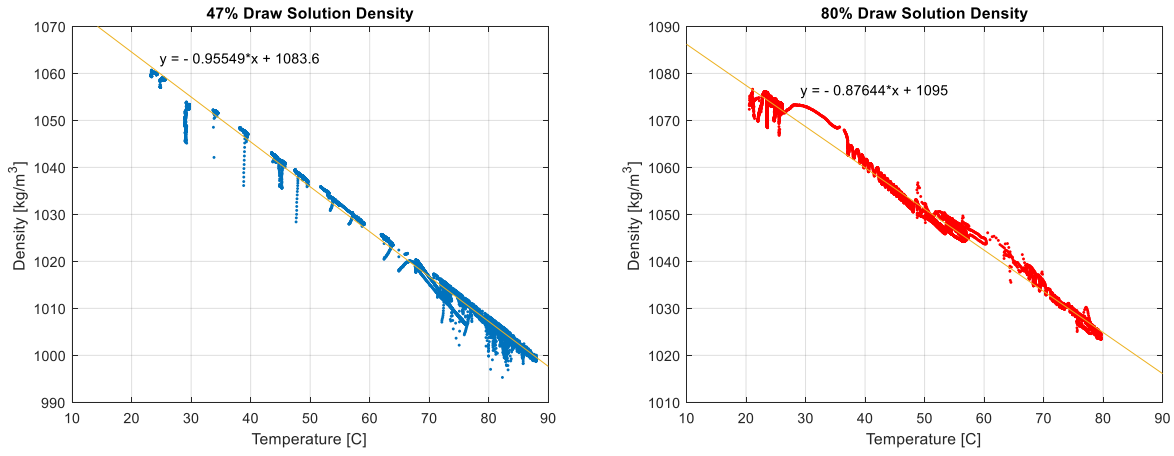

Figure 54. Density versus temperature of 47% and 80% draw solution.

Using the curve fits at each temperature, the pressure drop data were combined to plot the pressure drop vs temperature for lines of constant velocity.

The internal fluid pressure drop was measured in the pressure testing apparatus. The external channel is formed between stacked TFHX plates and was tested during performance testing (Figure 56), when multiple TFHX plates were stacked together.

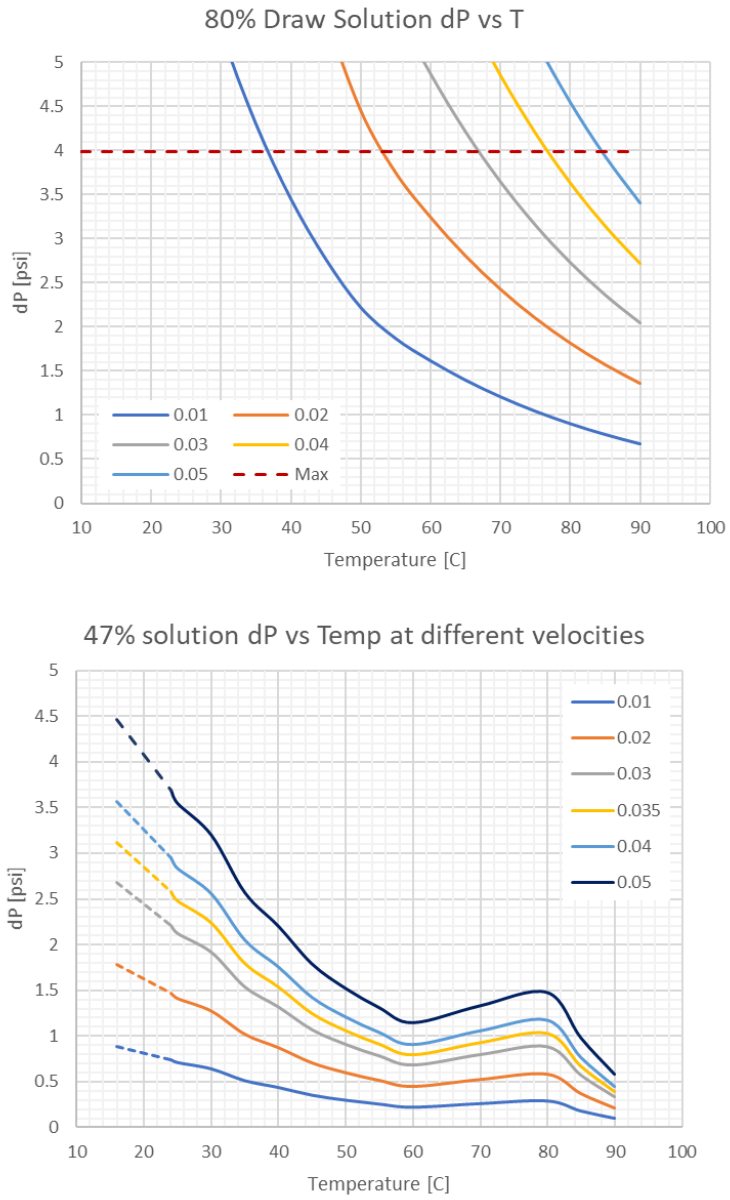

Figure 55. At a constant velocity, the pressure drop changes with fluid temperature. In the 80% draw solution, pressure drop decreases with increasing temperature. In the 47% draw solution, pressure drop decreases with increasing temperature until 60°C, increases between 60-80°C, and decreases again above 80°C. The increase in pressure drop occurs when the solution undergoes phase change. Dashed lines on lower graph indicate extrapolated data.

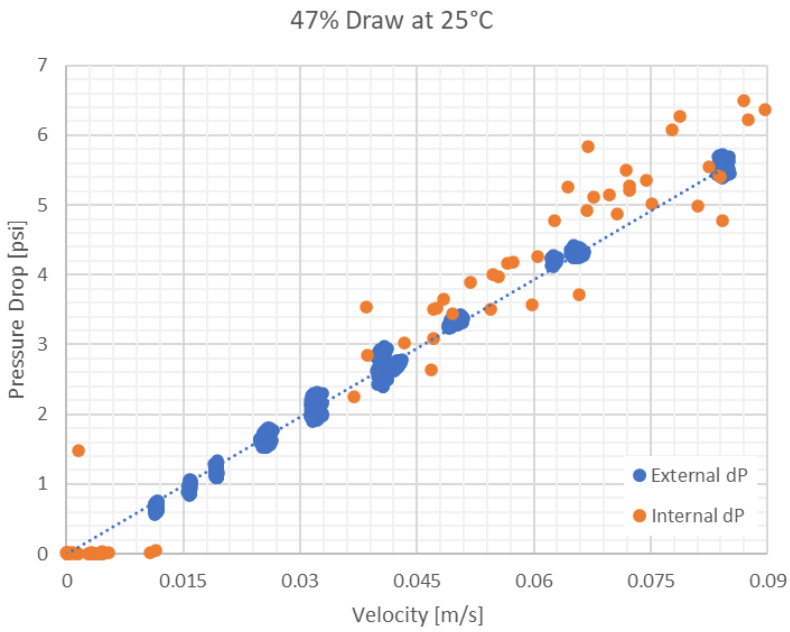

Figure 56. Pressure drop of 47% draw solution in an 0.55 mm external channel. The external pressure drop vs velocity is comparable to the internal pressure drop vs velocity at the same temperature.

The measured internal pressure drop was ~20% lower than the predicted pressure drop. This was expected as the pressure drop of water was previously measured in a comparable internal channel at room temperature.

The external pressure drop was 2.5-3X lower than predicted at 2B temperatures and 4X lower than predicted at 1C temperatures. A lower pressure drop enables a longer heat exchanger plate, fewer plates (higher velocity), a smaller external channel (higher velocity), and/or lower pumping power (electrical operating costs).

6.4.2. Performance Testing

A new test station was designed and constructed for performance testing, which used a counterflow configuration with hot water as the internal fluid and the 47% draw solution as the external fluid. Due to the temperature-dependent changes in draw solution fluid properties and phase, it was important to conduct performance testing at the specified operating temperatures of the desalination system. Two operating conditions, denoted 2B and 1C, were tested. The fluids were the same, but the temperatures and relative flow rates were different. The goal of performance testing was to determine convective coefficients of the draw solution under representative operating conditions to use in designing TFHXs for the desalination system.

Performance Testing Setup

The test setup included the test heat exchanger, a companion heat exchanger to recuperate the heating/cooling, the heating and cooling heat exchangers, a pump in each fluid loop, and instrumentation to measure temperature, pressure, and mass flow rates (Figure 57). The test heat exchanger was outfitted with instrumentation to measure the inlet and outlet temperatures and

pressures and mass flow rates of the internal and external fluids. Fluid mass flow rates were controlled by manually adjusting the VFD output to control the pump motor speed.

Makai previously used electric heaters to provide heating in air-water performance testing, but the heat load and high temperatures required to replicate the operating conditions made electrical heating elements impractical. The heating heat exchanger used a propane hot water heater as the heat source. The amount of heating was controlled by adjusting the propane flow rate and the hot water heater setting (winter vs summer, which changed the number of heating elements). The cooling heat exchanger used tap water as the cooling source. The amount of cooling was manually adjusted by throttling the flow rate of tap water.

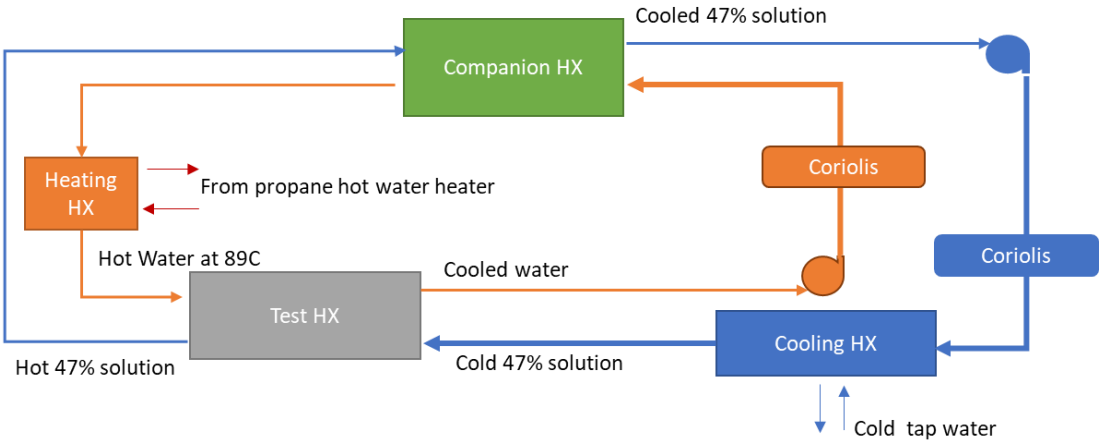

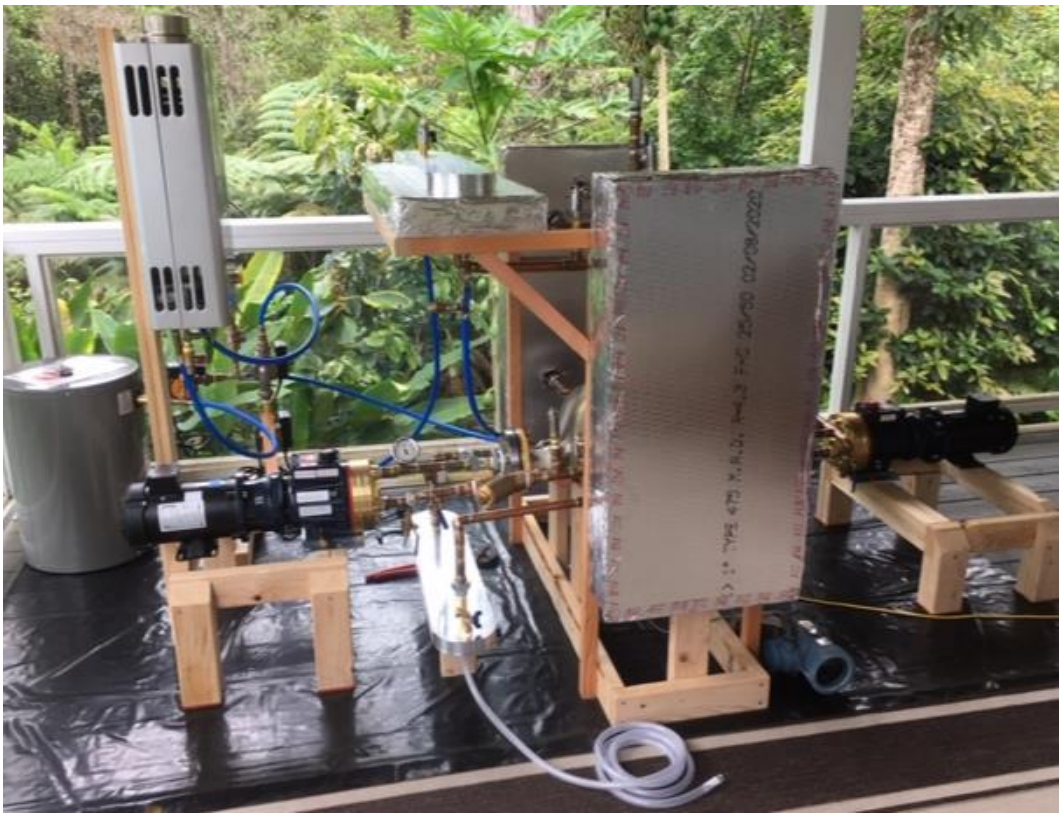

Figure 57. Schematic of test setup and constructed system.

TFHXs were used for all four heat exchangers in the test system. Although initial modeling suggested the optimal length to achieve the required approach temperature and to minimize cost (by reducing plates) was ~ 0.8m, testing was conducted using the existing (at the time of the project) fabrication equipment and tooling; i.e., TFHX plates were mid-length (0.39m) with 3E-style manifolds. Results were extrapolated to determine the performance for different TFHX plate lengths.

The test and companion heat exchangers were interlocking (1 mm plate spacing), 24-plate TFHX units (Figure 58). The test heat exchanger used TFHX plates with effective internal and external channel spacings of 0.25 mm and 0.55 mm, respectively. The total heat transfer area of the unit was 4.68 m^2. A custom aluminum housing (required because the operating temperature exceeded 90°C) was designed to house the 24-plate TFHX unit (Figure 59). The design and sizing of the test heat exchanger was at a $1/100^{th}$ scale. The heating and cooling heat exchangers used twelve 100-mm wide plates, similar to the plates used for pressure drop testing (Figure 60).

Calculations, and data processing details are the same as in previous performance testing and described in Appendix A.

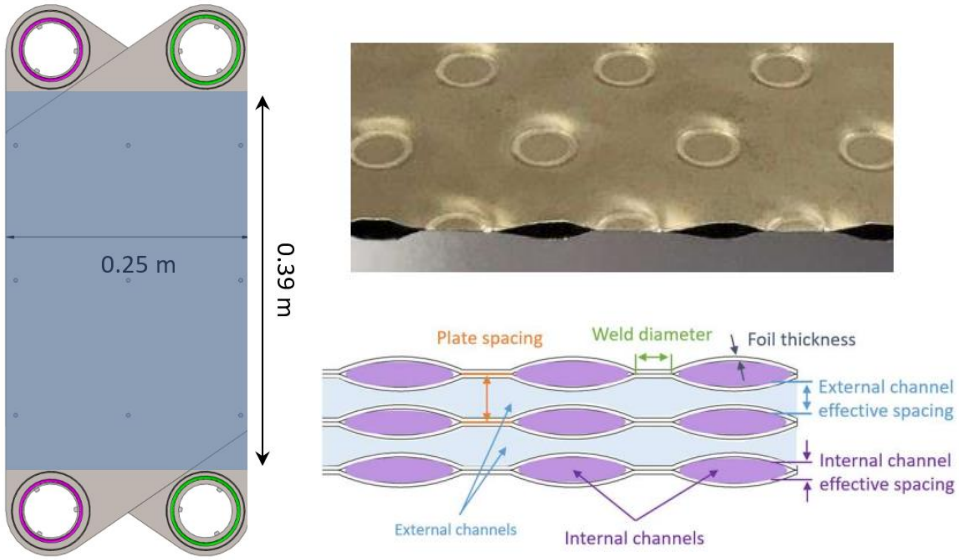

Figure 58. Interlocking plates use alternating manifold stacks to reduce the plate spacing from 2 mm to 1 mm. In the top right image, a TFHX plate is cut to show the internal channels. The bottom right image illustrates plate spacing and internal/external effective channel spacing.

Figure 59. Test HX housing and TFHX plates arranged in the housing.

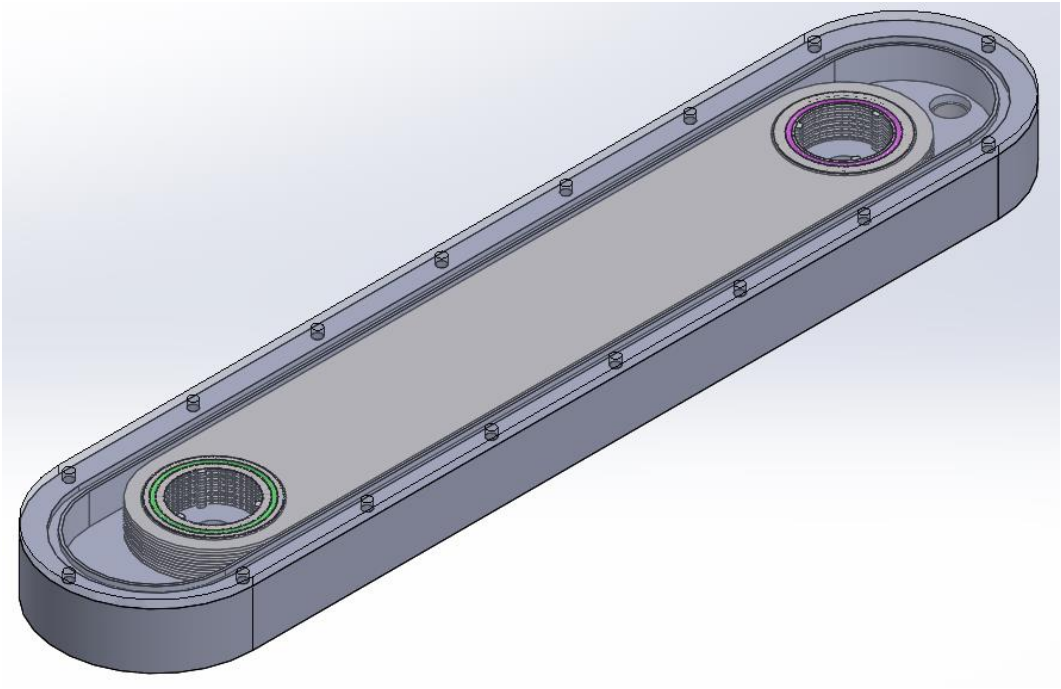

Figure 60. Schematic of the heating and cooling heat exchanger.

Performance Testing under 2B Conditions

In 2B testing, the mass flow rate ratio of water to draw solution was nominally 0.7, (Data 1 and Data 2 in Table 4). A reduced flow rate point was also tested (Data 3 and 4 in Table 4). The hot

water inlet temperature was kept as close to 89°C as possible and the draw was cooled to the maximum possible (i.e., tap water was at maximum flow).

There is some discrepancy between the measured heat of mixing in Data 1 and Data 2. The heat of mixing in Data 1 is significantly higher than expected and may have been a result of inaccurate draw mass flow rate measurement. In Data Points 2-4, draw solution increases about 41°C and the heat of mixing is ~ 44 kJ/kg. In Data Point 1, draw solution only increases 35°C and the heat of mixing is 50 kJ/kg. Data Point 1 was not used for further analysis.

The convective heat transfer coefficients of water and draw solution were adjusted in the TFHX model to match the measured temperatures for the recorded heat of mixing. This result is shown in the "Model" column in Table 4.

At the design flow rates, the maximum draw outlet temperature (assuming an infinitely long heat exchanger) was 78.2°C based on the measured heat of mixing and the draw inlet temperature. The hot-side approach temperature was 7.3°C and the cold-side approach temperature was 6.6°C (x and o dashed lines in Figure 61). Using the solved-for convective coefficients and extending the heat transfer length to 0.8 m, the hot and cold-side approach temperatures are 2.4°C and 2°C, respectively (triangle-dash lines in Figure 61).

At reduced flow rates, the hot and cold-side approach temperatures are 2°C and 1.6°C, respectively, for our 0.39-m long test heat exchanger and modeling predicts hot and cold-side approach temperatures of 0.8°C and 0.7°C with a 0.5-m long heat exchanger (Figure 62).

Table 4. 2B Test Data

		Data 1	Model 1	Data 2	Model 2	Data 3	Model 3	Data 4	Model 4
	Foil Thickness ["]	0.004	0.004	0.004	0.004	0.004	0.004	0.004	0.004
	Plate Spacing [mm]	1	1	1	1	1	1	1	1
	Width [m]	0.25	0.25	0.25	0.25	0.25	0.25	0.25	0.25
	Length [m]	0.39	0.39	0.39	0.39	0.39	0.39	0.39	0.39
	Plates	24	24	24	24	24	24	24	24
	Heat of Mixing [kW]	6.00	6.00	4.89	4.9	3.33	3.326	3.34	3.34
	Nominal Area [m2]	4.68	4.68	4.68	4.68	4.68	4.68	4.68	4.68
	% Eff Area	97.4	0.974	97.4	0.974	97.4	97.4	97.4	97.4
	Duty [kW]	17.91	17.87	17.56	17.58	12.17	12.17	12.34	12.33
	U [kW/m2/K]	0.48	0.33	0.32	0.29	0.30	0.23	0.34	0.24
	LMTD [C]	8.18	8.48	11.87	11.86	8.61	8.91	7.82	8.33
External (47% Draw)	mdot [kg/s]	0.119	0.119	0.111	0.111	0.075	0.075	0.078	0.078
	Spacing [mm]	0.55	0.00	0.55	0.55	0.55	0.55	0.55	0.55
	dP [psi]	1.44	3.61	1.03	3.08	0.86	2.36	0.99	2.47
	T in [C]	31.25	31.25	30.44	30.44	26.01	26.01	26.32	26.32
	Tout [C]	66.68	66.70	70.92	70.96	67.97	67.95	67.50	67.47
	velocity [m/s]	0.031	0.034	0.027	0.032	0.018	0.021	0.019	0.022
	h [kW/m2/K]		0.497		0.404		0.317		0.323
Internal (Water)	mdot [kg/s]	0.077	0.077	0.079	0.079	0.048	0.048	0.048	0.048
	Spacing [mm]	0.25	0.00	0.25	0.25	0.25	0.25	0.25	0.25
	dP [psi]	0.48	0.62	0.54	0.57	0.32	0.41	0.27	0.42
	T in [C]	89.06	89.07	90.36	90.35	89.18	89.17	89.63	89.62
	Tout [C]	33.07	33.29	37.02	37.03	28.40	28.64	27.93	28.28
	velocity [m/s]	0.051	0.053	0.053	0.054	0.032	0.033	0.032	0.033
	h [kW/m2/K]		0.956		1.022		0.819		0.874

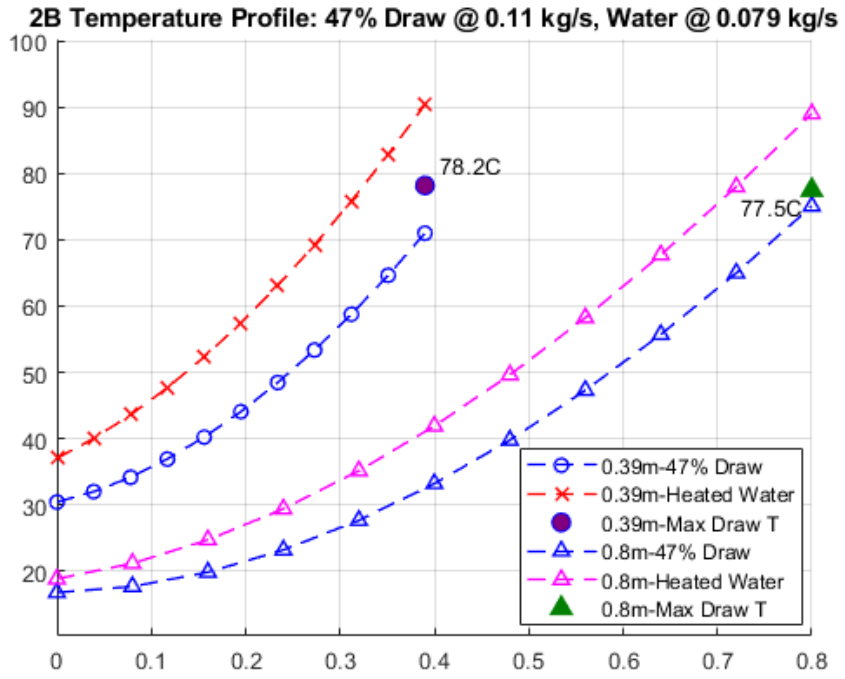

Figure 61. Temperature profiles for tested (0.39m) and modeled (0.8m) heat transfer length at design flow rates. The maximum draw temperature, based on the duty, heat of mixing, and draw inlet temperature for each case is also shown on the graph.

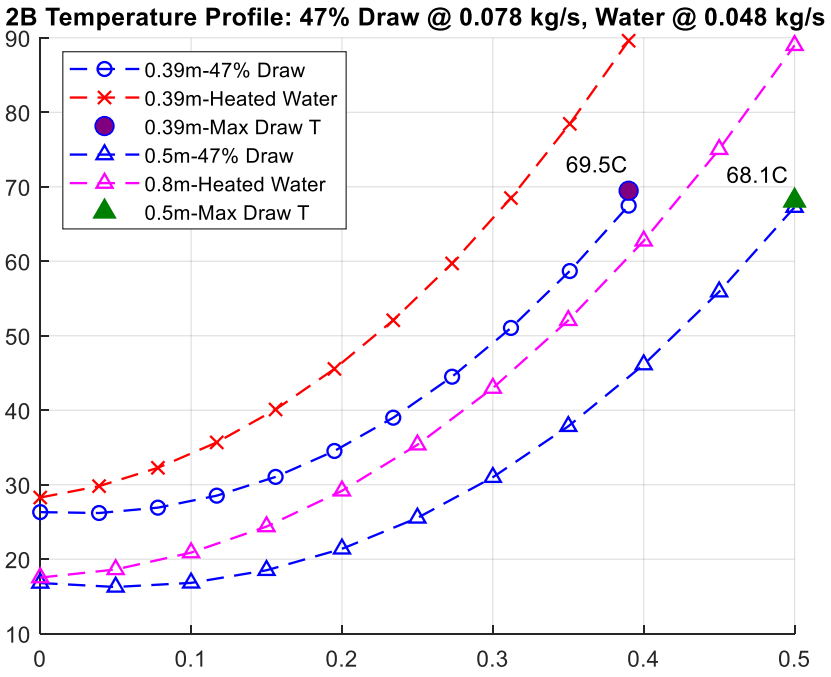

Figure 62. Temperature profiles for tested (0.39m) and modeled (0.5m) heat transfer length at reduced flow rates. The maximum draw temperature, based on the duty, heat of mixing, and draw inlet temperature for each case is also shown on the graph

Performance Testing under 1C Conditions

In the 1C test, the mass flow rate ratio of water to draw solution was 0.8. Although higher water flow rates were allowable according to the $1/100^{th}$ scaling, it was difficult to maintain the water inlet temperature > 91°C at higher water flow rates. The draw inlet temperature was held around 80°C. 2.6 kW of heat of mixing (7.6 kJ/kg for 6.9°C temperature change) was observed during under the test conditions.

As in 2B, the heat of mixing and measured temperatures were used to deduce the convective coefficients for both draw and water at the test conditions (Table 5). For the tested TFHX, the hot and cold-side approach temperatures were 3.1°C and 1.9°C, respectively. At the tested flow rates and using the same 2.6 kW for heat of mixing, for a draw inlet temperature of 70°C and hot water inlet temperature of 93°C, a 0.8m long TFHX will heat the draw solution to 89.8°C (Figure 63) with hot and cold-side approach temperatures of 3.2°C and 4°C.

Table 5. 1C Performance Testing and Model Results.

		Data	Model
	Foil Thickness ["]	0.004	0.004
	Plate Spacing [mm]	1	1
	Width [m]	0.25	0.25
	Length [m]	0.39	0.39
	Plates	24	24
	Heat of Mixing [kW]	2.6	2.6
	Nominal Area [m2]	4.68	4.68
	% Eff Area	97.4	97.4
	Duty [kW]	9.30	9.27
	U [kW/m2/K]	0.83	0.78
	LMTD [C]	2.47	2.49
External (47% Draw)	mdot [kg/s]	0.342	0.34
	Spacing [mm]	0.55	0.55
	dP [psi]	0.59	3.00
	T in [C]	81.19	81.19
	Tout [C]	88.11	88.12
	velocity [m/s]	0.094	0.10
	h [kW/m2/K]		1.03
Internal (Water)	mdot [kg/s]	0.271	0.27
	Spacing [mm]	0.25	0.25
	dP [psi]	1.52	1.90
	T in [C]	91.25	91.25
	Tout [C]	83.09	83.12
	velocity [m/s]	0.187	0.19
	h [kW/m2/K]		3.40

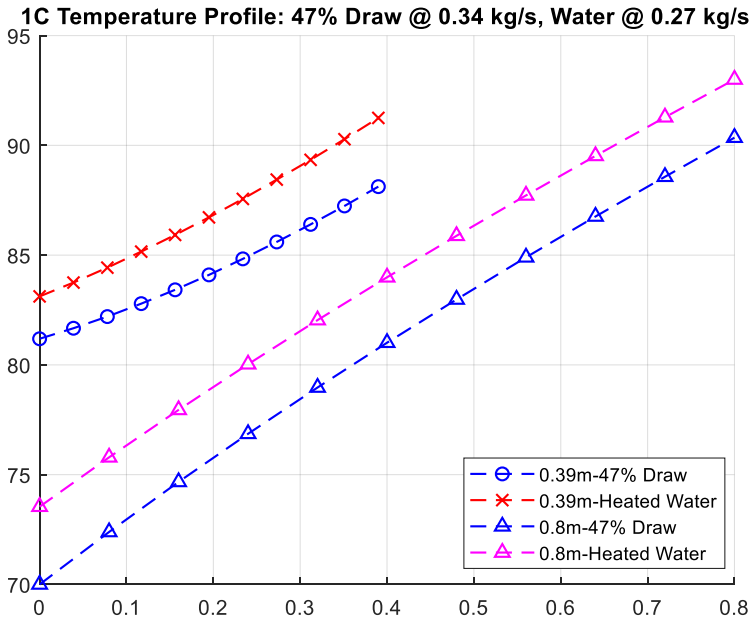

Figure 63. Temperature profile for tested TFHX and modeled 0.8m long TFHX.

Heat of Mixing

At 2B temperatures, the heat of mixing for 0.11 kg/s of 47% draw solution from 16.8-80°C was expected to by 4 kW. Instead, 4.9 kW was attributed to the heat of mixing for 0.11 kg/s from 30-70°C, or 1.07 kJ/kg/C using a simplification that applied the heat of mixing evenly throughout the entire temperature range. The heat of mixing was over 20% higher than expected at 2B conditions, particularly since the draw outlet temperature did not reach 80°C as initially predicted.

Heat of mixing was not expected, but was also observed at 1C conditions. The heat of mixing was 1.1 kJ/kg/C for measured temperature range of 81-88°C, which is comparable to the 1.07 kJ/kg/C measured under 2B conditions.

The high heat of mixing reduces the maximum possible 47% draw solution outlet temperature and requires additional heat transfer area to raise the draw solution outlet temperature. After discussion with Trevi, the lower draw outlet temperature was not a major issue as the operating conditions provided for the 1C heat exchanger is already oversized to accommodate start-up operations.

Performance Assessment

The operating velocities for the 2B condition, less than 0.05 m/s, were significantly lower than previously tested TFHX ranges (the lowest velocity in seawater testing was 0.2 m/s) and previous correlations for convective coefficients overpredicted the actual values.

2B testing revealed that while maintaining the same mass flow rate ratio, it is more advantageous to have higher mass flow rates. While the approach temperature is higher at higher mass flow rates, the maximum draw outlet temperature is limited at lower flow rates due to the heat of mixing (68.1°C vs 77.5°C) and the actual draw outlet temperature is also higher (75°C vs 67.3°C). Lower

flow rates also mean more plates and heat exchanger area is required to accommodate total overall flow rates in a desalination system.

Since the draw pressure drop was lower than expected, higher flow rates, (accomplished by using fewer plates or smaller channels) which improve the heat transfer efficiency, and longer heat exchanger lengths, which improve the outlet temperature, are possible.

6.4.3. TFHX Designs for Desalination System

The flow rates, pressure drop, and duty specifications for a demonstration-scale desalination system were provided by Trevi. Makai evaluated several TFHX configurations with different plate lengths and channel sizes. The TFHX design was balanced between competing priorities of efficiency, approach temperature, operating power, and heat exchanger cost. For example, for the same heat exchanger, higher flow velocities improve the heat transfer efficiency, but result in less favorable outlet temperatures and increased pumping power.

Makai used the pressure drop and convective coefficients from testing to design each of the three heat exchangers in the desalination system. The low pressure drop measured for the 47% draw solution enables: 1) higher flow rates by using fewer heat exchanger plates and reducing the initial heat exchanger cost, and 2) adding length to the heat exchanger to improve the outlet temperature. Although performance testing was not performed on the 1B operating configuration, Makai estimated the convective coefficient by applying a correction factor to 2B and 1C results to account for changes in channel size. Makai determined it was most economical to use the same overall plate size and shape in each of the three heat exchangers; tooling costs and custom-designed components would be used across all three heat exchangers.

Makai's baseline design (Table 6) utilizes full-length (0.8-m long fluid flow path) 0.002" SS316L TFHX plates at a 1-mm plate spacing and a modular concept to construct the heat exchangers, similar to the design introduced in Section 2.5, but with six ports to support the interlocking plate design. For the Trevi design, the 55-mm ID manifold sizes is appropriate for the internal fluid and the external fluid requires a 80-mm ID port.

2B and 1C have the same internal/external channel size whereas 1B has a larger internal channel to accommodate the more viscous 80% draw solution. The duty and pressure drop requirements met the requirements but the outlet temperatures of the external draw solution in 1B and 2B are lower than originally specified. This is because the heat of mixing was higher than expected.

6.4.4. Cost

Makai reported heat exchanger costs to Trevi based on \$247/m^2 heat transfer area and estimated \$50,000 in tooling costs. However, more recent estimates, which include modules, end plates, and current labor costs are closer to \$524/m^2 with the potential to target \$402/m^2 once optimized for the HSWS. With additional investment in automation, for example, in the stacking of plates in a module, reduced need for skilled labor, and price breaks for large quantity material orders a cost of \$285/m^2 can be realized in the near term.

Table 6. Baseline TFHX Design for Desalination System

	1B	2B	1C
Plates	3072	1632	864
Plate Width X Plate Length [m]	0.25 x 0.8	0.25 x 0.8	0.25 x 0.8
Total HX Area [m^2]	1229	653	346
Duty [kW]	1874	2247	1442
LMTD [C]	9.34	9.06	4.62
U [$kW/m^2/K$]	0.167	0.36	0.90
Internal Channel [mm]	0.5	0.35	0.35
Internal Mass Flow Rate [kg/s]	12.17	7.92	13.35
Internal dP [psi]	3.7	1	2.6
Internal T in [C]	89	89	95
Internal T out [C]	21.4	21.22	69.3
External Channel [mm]	0.4	0.55	0.55
External Mass Flow Rate [kg/s]	9.32	11.15	20.47
External dP [psi]	3.6	3.1	2.9
External T in [C]	16.8	16.8	65
External T out [C]	72.4	72.8	90

6.4.5. Discussion

Makai presented a design based on a standard TFHX shape and consistent plate spacing. This TFHX design can be fabricated with minimal modification to existing tooling.

For standard TFHX plates, Makai recommends an additional round of optimization to confirm pressure drop and performance results using slightly different internal channel sizes and to verify performance for the 80% draw solution.

For future work, Makai recommends exploring different overall heat exchanger designs (wedges instead of rectangular or pass-through instead of 4-port) and/or breaking each heat exchanger into two units to leverage the customizability of the TFHX and take advantage of low viscosity on the hot side of the heat exchanger while accommodating the high viscosity on the cold side of the heat exchanger. On a large-scale system, substantial performance improvements and cost savings may be realized by optimizing the heat exchanger for the different flow regions.

Trevi Systems, Inc. was impressed with the technical capabilities of the TFHX and the overall performance capabilities with additional optimization. However, the current cost and fabrication capability the TFHX was incompatible with their project timeline.

7. CONCLUSION

Between February 2020-July 2021, Makai made significant progress in advancing the TFHX design, reducing TFHX fabrication time/cost, and adding empirical data to TFHX thermal, hydraulic, and structural/mechanical performance database. In doing so, Makai continues to gain expertise in the fundamental principles of laser welding and further our understanding of the TFHX technology.

TFHX Design

A new, modular, 4-port, 1-m long, counterflow TFHX was designed for seawater-seawater and ammonia-seawater applications. This new plate design required a larger manifold opening and new forms and fixtures for fabrication. The modular design streamlines the assembly process for TFHX units but maintains TFHX customizability in internal/external channel sizes. Although some issues were identified during commissioning, Makai was still able to fabricate several full-length plates. In the next period, Makai's efforts will include assembling and performance testing several modules in the 100-kW Test Station.

Makai also demonstrated the ability to perform the internal manifold weld for the all-welded version of a TFHX. The all-welded technology eliminates the need for gaskets (and accompanying inserts and hardware) to seal the internal fluid. After successful demonstration of the all-welded concept, Makai developed and demonstrated a new method to perform the internal manifold weld that is transferrable to different manifold sizes. Fixturing to perform the weld on stacks of multiple plates has been procured and Makai intends to test the sealing capability of a stack of all-welded plates next.

A new short-length plate (and accompanying fabrication fixtures) was designed for the all-welded platform. The short-length plate can be fabricated entirely in-house from coils of foil; there is no external vendor-performed forming step. The short-length plate also provides a rapid and economical platform for future TFHX characterization.

TFHX Fabrication and Cost

Makai commissioned the High Speed Welding Station (HSWS) and has already reduced fabrication times from 30 minutes to produce a mid-length 3E-style plate on the stage to 17.5 minutes to produce a full-length plate on the HSWS. TFHX cost has been reduced from \$1297/m^2 for 3E-INT to \$679/m^2 at current HSWS capacity and projected to decrease \$608/m^2 in September after the arrival of new equipment for the HSWS. It is important to note previous costs did not include additional parts to build a TFHX unit, only the cost of plate fabrication; furthermore, current costs include more realistic contingency and operational expenses.

TFHX Characterization and Performance

In this period, Makai introduced additional weld parameters that expanded TFHX pressure capacity and channel sizes and began geometric and mechanical characterization of these new combinations. Makai developed a new plan for TFHX characterization that focuses on relevant TFHX design configurations, i.e., only testing plates fabricated with optimal weld parameters, expanded to required percentages, with appropriately designed seal welds and transition zones. In

addition to using static and cyclic pressure testing to evaluate TFHX designs, Makai also added optical microscopy to the array of tools used in characterization.

Makai continues to conduct performance testing of different TFHX configurations. A new round of counterflow seawater-seawater performance testing was conducted at the 100 kW Test Station. Makai also completed modifications to the 100 kW testing station in preparation for full-length, modular, 4-port TFHX testing in counterflow seawater-seawater and seawater-ammonia configurations.

Makai also completed air-water performance testing of 11 TFHX configurations. The Air Convection Test Station was upgraded to accommodate higher flow rates and higher duties for more robust data collection. Previous trends of higher convective coefficients in smaller channels for the same Reynolds number and higher convective coefficients in larger channels for the same pressure drop were observed. More significantly, at tested air flow rates, the TFHX does not exhibit a saturation point – unlike finned heat exchangers, TFHX duty and performance continue to increase with increasing air flow rates.

Makai also performed a commercial case study for Trevi Systems, a company specializing in desalination projects. Makai designed and tested a TFHX at provided operating conditions and used the data to design TFHXs for a full-scale desalination system. Trevi Systems was impressed with the technical performance and capabilities of the TFHX but the current fabrication capacity and cost did not meet their project timeline or budget.

Upcoming Work

The major points of focus for Makai's near-term work are to:

- Resolve weld reliability/quality issues on the HSWS and, in conjunction, reduce fabrication times and TFHX cost.
- Fabricate 3-4 full-length modules for performance testing in ammonia-seawater and seawater-seawater orientations.
- Advance the all-welded TFHX technology by fabricating a stack of all-welded plates and performing a seal test to evaluate the internal manifold weld strength. Further development in automating the process is also planned.
- Utilize the short-length platform for TFHX characterization with existing titanium foil thicknesses and new materials (e.g., SS316L, Haynes 230).

8. APPENDIX A – SEAWATER-SEAWATER HEAT EXCHANGER TESTING

8.1. DATA ACQUISITION AND INSTRUMENTATION

A custom developed Labview-based program was used to collect data. The instruments (Table 7) output a 4-20 mA signal, proportional to the measurement, which was read using National Instruments' NI 9208 Analog Input modules. Measurements were sampled 10X a second, averaged, and recorded every second.

Table 7. Sensors Used in Seawater-Seawater Performance Testing

Measurement	Model	Range	Accuracy
Internal/External Seawater Flow Rate	Rosemount 8705 Mag Meter	0-300 gpm	0.25% of rate
Internal Seawater Inlet/Outlet Temperature	Intempco MIST 55	0-50 C	0.1 C + 0.1% FS
External Seawater Inlet/Outlet Temperature	Intempco MIST 55	0-50 C	0.1 C + 0.1% FS
Internal Seawater Inlet/Outlet Pressure	GE UNIK5000	0-30 psia	0.25% FS*
External Seawater Inlet/Outlet Pressure	GE UNIK5000	0-30 psia	0.25% FS*

* Another +/- 0.5% FS due to temperature error band needs to be added to the stated static accuracy. In practice, the pressure sensors are accurate to +/- 1 kPa.

8.2. CALCULATED VALUES

Several values are calculated by the 100 kW control software in real time. These values are used in determining steady state operation and characterizing heat exchanger performance.

8.2.1. Seawater Mass Flow Rate

Seawater mass flow rate is calculated from the measured volumetric flow rate:

$$\dot{m} = \frac{gpm}{15850.3\ {}^{gpm}/_{m^3/s}} \times \rho$$

The density of cold seawater is taken to be 1027.7 kg/m^3 and the density of warm seawater is taken to be 1022.8 kg/m^3.

8.2.2. LMTD

LMTD is a measure of the average temperature difference across the heat exchanger. It is used in the calculation of overall heat transfer coefficient, U. LMTD is calculated according to:

$$LMTD = \frac{(T_{wsw\ in} - T_{csw\ out}) - (T_{wsw\ out} - T_{csw\ in})}{\ln \frac{T_{wsw\ in} - T_{csw\ out}}{T_{wsw\ out} - T_{csw\ in}}}$$

8.2.3. Duty

Duty is a measure of the heat transferred between warm and cold seawater and is used in the calculation of overall heat transfer coefficient. Duty can be calculated based on eitherseawater or based on the ammonia. The equations used to calculate the duty are:

$$Duty_{wsw} = \dot{m_{wsw}} * c_{p,wsw} * (T_{wsw\ in} - T_{wsw\ out})$$

$$Duty_{csw} = \dot{m_{csw}} * c_{p,csw} * (T_{csw\ out} - T_{csw\ in})$$

$\dot{m}$ = mass flow rate [kg/s],

c_p = specific heat capacity of seawater [kJ/kg],

T = seawater temperature [C], and

8.2.4. Overall Heat Transfer Coefficient

The overall heat transfer coefficient, U, is a measure of the overall efficiency of a heat exchanger. It is calculated according to:

$$U = \frac{Duty}{LMTD * Area}$$

LMTD = log mean temperature difference [C]

Area = heat transfer area of the heat exchanger [m^2]

Both duty and LMTD directly impact the calculation of overall heat transfer coefficient. The duty used to calculate the heat transfer coefficient is the ammonia duty.

8.2.5. Convective Heat Transfer Coefficients

The overall heat transfer coefficient is a function of the convective and conductive heat transfer coefficients:

$$\frac{\mathbf{1}}{\boldsymbol{UA}} = \frac{\mathbf{1}}{\boldsymbol{h_{csw}A}} + \frac{\boldsymbol{t}}{\boldsymbol{k_{foil}A}} + \frac{\mathbf{1}}{\boldsymbol{h_{wsw}A}} \qquad \textit{Equation 8-1}$$

where

A = heat transfer area [m^2],

h_{csw} = internal seawater convective coefficient [kW/m^2C],

h_{wsw} = external seawater convective coefficient [kW/m^2C],

t = foil thickness [m], and

k_{foil} = thermal conductivity of titanium foil [kW/mC],

The heat transfer area for each component in Equation 3-1 is the same; Equation 3-1 reduces to:

$$\frac{1}{U} = \frac{1}{h_{SW}} + \frac{t}{k_{foil}} + \frac{1}{h_{NH3}}$$ *Equation 8-2*

1/U is calculated from the data as described in Section 8.2.4. t/k_{foil} is a constant based on the physical and thermodynamic properties of the foil.

In order to determine h_{csw} and h_{wsw}, the internal and external seawater-side heat transfer coefficient was assumed to be constant for a fixed seawater flow rate and independent from the other side. By holding internal seawater flow rate constant and changing the external seawater flow rate and vice versa, a matrix of U-values for each combination of internal/external seawater flow rates was generated. The entire set of equations was solved simultaneously using the method of constrained least squares.

8.3. DATA PROCESSING

Raw data were first graphed in a custom analysis program. Large sections of data could be quickly reviewed and steady-state data was averaged and added to a summary file. Sections of steady-state data were added to a separate file.

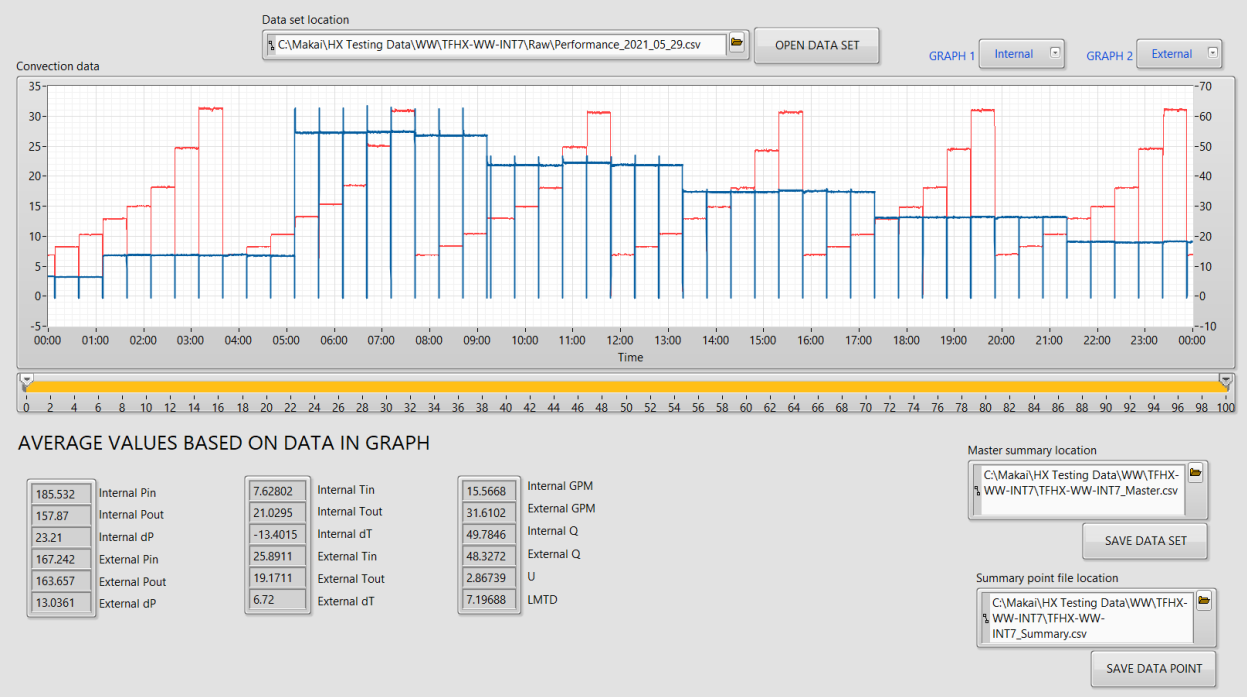

Figure 64. Data review program is first used to identify sections of steady-state data. For each section, an averaged set of values is saved in a summary file and all points in the section are saved in a master data file.

Summarized data points were grouped by internal/external flow rates, with a range of +/- 3% of gpm for most flows but up to +/-10% for the lowest flow rates. The lower flow rates were highly sensitive to fluctuations in system pressure and difficult to consistently return to the same flow rate.

9. APPENDIX B - AIR CONVECTION TESTING

9.1. DATA ACQUISITION AND INSTRUMENTATION

A custom developed Labview-based program was used to collect data. The instruments (Table 8) output a 4-20 mA signal, proportional to the measurement, which was read using National Instruments' NI 9208 Analog Input modules. Measurements were sampled 10X a second, averaged, and recorded every second. RefProp 10 was used obtain density and specific heat capacity for dry air and water at the testing temperatures and pressures, and used in calculating velocity/mass flow rate and duty.

Table 8. Instrumentation used in air convection testing

Measurement	Model	Range	Accuracy
Air Mass Flow Rate	Coriolis CMFS150M	0-0.075 kg/s	±0.25% of reading
Air Inlet/Outlet Temperature	Intempco MIST 55	0-50°C	±0.15°C
Air Inlet/Outlet Pressure	GE Unik 5000	0-5 psia	±0.04% FS
Water Flow	N/A	0.2-10 gpm	±2%
Water Inlet/Outlet Temperature	Intempco MIST 55	0-50°C	±0.15°C
Water Inlet/Outlet Pressure	GE 5000	0-30 psia	±0.2% FS

9.2. CALCULATIONS

9.2.1. Air Velocity

The in-channel air velocity was calculated by dividing the mass flow rate by the outlet air density and the air cross-sectional flow area.

Table 9. Relevant dimensions for tested air-water TFHX configurations

	Internal	External	Plates	Air XC Flow Area [m^2]
TFAC-3E-10	0.342	0.771	18	0.00142
TFAC-3E-11	0.342	0.771	18	0.00142
TFAC-3E-12	0.342	0.932	16	0.00153
TFAC-3E-13	0.342	1.136	14	0.00164
TFAC-3E-14	0.144	0.965	18	0.00182

TFAC-3E-15	0.144	0.836	20	0.00175
TFAC-3E-16	0.144	0.730	22	0.00169
TFAC-3E-17	0.144	0.730	22	0.00168
TFAC-3E-18	0.229	0.803	20	0.00160
TFAC-3E-19	0.229	0.931	18	0.00168
TFAC-3E-20	0.229	1.091	16	0.00176

9.2.2. Duty

Air and water duties are calculated using $Q = \dot{m}\ c_p\ (T_{in} - T_{out})$ where $\dot{m}$ = measured mass flow rate (Coriolis):

	volumetric flow rate [m^3/s]	**density [kg/m^3]**	**c_p [kJ/kg]**
air	measured mass flow rate	Determined using Refprop at the averaged outlet temperatures and outlet pressure	Determined using Refprop at the averaged the inlet and outlet temperatures and outlet pressure
water	$\frac{measured\ gpm}{15850.3\ \frac{gpm}{m^3/s}} \times \rho$	Determined using Refprop at water inlet temperature and pressure.	Determined using Refprop at water inlet temperature and pressure.

9.2.3. LMTD

The log mean temperature difference is calculated from the measured inlet and outlet water temperatures, the measured inlet air temperature, and the averaged outlet air temperature.

$$LMTD = \frac{\left(T_{water,in} - T_{air,out}\right) - \left(T_{water,out} - T_{air,in}\right)}{\ln \frac{\left(T_{water,in} - T_{air,out}\right)}{\left(T_{water,out} - T_{air,in}\right)}}$$

Typically, a correction factor is applied to LMTD to account for the cross-flow configuration, but for the tested conditions, the correction factor is ~1.

9.2.4. Overall Heat Transfer Coefficient

The overall heat transfer coefficient, U-value, is calculated by Q = U A LMTD where the area for each configuration is listed in Table 9.

9.2.5. Determination of Air-Side Heat Transfer Coefficients

Air-side heat transfer coefficients were calculated using $\frac{1}{U} = \frac{1}{h_{water}} + \frac{t}{k} + \frac{1}{h_{air}}$ and assuming a constant water-side heat transfer coefficient of 20 $kW/m^2/K$, regardless of the water-side internal channel spacing and flow rate.

Previous analysis compared four methods of calculating the air-side heat transfer coefficient: using a constant water-side Nusselt number, functional Wilson plot, two-coefficient Wilson plot, and a weighted least-squares solution simultaneous equation solver. The resulting water-side heat transfer coefficient ranged from 1 - 15 $kW/m^2/K$. The functional Wilson plot produced conflicting water-side convective coefficients for the same water flow rate. The 2-coefficient Wilson plot produced a range of air and water convective coefficients depending on the chosen correlation. Additionally, the linear fit to the Wilson plot x and y coordinates was poor which lowers the confidence in the results.

Using correlations developed for pillow-plate heat exchangers, the water-side heat transfer coefficients are more likely in the range of 10-30 $kW/m^2/K$. There is < 10% increase in air-side convective coefficients for a decrease in water-side heat transfer coefficient from 30 $kW/m^2/K$ to 5 $kW/m^2/K$. Therefore, Makai has chosen a constant water-side heat transfer coefficient of 20 $kW/m^2/K$ to calculate air-side convective coefficients.